

Reference Spectrum Method for Nuclear Matter*

H. A. BETHE, B. H. BRANDOW, AND A. G. PETSCHET†

Laboratory of Nuclear Studies, Cornell University, Ithaca, New York

(Received 27 June 1962)

A new method is presented for the calculation of the reaction matrix G of the Brueckner-Goldstone theory. The spectrum of the intermediate states is replaced by a "reference spectrum" of the form $A+Bk^2$ where the constants A and B are chosen so as to approximate, as closely as possible, the actual particle energies for k between 3 and $6 F^{-1}$. The reason for this choice is explained. With the reference spectrum, the Brueckner integral equation reduces to a differential equation which is easily solved. The case of a repulsive core can be solved explicitly, and can be summed over angular momentum, taking into account the correct statistical weights. If an attractive potential is added to the repulsive core, a simple "modified Born approximation" can be developed. Noncentral forces, such as tensor forces, are considered.

The actual G matrix, G^N , is calculated from the reference matrix G^R . It is shown that this can be done to sufficient accuracy (0.1 to 0.2 MeV per nucleon) by a simple quadrature. The difference $G^N - G^R$ arises mainly from the Pauli principle which is not taken into account in G^R . A small correction, less than 1 MeV per nucleon, arises from the inaccuracy of the reference spectrum.

1. INTRODUCTION

THE theory of Brueckner and co-workers¹ permits, in principle, the calculation of the properties of complex nuclei in terms of the potential between two nucleons. The theoretical foundation of the theory has been given by Goldstone² whose proof was generalized by Hugenholtz³. Brueckner and Gammel,⁴ aside from further developing the method, did extensive numerical calculations, using the best results then available on the interaction between two nucleons,⁵ and obtained results in good agreement with experiment.

The Brueckner-Goldstone (BrG) method can be criticized from two points of view: From the basic point of view it may be questioned whether it actually leads to the ground state of nuclear matter, and from the practical point of view the numerical calculations required are complicated and not very transparent. On the basic side, there are two questions, (a) whether perturbation theory is valid, and (b) whether the BrG theory gives the correct perturbation result. On question (b), Luttinger, Kohn, and Ward^{6,7} have shown that the BrG method is indeed correct to all orders of perturbation theory if (1) the particles have spin 1/2, (2)

This shows that the details of the particle energy spectrum are not important for the calculation of the nuclear binding energy.

The particle energy spectrum is carefully investigated. In agreement with Brueckner and Goldman, the G matrices determining the potential energy of states in the Fermi sea are calculated "on the energy shell," and a more detailed justification is given for this procedure. Those for states above the Fermi sea are calculated "off the energy shell." This, in combination with the repulsive core, has the consequence of making the potential energy very large and positive for large k , corresponding to an effective mass between 0.8 and 0.9 for highly excited states. In addition, there is an energy gap at the Fermi momentum, a feature which helps to justify the reference spectrum.

A modified Moszkowski-Scott separation into short- and long-range potentials is developed and gives, in second order, results accurate to better than 0.1 MeV per particle. The wave functions of interacting particles are calculated in the reference spectrum approximation for central and tensor forces.

the interaction between them is isotropic, and (3) the Fermi surface without interactions is isotropic in momentum space. These conditions are evidently satisfied for nucleons interacting with central forces. For electrons in solids, condition (3) is obviously violated, and Kohn and Luttinger⁶ show that a correct perturbation calculation deviates from BrG in second order. For the case of nucleons interacting with tensor forces, they showed that the BrG theory is correct in second order⁶; it is likely that it is correct in all orders but we have not seen a proof of this.

On problem (a), i.e., whether perturbation theory is valid, the chief argument is that nuclear matter may exhibit a phenomenon similar to superconductivity. This was first suggested by Bohr *et al.*⁸ who pointed out that the first intrinsic excited states of heavy, deformed, even-even nuclei lie at about 1 MeV while the spacing between single-nucleon levels is expected to be only about $\frac{1}{4}$ MeV. Bohr *et al.*, attribute this to a pairing energy similar to that found by Bardeen, Cooper, and Schrieffer⁹ in superconductors. Emery and Sessler¹⁰ developed a theory of the energy gap in infinite nuclear matter, using for the interaction between two nucleons the singlet-even¹¹ potential of Gammel and Thaler.⁵ They found that the energy gap is very sensitive to the density of nuclear matter and to the effective mass M^* of the nucleons near the Fermi surface. For the observed nuclear density which Emery and Sessler¹⁰ used, corresponding to a Fermi momentum $k_F = 1.4 F^{-1}$

* Supported in part by the joint program of the Office of Naval Research and the U. S. Atomic Energy Commission.

† Permanent address: Los Alamos Scientific Laboratory, Los Alamos, New Mexico.

¹ K. A. Brueckner and C. A. Levinson, Phys. Rev. **97**, 1344 (1955); K. A. Brueckner, *ibid.* **97**, 1353 (1955).

² J. Goldstone, Proc. Roy. Soc. (London) A293, 267 (1957).

³ N. M. Hugenholtz, Physica **23**, 481, 533 (1957).

⁴ K. A. Brueckner and J. L. Gammel, Phys. Rev. **109**, 1023 (1958). See this paper for other references.

⁵ J. L. Gammel and R. M. Thaler, Phys. Rev. **107**, 291, 1337 (1957).

⁶ W. Kohn and J. M. Luttinger, Phys. Rev. **118**, 41 (1960).

⁷ J. M. Luttinger and J. C. Ward, Phys. Rev. **118**, 1417 (1960).

⁸ A. Bohr, B. R. Mottelson, and D. Pines, Phys. Rev. **110**, 936 (1958).

⁹ J. Bardeen, L. N. Cooper, and J. R. Schrieffer, Phys. Rev. **108**, 1175 (1957).

¹⁰ V. J. Emery and A. M. Sessler, Phys. Rev. **119**, 248 (1960).

¹¹ This state is likely to give the largest energy gap. See reference 10.

($F \equiv \text{fermi} \equiv 10^{-13}$ cm), the calculated gap is only 0.1 MeV at $m^* = M^*/M = 1$, and falls to a negligible value when the effective mass is reduced to 0.75 which should be close to the actual value. At reduced density, $k_F = 1.0 F^{-1}$, the calculated gap is much larger, from 1 MeV at $m^* = 0.75$ to 4 MeV at $m^* = 1$. Thus, the calculated energy gap tends to be less than that deduced⁸ from empirical data. To be on the safe side, we assume the latter, viz., $\Delta E = 1$ MeV. But even then, the effect on the average energy per nucleon is likely to be *less* than

$$\Delta W = \frac{3}{8} \Delta E^2 / E_F = 0.008 \text{ MeV}, \quad (1.1)$$

where E_F is the Fermi energy, 47 MeV for $k_F = 1.5 F^{-1}$ (which is the value we use), and the factor $\frac{3}{8}$ is the statistical probability of having a pair of nucleons in a state of even relative angular momentum. We therefore believe that the "superconductivity pairing," while probably of interest for the detailed level structure of even-even nuclei, has a negligible influence on the average binding energy of nuclei.

We therefore consider the Brueckner-Goldstone method as sufficiently established on theoretical grounds. However, the numerical work is complicated, especially due to the repulsive core in the nucleon interaction. It has therefore been suggested, especially by Levinger, Peierls, and collaborators,¹² to ignore the repulsive core and to replace its effect by a velocity-dependent potential. They have fitted the parameters of this potential so as to reproduce the observed phase shifts for nucleon-nucleon scattering. The resulting velocity-dependent potential is then "weak" enough to justify the use of ordinary perturbation theory, rather than BrG theory.

There is no objection, in principle, against the use of velocity-dependent potentials. It is well known that the measurement of scattering phase shifts of real nucleons, on the energy shell, does not fully determine the interaction of nucleons. The interaction off the energy shell is still largely arbitrary, and can only be determined experimentally by studying processes involving more than two nucleons, e.g., the photoeffect on the deuteron, the structure of the triton and heavier nuclei, scattering processes involving these, etc. The velocity-dependent potential of Levinger *et al.*, while agreeing (by definition) with the standard, static potentials for processes on the energy shell, differs from them in its predictions of phenomena off the shell. The theory of nuclear matter involves off-shell matrix elements to an important de-

¹² R. E. Peierls, in *Proceedings of the International Conference on Nuclear Structure, Kingston, Canada, 1960*, edited by D. A. Bromley and E. Vogt (University of Toronto Press, Toronto, 1960), p. 7; J. S. Levinger and L. M. Simmons, Phys. Rev. **124**, 916 (1961); M. Razavy, G. Field, and J. S. Levinger, *ibid.* **125**, 269 (1962); O. Rojo and L. M. Simmons, *ibid.* **125**, 273 (1962).

See especially the recent calculations of A. M. Green [A. M. Green, Nuclear Phys. **33**, 218 (1962); Phys. Letters **1**, 136 (1962)]. These show a distinct difference between the effects of a hard core and a velocity-dependent potential in nuclear matter. It does not seem that a velocity-dependent potential can account for the observed saturation.

gree. *A priori* it is hard to tell whether a velocity-dependent or a static potential gives better results. However, Charap, Fubini, and Tausner¹³ have shown that at least at moderate energies, dispersion theory leads to an unambiguous definition of a (static) potential which can be calculated in terms of the exchange of one, two, etc., pions. The exchange of many pions or other particles influences the interaction at small distance which may no longer be describable by a potential. Now in nuclear matter, the filled states have momenta up to $k_F = 1.5 F^{-1}$ which is moderate—a *relative* momentum of this magnitude corresponds to a free nucleon of less than 200-MeV laboratory energy colliding with a nucleon at rest. We therefore believe that an ordinary, static, nucleon-nucleon potential should give a good description of nuclear matter. However, in calculating the energies of individual particles in nuclear matter we need (Sec. 9) the interaction of particles up to about $3.5 F^{-1}$ with particles essentially at rest; this corresponds to about 450-MeV laboratory energy where the static repulsive core is no longer clearly established by nucleon-nucleon scattering.

Thus we are led back to the nuclear matter problem for a static potential with a repulsive core. Very important progress in this problem was made by Moszkowski and Scott¹⁴ (quoted as MS). They showed that the theory is greatly simplified if the nucleon-nucleon interaction is separated into a short-range part, v_s , and a long-range part, v_l . The short-range part is then represented by a reaction matrix G_s which is not very different for nuclear matter and for free nucleons. The long-range part can be treated by Born approximation in nuclear matter while for free nucleons this is not possible and a very different result is obtained. The separation between short and long range is made in such a way that the short-range reaction matrix for *free* nucleons, G_s^F , vanishes. Then the total reaction matrix G consists of two main parts, the first Born approximation for v_l , and the difference between G_s in nuclear matter, G_s^N , and for free nucleons, G_s^F ; in addition, there are some small corrections. There is no problem about v_l , and MS show how to calculate $G_s^N - G_s^F$ in terms of the spectrum of nucleons in nuclear matter, $E(k)$.

Köhler¹⁵ has further investigated the MS method. He finds that the MS calculation of $G_s^N - G_s^F$ may not be sufficiently accurate and suggests an improved method which, however, may still leave appreciable errors. Thus the MS method, while a great simplification over the direct solution of the Brueckner integral equation, should be improved in accuracy. This is the first main task of this paper. In addition, we have been able to develop a method, even simpler than MS be-

¹³ J. M. Charap and S. P. Fubini, Nuovo Cimento **14**, 540 (1959); **15**, 73 (1960); J. M. Charap and M. J. Tausner, *ibid.* **18**, 316 (1960).

¹⁴ S. A. Moszkowski and B. L. Scott, Ann. Phys. (New York) **11**, 65 (1960).

¹⁵ S. Köhler, Ann. Phys. (New York) **16**, 375 (1961).

cause it does not require separation into short and long range, which is probably more accurate than the original MS method.

The second problem discussed in this paper is the calculation of the energies of individual nucleons, $E(k)$. We do not attempt here to calculate the *actual* energy required to remove a nucleon of given momentum $k < k_F$ from the nucleus, nor to calculate the optical potential seen by a real nucleon entering from the outside. We merely wish to define an energy spectrum $E(k)$ in such a way that the calculation of the total energy of the nucleus converges as rapidly as possible. As we show in Sec. 4, this may be accomplished by requiring that the potential energy, $U(k)$, compensate certain diagrams occurring in the third order of the BrG expansion. These diagrams correspond to the interaction of a nucleon in an intermediate state with all the nucleons in the Fermi sea. If the intermediate state is a hole in the Fermi sea, $k < k_F$, the interaction should be calculated on the energy shell, as proposed by Brueckner and Goldman.¹⁶ If the intermediate state is above the Fermi sea, $k > k_F$, the interaction must be calculated off the energy shell, as was indeed done by Brueckner and Gammel.⁴ The “potential energies” for these states $k > k_F$, therefore, have nothing to do with the actual potential energy of a real nucleon of such a momentum, i.e., with the optical potential; our $U(k)$ turns out much more positive than the optical potential (Secs. 4, 7, 8). In fact, we find that $U(k)$, for large k , becomes large and positive, and proportional to the kinetic energy of the nucleon, thus giving the virtual nucleon an effective mass less than unity even in this limit.

The aim of this paper is to provide a method for the calculation of the binding energy of nuclear matter which is *accurate and simple once the potential between nucleons is known*. At present our knowledge of this potential is still very incomplete although a lot of progress has been made, both experimentally and theoretically.¹⁷ For instance it is quite uncertain what part of the binding energy of the deuteron is due to tensor and what part to central forces, and in nuclear matter the central forces seem to be more effective than the tensor. Also the repulsive core in odd- L states is not well known from nucleon-nucleon data. Once a reliable theory of nuclear matter is available the experimental properties of nuclear matter may shed light on these questions. In this paper we do not make any attempt to calculate nuclear binding energies quantitatively.

¹⁶ K. A. Brueckner and D. T. Goldman, Phys. Rev. **117**, 207 (1960).

¹⁷ See the review articles by M. J. Moravcsik and H. P. Noyes, Ann. Rev. Nuclear Sci. **11**, 95 (1961), and by H. P. Stapp, M. H. MacGregor, and M. J. Moravcsik, Ann. Rev. Nuclear Sci. **10**, 291 (1960).

2. GENERAL THEORY AND MOSZKOWSKI-SCOTT METHOD

The basic quantity of the Brueckner-Goldstone theory is the reaction matrix G which satisfies the integral equation

$$G = v - \frac{Q}{e} G, \quad (2.1)$$

where v is the potential between two nucleons, Q is the Pauli operator, and e is the energy denominator which we define¹⁸ so as to be positive definite. Throughout this paper, except where specially indicated otherwise, we define all energy quantities, such as e , v , and G , as the actual energy multiplied by $M\hbar^2$. Thus, e has the dimension fermi⁻². This choice of units, similar to atomic units in the theory of atoms, has the advantage that, e.g., the energy of a free nucleon is simply $\frac{1}{2}k^2$. To translate back to familiar units, we note the relation ($F \equiv \text{fermi}$)

$$1 F^{-2} = 41.467 \text{ MeV}. \quad (2.1a)$$

G and v , being volume integrals of energies, have the dimension of a length which makes G directly related to the scattering length. (2.1) may be written explicitly:

$$\begin{aligned} \langle \mathbf{k} | G | \mathbf{k}_0, \mathbf{P} \rangle = & \langle \mathbf{k} | v | \mathbf{k}_0 \rangle - (2\pi)^{-3} \int d^3 \mathbf{k}' \langle \mathbf{k} | v | \mathbf{k}' \rangle \\ & \times \frac{Q(k')}{e(k', k_0)} \langle \mathbf{k}' | G | \mathbf{k}_0, \mathbf{P} \rangle. \end{aligned} \quad (2.2)$$

Here \mathbf{k}_0 , \mathbf{k}' , \mathbf{k} denote the initial, intermediate, and final relative momentum of the two interacting nucleons, and \mathbf{P} is their *average* momentum¹⁹ so that, e.g., the laboratory momenta of the two nucleons in the intermediate state are $\mathbf{P} + \mathbf{k}'$ and $\mathbf{P} - \mathbf{k}'$. The Pauli operator is then

$$\begin{aligned} Q = 1 & \text{ if } |\mathbf{P} + \mathbf{k}'| > k_F \text{ and } |\mathbf{P} - \mathbf{k}'| > k_F, \\ Q = 0 & \text{ otherwise.} \end{aligned} \quad (2.3)$$

The energy denominator is

$$e(k', k_0, P) = E(\mathbf{P} + \mathbf{k}') + E(\mathbf{P} - \mathbf{k}') - H(k_0, P). \quad (2.4)$$

Note again that e is positive definite. If $|\mathbf{P} + \mathbf{k}_0|$ and $|\mathbf{P} - \mathbf{k}_0|$ are both $< k_F$, i.e., if we calculate the interaction of two nucleons actually present in the nucleus, then the “starting energy” H is simply

$$H(k_0, P) = E(\mathbf{P} + \mathbf{k}_0) + E(\mathbf{P} - \mathbf{k}_0). \quad (2.5)$$

If, however, $|\mathbf{P} + \mathbf{k}_0|$ or $|\mathbf{P} - \mathbf{k}_0|$ is $> k_F$, then the starting energy is much less than (2.5); this is discussed in Sec. 4. $E(k)$ denotes the energy of an individual particle of momentum k ; the function $E(k)$ is assumed to

¹⁸ This is opposite to the definition in most of the literature, but far more convenient.

¹⁹ The momentum of the center of mass is thus $2\mathbf{P}$; the factor of 2 by which we differ from Brueckner and Gammel, Moszkowski and Scott, and others, makes the definitions of \mathbf{P} and \mathbf{k} symmetrical and greatly simplifies the formulas.

be known before the calculation of G is begun. For the sake of rapid convergence, $E(k)$ must satisfy conditions of reasonable self-consistency (see Sec. 4). If v is a simple, local potential, then its matrix elements depend only on the difference of the momenta occurring,

$$\langle \mathbf{k} | v | \mathbf{k}_0 \rangle \equiv v(\mathbf{k} - \mathbf{k}_0) = \int v(r) e^{i(\mathbf{k}-\mathbf{k}_0) \cdot \mathbf{r}} d\tau, \quad (2.6)$$

but for an exchange potential, also $\mathbf{k} + \mathbf{k}_0$ appears.

Equation (2.2) should be considered an integral equation in the variable \mathbf{k} only; the quantities \mathbf{P} and \mathbf{k}_0 are merely parameters. According to general scattering theory,²⁰

$$G\phi = v\psi, \quad (2.7)$$

where ϕ is the free-particle wave function for the state \mathbf{P} , \mathbf{k}_0 and ψ is the actual wave function of the two particles interacting in nuclear matter. It is useful to introduce the wave operator, Ω , thus:

$$\psi = \Omega\phi, \quad (2.8)$$

so that (2.7) is equivalent to the operator equation

$$G = v\Omega. \quad (2.9)$$

The Schrödinger equation for ψ then shows that

$$\Omega = 1 - \frac{Q}{e}G. \quad (2.10)$$

(2.9) together with (2.10) yields (2.1). Matrix elements in momentum space may easily be taken of all these equations, but it is also useful to consider ψ as a function of the relative coordinate r of the nucleons.

The structure of the reaction matrix has been greatly clarified by the work of Moszkowski and Scott.¹⁴ They suggested the separation of the potential into a short- and a long-range part, v_s and v_l , assuming a separation distance d , and denoting the part of v for $r < d$ by v_s , that for $r > d$ by v_l . In discussing the MS method, we leave d undetermined until Sec. 10.

With these assumptions, Köhler¹⁵ has shown that

$$G = G_s + \Omega_s^\dagger v_l \Omega, \quad (2.11)$$

where G_s is the contribution to G from the short-range forces alone, and Ω_s is the corresponding wave operator, Eq. (2.10). For a simple proof, see Appendix A, Eq. (A16). It is easy to show (Sec. 10) that the second term in (2.11) is approximately v_l . Using this in (2.10) we may write

$$\Omega \approx \Omega_s - \frac{Q}{e}v_l, \quad (2.12)$$

and inserting into (2.11) we get

$$G = v_l + G_s + (\Omega_s^\dagger - 1)v_l + v_l(\Omega_s - 1) - \frac{Q}{e}v_l, \quad (2.13)$$

²⁰ See, e.g., H. A. Bethe and J. Goldstone, Proc. Roy. Soc. (London) A238, 531 (1957).

neglecting such higher order terms as

$$(\Omega_s - 1)^2 v_l, \quad \frac{Q}{e}v_l(\Omega_s - 1), \quad \frac{Q}{e}\frac{Q}{e}v_l, \quad (2.14)$$

which can be shown to be very small (see Sec. 10).

Equation (2.13) shows that G is given by five terms, the first two of which are large while the other three are small corrections. The first term is the first Born approximation due to the long-range forces alone; it is by far the largest contribution to the nuclear binding energy per particle, amounting to about 50 MeV per particle.¹⁴ The last term is the second Born approximation due to the long-range forces and is¹⁴ less than 1 MeV per particle; its smallness is due to the Pauli principle; the first Born approximation is even better for the long-range forces, v_l , than for "conventional" nuclear forces²¹ (such as exponential and Yukawa, without repulsive cores). The second term in (2.13) is the contribution of short-range forces; it arises in the MS theory from the "dispersion effect," i.e., the fact that the one-particle energy $E(k)$ in nuclear matter differs from that for free nucleons. According to MS (reference 14, Table I) this contribution G_s is only about 10% of v_l , but it is very important for the saturation of nuclear forces because it increases strongly with density: It represents the residual effect of the repulsive core on nuclear matter. This is further discussed in Secs. 7 and 10. Finally, the third and fourth terms in (2.13) which are in many cases equal represent an interference between short- and long-range potential; they are together about 2 MeV per particle according to MS (Table I).

Thus a successful calculation of G requires primarily the calculation of v_l which is straightforward, and a good approximation for G_s . All other terms are small, as is discussed in Sec. 10.

3. REFERENCE SPECTRUM

We have shown that it is important to get a good approximation to the short-range reaction matrix in nuclear matter, G_s^N , which satisfies (2.1) with v replaced by v_s . MS point out that G_s has matrix elements mostly to intermediate states of high momentum (of order $3k_F$, according to Secs. 7 and 9 of this paper). Consequently the Pauli principle (the operator Q) does not have much influence on G_s^N but the energy spectrum "e" of the intermediate states does.

This suggests that we approximate G_s^N by another matrix which is easier to calculate. We define the "reference matrix"

$$G_s^R = v_s - v_s(1/e_R)G_s^N, \quad (3.1)$$

i.e., we omit the Pauli principle in this definition. The G_s^R is easy to calculate if e_R is a quadratic function of the momentum k' in the intermediate state. Accord-

²¹ H. A. Bethe, Phys. Rev. 103, 1353 (1956).

ingly, we define the *reference energy* of a particle by

$$E_R(k') = A + k'^2/2m^*, \quad (3.2)$$

where m^* is an effective mass. Because of our choice of energy units, m^* is dimensionless, viz.,

$$m^* = M^*/M, \quad (3.3)$$

in terms of the usual definition of effective mass. With (3.2), the energy denominator in (3.1) becomes

$$e_R = k'^2/m^* + 2A + P^2/m^* - H(k_0, P). \quad (3.4)$$

It is important to note that (3.1) is easy to solve regardless of the value of $H(k_0, P)$, since H enters the integral equation only as a parameter, not as a variable; therefore the *actual* value of the "starting energy" H can be chosen, without approximation; it is not necessary and in general not desirable to use the reference spectrum in calculating H . The coefficients A and m^* in (3.2), of course, can be chosen so as to give the best average fit to the actual energy spectrum $E(k')$ in that region of k' which matters most for the solution of (3.1). Suitable choices are discussed in Secs. 7, 8.

The reference spectrum can, of course, also be used to advantage to calculate a reference reaction matrix for the *complete* potential

$$G^R = v - v(1/e_R)G^R, \quad (3.5)$$

rather than for its short-range part only. In many cases G_R provides a sufficient first approximation, and whenever this is the case it is unnecessary to use the MS separation into short- and long-range potential. This simplifies the calculation.

MS have already shown how to solve (3.5) with e_R given by (3.4), only assuming $m^* = 1$ (see Appendix of reference 14). The solution is most easily obtained by using (2.9) on both sides of (3.5) to replace G by Ω ,

$$e^R(1 - \Omega^R) = v\Omega^R. \quad (3.6)$$

Applying this operator to the unperturbed wave function $\phi(k_0, P, r)$ gives, according to (2.8),

$$e^R(\phi - \psi^R) = v\psi^R. \quad (3.7)$$

The operator e_R , by virtue of its quadratic dependence on k' , may be written in coordinate space in terms of ∇^2 . It is convenient to introduce the abbreviation

$$\gamma^2 \equiv P^2 + m^*[2A - H(k_0, P)], \quad (3.8)$$

which is an effective energy in (3.7), and also

$$\zeta \equiv \phi - \psi = (1 - \Omega)\phi, \quad (3.9)$$

i.e., the difference between the free and the actual wave function. Then (3.7) becomes

$$(\gamma^2 - \nabla^2)\zeta^R = m^*v\psi^R. \quad (3.10)$$

This is our fundamental differential equation. We solve this equation by means of the usual partial-wave expansion, with the notation $\zeta(L) = \chi_L/k_0 r$, in analogy

to $\psi(L) = u_L/k_0 r$. The resulting radial equations are given in (5.11).

To discuss (3.10), the approximation to G^N obtainable from the reference spectrum, we now consider the short-range potential v_s alone. Formulas (3.6) to (3.10) can be taken over, with a subscript s attached. Since v_s is defined to vanish for $r > d$, an $L=0$ solution of (3.10) behaves for $r > d$ as

$$\chi_{s, L=0}^R = e^{-\gamma r}. \quad (3.11)$$

Other angular momentum components behave similarly. Thus χ and ζ tend rapidly to zero, the more so the larger γ . Typical values of γ for states inside the Fermi sea are of order $2 F^{-1}$, and for states outside the sea even larger, insuring a very rapid decay of ζ_s^R . The reference wave function ψ_s^R , Eq. (2.8), thus tends rapidly towards the free-particle wave function ϕ , corresponding to rapid "healing" in the sense of Gomez, Walecka, and Weisskopf.²² The "healing distance" is 0.5 F or less, beyond the separation distance d .

In its rapid healing property, the reference wave function is similar to the Bethe-Goldstone (BG) wave function.²⁰ The BG function takes the Pauli principle into account but replaces, in general,²³ the energy spectrum by the free nucleon spectrum, thus

$$G_{BG} = v - v \frac{\Omega}{e_0} G_{BG}. \quad (3.12)$$

The BG wave function has the disadvantage that $\zeta^{BG} = \phi - \psi^{BG}$ oscillates for large r , with frequency k_F , rather than decreasing exponentially, like our (3.11). Therefore, our reference wave function is easier to work with and, hence, preferable. Moreover, ψ^R is a good approximation to the true wave function at small r while ψ^{BG} is not, because at small r the correct energy spectrum of the intermediate states is much more important than the Pauli principle (see the beginning of this section).

We now consider the solution ζ^R of (3.10) if v is the *complete* potential rather than just its short-range part, v_s . The asymptotic behavior of ζ^R then depends on that of v : If v decreases faster than $e^{-\gamma r}$, Eq. (3.11) still holds for ζ^R ; but if it decreases more slowly, then

$$\zeta^R \sim v \quad \text{as } r \rightarrow \infty. \quad (3.13)$$

In any case, however, rapid "healing" is assured.

The question is now whether G^R so defined is a good approximation to G^N . We have already shown that G_s^R is a good approximation to G_s^N (see Sec. 10 for further discussion), thus we are mainly concerned with the long-range part of the potential. Now it is well known that for the long-range potential the first Born approximation is good,¹⁴ i.e., $G_l^N \approx v_l$. This means that

²² L. C. Gomez, J. D. Walecka, and V. F. Weisskopf, Ann. Phys. (New York) 3, 241 (1958).

²³ A spectrum of the form (3.2) is, however, also considered as a possibility, cf., Eq. (2.27) of reference 20.

the wave function ψ^N in nuclear matter for $r > d$ must be close to the unperturbed wave function ϕ , i.e., healing must be rapid. But this is precisely the property of our reference wave function ψ^R . It does not matter greatly how ψ approaches ϕ for larger r , the leading term in G_l is just

$$\langle \mathbf{k} | G_l | \mathbf{k}_0 \rangle \approx \langle \phi(\mathbf{k}) | v_l | \phi(\mathbf{k}_0) \rangle. \quad (3.14)$$

Therefore any ζ which goes rapidly to zero is acceptable, and our ψ^R is thus a reasonable first approximation also for calculating the long-range contribution G_l .

It is a quantitative question whether G^R is a sufficiently good approximation to the actual reaction matrix G^N . If it is, we can use G^R directly and thus avoid the MS separation. If it is not, we can use the MS separation and calculate G_s^R . This is discussed in detail in Sec. 10. In the following we speak of G^R but the argument is essentially the same for G_s^R .

To determine G^R , the wave equation (3.10) is solved (Secs. 5–9), then

$$\langle \mathbf{k} | G^R | \mathbf{k}_0, \mathbf{P} \rangle$$

$$= \int \phi(\mathbf{k}, \mathbf{r}) v \psi^R(\mathbf{k}_0, \mathbf{r}) d\tau, \quad (3.15)$$

$$= (m^*)^{-1} \int \phi(\mathbf{k}, \mathbf{r}) (\gamma^2 - \nabla^2) \zeta^R(\mathbf{k}_0, \mathbf{r}) d\tau, \quad (3.16)$$

$$= (m^*)^{-1} (\gamma^2 + k^2) \int \phi(\mathbf{k}, \mathbf{r}) \zeta^R(\mathbf{k}_0, \mathbf{r}) d\tau. \quad (3.17)$$

This last step involves integration by parts. It is equivalent to taking the matrix element of the identity

$$G^R = e^R (1 - \Omega^R). \quad (3.18)$$

In various connections, different expressions are preferable.

Once G^R is obtained, the actual nuclear reaction matrix can be calculated from the exact integral equation (see Appendix A)

$$G^N = G^R + G^{R\dagger} \left(\frac{1}{e_R} - \frac{Q}{e} \right) G^N. \quad (3.19)$$

We have chosen e_R to be a good approximation to e in the region of k' important for the short-range forces so that the second term in (3.19) should be small for these. For the long-range forces, the second term is also likely to be small, partly because of the Pauli operator and partly because e_R is fairly large for all intermediate states.²⁴ Therefore, it should be a good approximation

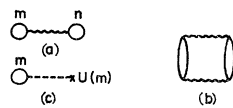


FIG. 1. Lowest order diagrams in the Goldstone expansion. Diagram 1(b) does not enter in the expansion.

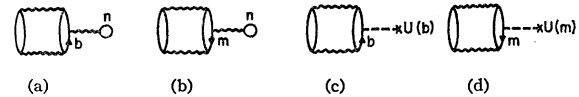


FIG. 2. Lowest order of class A diagrams, as defined in Sec. 4. These may be made to cancel “on the average” by a suitable choice of $U(b)$, $U(m)$.

to replace G^N by G^R in the second term. If this is done G^N can be obtained simply by quadrature; the diagonal terms are

$$\begin{aligned} \langle \mathbf{k}_0 | G^N | \mathbf{k}_0 \rangle &\approx \langle \mathbf{k}_0 | G^R | \mathbf{k}_0 \rangle + (2\pi)^{-3} \int d^3 \mathbf{k}' |\langle \mathbf{k}' | G^R | \mathbf{k}_0 \rangle|^2 \\ &\times \left(\frac{1}{e_R(k')} - \frac{Q(k')}{e(k')} \right), \end{aligned} \quad (3.20)$$

where we have used the fact that G^R is Hermitean (Appendix A).

In Sec. 10 we further discuss the second term of (3.20), especially the accuracy of the approximation $G^N = G^R$ in the second term of (3.19). We also give the additional terms introduced by the MS separation.

4. PARTICLE ENERGIES

In the Goldstone formalism the initial choice of the particle energies $E(k)$ is arbitrary. This, in fact, is an important reason for the power of the method, as compared with perturbation theory. The freedom of choice can be used to make the contributions of the third-order diagrams very small if not zero.

It is well known that in the Goldstone theory there is no second-order diagram because the only possible one, Fig. 1(b), is made up of Goldstone v -interaction diagrams that have already been included in the first-order one, Fig. 1(a). Wavy lines denote interactions by G , dashed lines by v , solid lines going up are nucleons in “particle” states $k_b > k_F$, lines going down are “holes” in states $k_m < k_F$, and circles denote nucleons in normally occupied states, $k_n < k_F$. Throughout this paper we follow the convention that a, b, c , etc., refer to states above the Fermi sea, while l, m, n , etc., denote states in the sea. The latter may or may not represent “holes,” depending on the context.

The third-order diagrams fall into two classes, A and B (as do the higher order diagrams). In class A diagrams, such as Figs. 2(a) and 2(b), one of the lines produced by the original interaction, either a particle [Fig. 2(a)] or a hole [Fig. 2(b)] interacts with an additional particle in the sea. We may say, in analogy to field theory, that the class A diagrams are self-energy diagrams. The diagrams 2(a), 2(b) represent the simplest self-energy insertions, namely, single “bubbles,” which can be made into Fig. 1(a). Class B diagrams do not have the character of insertions, thus they correspond to genuine many-body clusters, examples of which in third order are the “particle-hole” and “hole-hole”

²⁴ This is another way of arguing that G^R should also be a good approximation for the long-range forces.

diagrams of Figs. 3(a) and 3(b). [The so-called “three-body cluster” diagram, Fig. 3(c), can be considered an exchange graph associated with Fig. 3(a).]

There has been a tendency to regard class *B* diagrams as small. This was apparently confirmed by Köhler²⁵ who used the MS separation method and found the total contribution of third-order clusters to be only 0.1 MeV. However, Rajaraman²⁶ has pointed out that, in third order, the class *B* diagrams are quite similar to class *A*. If they are suitably interpreted, they may also be considered as self-energy diagrams. This involves an approximation, which, however, works quite well. Rajaraman estimates that class *B* diagrams are about as important as class *A*, which is reasonable. We have estimated that their influence on the binding energy per nucleon may be several MeV unless there is an accidental cancellation. The reason for the difference from previous estimates is that our theory attributes much greater importance to the hard core interaction far “off the energy shell.” For simplicity, however, we ignore class *B* diagrams in this section and return to Rajaraman’s suggestion at the end of this section and again at the end of Sec. 8.

The free choice of $E(k)$ can now be used to compensate, as far as possible, the diagrams of Fig. 2. If we choose

$$E(k) = \frac{1}{2}k^2 + U(k), \quad (4.1)$$

then $-U(k)$ is part of the perturbation Hamiltonian. We therefore try, as closely as possible, to make the diagrams of Figs. 2(a) and 2(c) cancel by defining

$$U(b) = \sum_{kn < k_F} \langle bn | G | bn - nb \rangle, \quad (4.2)$$

where we have indicated the direct minus the exchange elements of the reaction matrix²⁷ for the interaction of nucleons *b* and *n*, summed over all nucleons *n* in the Fermi sea. Equation (4.2), in fact, is the definition used by Brueckner in all his papers.²⁸

However, (4.2) does not completely define *U* because *G* depends not only on *k_b* and *k_n* but also on *H*, see Eq. (2.4). But *H* depends generally on all the particles and holes present while the interaction occurs,²⁹ not only on the two interacting particles, *b* and *n*. For instance, in order to find out the proper *H* for Fig. 2(a) we expand

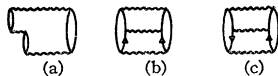


FIG. 3. Lowest order of class *B* diagrams, as defined in Sec. 4. Rajaraman has shown that these may be considered approximately equivalent to class *A* diagrams, i.e., insertions. Diagrams (a), (b), and (c) are commonly called the particle-hole, hole-hole, and three-body-cluster diagrams.

²⁵ S. Köhler, Ann. Phys. (New York) **12**, 444 (1961).

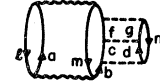
²⁶ R. Rajaraman, following paper [Phys. Rev. **129**, 265 (1963)].

²⁷ The notation is different from that in Secs. 2 and 3; we have $\mathbf{k}_b = \mathbf{P} + \mathbf{k}$ and $\mathbf{k}_n = \mathbf{P} - \mathbf{k}$ in terms of the previous notation.

²⁸ See especially reference 16.

²⁹ Reference 21, Sec. 3, especially Eq. (3.13).

FIG. 4. Typical *v*-interaction ladder diagram contained in Fig. 2(a).



the interaction with the bubble on the right into ladder diagrams such as Fig. 4. Then in the step which contains the particle states *c* and *d*, the energy denominator is obviously³⁰

$$e = E(c) + E(d) + E(a) - E(l) - E(m) - E(n), \quad (4.3)$$

so that, using the definition of *H* in (2.4),

$$H = E(l) + E(m) + E(n) - E(a). \quad (4.4)$$

Since state *a* is above the Fermi sea, and *l*, *m*, and *n* are all in the sea, it follows that

$$H \ll E(n) + E(k_F - \epsilon), \quad (4.5)$$

whereas, if *b* and *n* interacted “on the energy shell,” we would have

$$H' = E(n) + E(b) \gg E(n) + E(k_F - \epsilon). \quad (4.6)$$

This shows that the interaction is “off the energy shell,” and that the “starting energy” *H* is always considerably less than the on-energy-shell value *H'*. Furthermore, (4.4) shows that *H* is not uniquely determined by *b* and *n*, but depends also on *l* and *m*, the nucleons which originally interacted. It should be noted that

$$\mathbf{k}_a = \mathbf{k}_l + \mathbf{k}_m - \mathbf{k}_b, \quad (4.7)$$

so \mathbf{k}_a is not an additional variable.

The dependence on *l* and *m* means that the definition (4.2) is ambiguous for states $k_b > k_F$, since the right-hand side depends on three parameters while the left side must depend only on state *b*. The best that can be achieved then is to make

$$U(b) = \text{average}_{l,m} \sum_{kn < k_F} \langle bn | G | bn - nb ; lm \rangle. \quad (4.8)$$

Then the potential is not truly self-consistent; for a given *l* and *m* the sum of the diagrams 2(a) over all *n* do not cancel Fig. 2(c). But we may expect that after summation over *l* and *m* the cancellation will be quite close.³¹ Fortunately, the dependence on *l* and *m* is not very strong because *H* is not very sensitive to these parameters. For instance, if *k_b* is very large, (4.7) gives $k_a \approx k_b$, and (4.4) yields³²

$$H \approx E(n) + 2E_{av} - E(b), \quad (4.9)$$

³⁰ This is essentially in agreement with Brueckner and Gammel, reference 4, Appendix A.

³¹ That “cancellation on the average” is the best we can hope to achieve was pointed out by Goldstone, reference 2, and by D. J. Thouless, Phys. Rev. **112**, 906 (1958).

³² It may be noted that if (4.9) is rewritten as $H = 2E_{av} - \Delta$, then $\Delta = E(b) - E(n)$. Clearly Δ depends strongly on *k_b*. In view of the influence of *H* on the resulting *U(b)*, it is not a good approximation to replace $\Delta(b)$ by an average value, as done by Brueckner and Gammel. They justified this by the weak dependence of their *U(b)* on Δ , but, as shown below, this was a result of their incorrect treatment of the hard cores.

where E_{av} is the average energy of a nucleon in the Fermi sea.

The definition (4.2), or more accurately (4.8), is of course in the spirit of the Hartree-Fock method. It is reasonable to hope, but it still has to be proved, that this choice also minimizes contributions from the most important fourth and higher order graphs.

For the potential energy of states m below the Fermi sea, or "holes," Brueckner has always calculated G on the energy shell, i.e., with

$$H = E(m) + E(n). \quad (4.10)$$

This is reasonable, but not obviously the best choice. At first sight, (4.10) is suggested by the fact that it makes diagram 1(c) cancel the sum over diagrams 1(a). But this is not particularly useful: In the total energy of nuclear matter, in first order in G , there is no such cancellation because we must take one-half the sum of diagrams 1(a) over m and n , minus the full sum of diagrams 1(c) over m . Instead, as we have said in connection with (4.2), $U(m)$ in Fig. 2(d) should compensate the diagrams of Fig. 2(b). In fact, as Goldstone has demonstrated, the Hartree-Fock definition of $U(m)$ in perturbation theory does even better: The term $-U(m)$ in the perturbing Hamiltonian identically cancels all diagrams which contain a "bubble interaction" inserted into an upgoing or downgoing line of some simpler diagram. This is no longer true in the G -diagram expansion, because the starting energies for the G 's associated with the bubble interactions depend on the remainder of the diagram.

From the foregoing it might seem reasonable to proceed by analogy to our choice for $H(b)$, but this leads to a difficulty when we follow the Goldstone theory in a straightforward manner. In this theory, the ladders of v interactions which combine to form G can only exist between particle states $k > k_F$, so that a typical ladder contained in Fig. 2(b) is shown in Fig. 5. The energy denominator in the section involving c, d can easily be read from the diagram, and the starting energy is

$$H = E(l) + 2E(m) + E(n) - E(a) - E(b). \quad (4.11)$$

It is easily seen that this is even lower than (4.4) since it involves four hole energies minus two particle energies, rather than 3 and 1. On the basis of this definition of H , Bethe and Goldstone³³ concluded that the G matrix due to a pure repulsive core is about the same for Figs. 4 and 5 if k_b is large. We have confirmed this conclusion under the assumption (4.11).

Unfortunately, in attempting to find the potential energy as a function of k_m only, we have obtained a

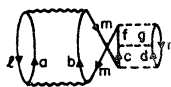


FIG. 5. Typical v -interaction ladder diagram contained in Fig. 2(b).

³³ Reference 20, Note added in proof.

result (4.11) which depends strongly on k_b . We mention two ways out of this difficulty. One is to adopt the on-energy-shell definition of $U(m)$ as done by Brueckner, and then to consider the difference between Figs. 2(b) and 2(d) as a contribution to $U(b)$. The hole-bubble G matrix depends strongly on k_b and only weakly on k_m , so it is reasonable to average over m states as in Eq. (4.8). This contribution to $U(b)$ has a strong quadratic dependence on k_b , of sign opposite to that from Fig. 2(a). We show below, and in Secs. 5 and 7, that the quadratic term from Fig. 2(a) leads to an effective mass considerably less than unity. The result of including Fig. 2(b) in this manner is to cancel most of this quadratic term so that m^* is much closer to unity. This interpretation of Fig. 2(b) is due to Bethe and Goldstone.³³

The method which we adopt, however, is based on a suggestion of Brueckner and Goldman.¹⁶ A fourth-order v diagram contained in Fig. 2(b) is shown in Fig. 6(a). They argue that another fourth-order diagram, Fig. 6(b), should be combined with this because it is of the same order of magnitude (see Appendix B). They show that in perturbation theory the energy denominators of Figs. 6(a), 6(b) combine to give the same result as if

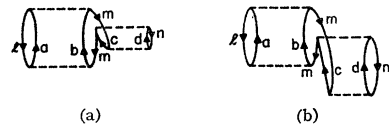


FIG. 6. Fourth-order diagrams combined by Brueckner and Goldman (reference 16) to suggest that the hole-bubble interaction be evaluated "on the energy shell."

Fig. 2(b) were evaluated with the "bubble" energy denominator evaluated on the energy shell, corresponding to (4.10). The basic idea is then that by including suitable higher order diagrams together with Fig. 2(b) one obtains the same result as by evaluating the complete hole-bubble interaction on the energy shell. Although Brueckner and Goldman only showed this to fourth order, the result is, in fact, valid to all orders of perturbation theory and thus can be used for G matrices. We prove this in Appendix B. We must include all diagrams of the type shown in Fig. 7. Two holes are created in the state m , by interaction with holes l and n . (It does not matter which interaction occurs first.) The particles b, c which arise from the two holes in m , interact alternately with the particles a, d which originated from the holes in l and n . Ultimately, the two holes in m are filled again, the first by interaction with n , the second with l . Summing over all diagrams of this type, and adding 2(b), we obtain exactly the same result as by evaluating 2(b) on the energy shell.

It is interesting that when we evaluate 2(b) on the energy shell the result depends only on the energy of the interacting particles m and n , not on that of any

other particles as in (4.4). Therefore the cancellation of 2(b) and 2(d) can now be made exact, while Figs. 2(a) and 2(c) only cancel in an average sense. Furthermore, this method can be applied to any hole bubble appearing in any diagram, so that this useful cancellation feature of Hartree-Fock perturbation theory may be carried over into the G -matrix expansion, *but for hole states only*. (For the difference between particle and hole states, see end of Appendix B.)

Note that this discussion has led us back to just the definitions of $U(m)$ and $U(b)$ used by Brueckner, which are obtained by ignoring Fig. 5. However, our results for the G -matrix elements which contribute to $U(b)$ differ from his in the region of large k_b . We find that $U(b)$ should asymptotically be quadratic in k_b , corresponding to an effective mass m^* less than unity, whereas Brueckner and Gammel⁴ obtain $U(b) \rightarrow 0$ as $k_b \rightarrow \infty$. The reason for the quadratic term in k_b may easily be seen as follows.

Consider Fig. 2(a), as shown in more detail in Fig. 4. It is easier to visualize the relations between the various momenta by means of a "momentum diagram," Fig. 8. A number of simplifications result from considering the asymptotic limit of large k_b . Figure 8 shows that inter-

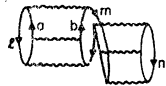


FIG. 7. Typical Goldstone diagram included along with Fig. 2(b) when the hole-bubble interaction in Fig. 2(b) is evaluated "on the energy shell."

mediate states c, d with small momenta should not be important. For this reason the Pauli exclusion operator, Q , may be neglected and the reference spectrum approximation should be very good. For the same reason, and because we are only interested in quadratic effects, we need only consider the hard core part of the two-nucleon interaction. Now we use Eqs. (4.4) and (3.8) to write, for the interaction of b and n ,

$$\gamma^2 = P^2 + m^* [2A - E(l) - E(m) - E(n) + E(a)], \quad (4.12)$$

$$P^2 = \frac{1}{4}(\mathbf{k}_b + \mathbf{k}_n)^2, \quad (4.13)$$

$$k_0^2 = \frac{1}{4}(\mathbf{k}_b - \mathbf{k}_n)^2. \quad (4.14)$$

Now use Eqs. (3.2) and (4.7) to define $E(a)$. After averaging over directions of the momenta l, m, n , no terms remain which are linear in k_b . Dropping terms which are small compared to k_b^2 ,

$$\gamma^2 \approx \frac{3}{4}k_b^2, \quad (4.15)$$

$$k_0^2 \approx \frac{1}{4}k_b^2. \quad (4.16)$$

Inside the core, ψ vanishes but $v = \infty$. Their product is finite, however, and is found from Eqs. (3.9) and (3.10) to be

$$v\psi = (m^*)^{-1}(\gamma^2 + k_0^2)\phi \approx (m^*)^{-1}k_b^2\phi. \quad (4.17)$$

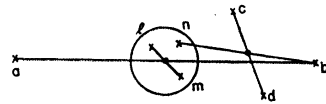


FIG. 8. Momentum-space diagram for Fig. 4, showing the relations among the states due to momentum conservation. The Fermi sea is represented by the circle.

There is also a core boundary term in $v\psi$, which arises from the discontinuous change in slope of ψ at $r=c$. This term is proportional to the radial slope of ψ just outside of the core boundary, and from Eqs. (3.11) and (4.15) it is seen to be linear in k_b . For the present we may neglect this term in comparison to k_b^2 . Then the (direct) G -matrix element becomes simply

$$\langle bn | G | bn \rangle \approx \int_{r < c} \phi^* v \psi d\tau \approx \frac{4\pi}{3} c^3 k_b^2 (m^*)^{-1}. \quad (4.18)$$

The exchange matrix element becomes

$$\langle bn | G | nb \rangle \approx (m^*)^{-1} k_b^2 \int_{r < c} e^{-2i\mathbf{k}_0 \cdot \mathbf{r}} d\tau, \quad (4.19)$$

which vanishes in the limit $k_0 \rightarrow \infty$. The summation over the states n reduces to a multiplication of Eq. (4.18) by the density,

$$\rho = 4 \left(\frac{k_F}{2\pi} \right)^3 = \left(\frac{4\pi}{3} r_0^3 \right)^{-1}, \quad (4.20)$$

where r_0 is given approximately by the constant in the empirical nuclear radius formula. Then from (4.18) and (4.20)

$$U(b) \approx \frac{c^3 k_b^2}{r_0^3 m^*}, \quad (4.21)$$

and using

$$U(b) + \frac{k_b^2}{2} \approx \frac{k_b^2}{2m^*}, \quad (4.22)$$

we find

$$m^* \approx 1 - 0.566(k_F c)^3 = 1 - 2(c/r_0)^3. \quad (4.23)$$

This result was obtained before by Bethe and Goldstone,²⁰ but was then rejected by them in a note added in proof. This was because they considered only diagrams like Fig. 5 for the hole-bubble interaction, as mentioned above.

Inserting the values $k_F = 1.5 \text{ F}^{-1}$, $c = 0.4 \text{ F}$, we obtain $m^* = 0.88$. The value of m^* obtained in Sec. 8 is smaller than this, due to the effects, for finite values of k_b , of the core boundary term and the different statistical weights of even and odd angular momentum states. In fact, the quadratic part of $U(b)$ is approximately doubled by these effects.³⁴ The contribution to m^* from the potential beyond the core is indeed negligible.

³⁴ Because of these corrections for finite k_b , the cancellation in Figs. 2(a) and 2(b) in the Bethe-Goldstone treatment is not complete, and one still obtains an $m^* < 1$.



FIG. 9. Typical v -interaction ladder diagram contained in Fig. 1(a).

If we interpret Fig. 2(b) according to the suggestion of Brueckner and Goldman, an effective mass $m^* < 1$ is unavoidable for large k_b . We may inquire, then, why Brueckner and Gammel⁴ did not find this result. One reason is their neglect of the "core volume" term, Eq. (4.18), which we have shown to be the only contribution to $1 - m^*$ in the asymptotic region. In the calculation of $U(m)$, however, this "core volume" term is negligible, as shown by Bethe and Goldstone.²⁰ Another reason is Brueckner and Gammel's neglect of any interaction, including the repulsive core, in odd angular momentum states. Using the results of the next section, we have found (Sec. 8) that most of the quadratic part of $U(b)$, in the important region of k_b , comes from P states (cf. Fig. 10).^{34a}

We now want to return to the contribution of Class B diagrams, Fig. 3. Rajaraman has observed that these diagrams can also be considered, with good accuracy, as self-energy insertions in the particle line b of Fig. 9, hence they may be cancelled by a suitable choice of $U(b)$. This means that a first-order calculation of the nuclear binding energy with this $U(b)$ is, in fact, approximately correct to third order. Rajaraman's preliminary estimates indicate that the effect of including the third-order diagrams of Class B , shown in Fig. 3, in $U(b)$, is to roughly halve the contribution to $1 - m^*$ from Fig. 2(a) alone. We return to this point at the end of Sec. 8.

We do not consider this to be a sufficiently thorough discussion of the single-particle energies for states above the Fermi sea. It is quite possible that other higher order diagrams may be important; if so, it is likely that most of these may be cancelled or minimized by further modifications of $U(b)$. Note that the requirement of self-consistency for U (Sec. 7) amounts to making the assumption that our $U(b)$, Eq. (4.8), is a good choice also for the intermediate states occurring in the particle-bubble interaction.

In conclusion we want to make two general remarks about our particle energies. In the first place, these energies are not meant to give the observable energies of particles in the nucleus. For example, for states in the Fermi sea, $-E(m)$ does not give the energy necessary to remove particle m from the nucleus. This removal energy is the analog, for hole states, of the optical potential and is a measurable quantity, at least in principle. It can be calculated within the Brueckner-Goldstone formalism, as the difference between the total energies of nuclei containing A and $A-1$ particles. The removal energy differs from our $-E(m)$ by

^{34a} Note added in proof. A further, and important, reason for their different result is that their approximation to the off-energy-shell starting energies, H , was independent of k_b . See our footnote 32.

the oft-discussed rearrangement energy.¹⁶ Likewise, for states above the Fermi sea, $U(b)$ does not give the optical potential: Our states b are intermediate states occurring inside a complicated diagram; for a real state b interacting with n the starting energy is on the energy shell,

$$H = E(b) + E(n),$$

rather than (4.4), and the resulting $U(b)$ is, therefore, quite different from ours. The only purpose of our single-particle energies is to facilitate the calculation of the total energy of nuclear matter, by making the sum over Goldstone diagrams converge rapidly.

The second remark concerns the occurrence of Cooper singularities, analogous to the Bardeen-Cooper-Schrieffer theory⁹ of superconductivity. Such singularities are apt to occur if the single-particle energies $E(k)$ are continuous at the Fermi surface.¹⁰ Our particle energies are discontinuous because of the different choice of "starting energy" below and above k_F , Eqs. (4.10) and (4.4). The averaging over l and m required in (4.8) then ensures an energy gap at k_F . [If we choose specifically $\mathbf{k}_l + \mathbf{k}_m = 0$, k_l and $k_m = k_F - \epsilon$, and $k_b = k_F + \epsilon$, then H in (4.4) joins continuously to (4.10) below k_F ; therefore for this particular choice of momenta, there is no jump in E at the Fermi surface, and the BCS phenomenon could occur.] With such a gap there are no Cooper singularities. It has been made plausible by the work of Emery and Sessler¹⁰ that the Cooper singularities do not have a substantial influence on the bulk properties of nuclear matter. Our theory, which avoids formal difficulties from these singularities, has the advantage, compared with other theories, of (a) preserving the simplicity of the Goldstone approach, (b) giving a logical reason for the appearance of an energy gap, therefore (c) avoiding difficulties associated with vanishing energy denominators, (d) including the Pauli principle in a simple way, (e) permitting accurate calculations of the total energy, and (f) avoiding reformulation of the two-body problem in terms of an artificial, e.g., velocity-dependent, potential.

5. METHOD OF CALCULATING G^R

The introduction of $1/e^R$ in place of Q/e^N in the G -matrix equation has reduced this equation to a set of ordinary second-order differential equations for the various partial waves. This has the great advantage that a number of standard techniques may now be applied. It also leads to some new features that are quite helpful in understanding the essential physics of nuclear matter.

We show in this section that G^R may be separated into two contributions, one representing the effect of a pure hard-core interaction only, and the other the effect of the outer potential. By outer potential we mean the total interaction beyond the hard-core radius. Given the

reference spectrum, this separation is exact.³⁵ This is convenient for several reasons. There is less controversy about the existence of a core than there is about the detailed form of the interaction for $r > c$. It is easier to study the consequences of various assumptions for the outer potential after the core effects have been isolated. Also there are several subwaves, with various statistical weights, for each value of L . The situation for the outer contributions is rather complicated, and this discussion is deferred to the next section. However, the core contributions from all the subwaves combine to give this term a simple statistical behavior. If we assume the same c in all states, several Bessel function identities may be used to express the total core contribution in closed analytic form. This requires only a very minor approximation so that the core expression is essentially exact. We then show that there is an iteration expansion for the outer contribution which is directly analogous to the usual Born series. We call this the modified Born expansion, leading to various orders of modified Born approximation (MBA).

To illustrate the method we first discuss the "direct" diagonal element of G^R for two particles of relative momentum $k_0 = \frac{1}{2}|\mathbf{k}_a - \mathbf{k}_b|$, and distinct (spin, isospin) states. (In this section and in Sec. 6, we assume that $m^* = 1$. Modifications for $m^* \neq 1$ are discussed in Sec. 7.) Using Eq. (2.7) and the partial wave Eq. (5.11) obtained by separating (3.10), we find, similar to (3.17):

$$\langle k_0 | G^R | k_0 \rangle = 4\pi \sum_L (2L+1) k_0^{-1} \int_0^\infty j_L(k_0 r) v u_L R r dr \quad (5.1)$$

$$= 4\pi (\gamma^2 + k_0^2) \sum_L (2L+1) k_0^{-1} \int_0^\infty j_L(k_0 r) \chi_L R r dr. \quad (5.2)$$

The χ 's are defined by

$$\xi = \phi - \psi = (k_0 r)^{-1} \sum_L (2L+1) i^L \chi_L P_L(\cos\theta). \quad (5.3)$$

We omit the R labels from now on. It is convenient to introduce the following definitions:

$$\mathcal{J}_L(r) = k_0 r j_L(k_0 r), \quad (5.4)$$

$$\mathcal{K}_L(r) = \mathcal{J}_L(c) \frac{H_L^{(-)}(\gamma r)}{H_L^{(-)}(\gamma c)}, \quad (5.5)$$

where $H_L^{(\pm)}(\gamma r)$ are the solutions of (5.10) with the asymptotic forms $e^{\pm\gamma r}$. In terms of the usual spherical Hankel functions,

$$\begin{aligned} H_L^{(\pm)}(x) &= i^{(L+1)} (\mp ix) h_L^{(1)}(\mp ix) \\ &= i^{-(L+1)} (\pm ix) h_L^{(2)}(\pm ix). \end{aligned} \quad (5.6)$$

It is clear that

$$\chi_L = \mathcal{J}_L - u_L. \quad (5.7)$$

³⁵ Brueckner and Gammel, reference 4, mention such a separation, but they are unable to do this in an exact manner since they use the complete nuclear propagator Q/e^N .

For $r < c$, $\chi_L = \mathcal{J}_L$ since ψ vanishes. Thus, the integration of (5.2) over the core interior region is straightforward. If there were no interaction beyond the core, we would find $\chi_L = \mathcal{K}_L$ for $r > c$. Note especially that

$$\mathcal{J}_L(c) = \mathcal{K}_L(c) = \chi_L(c) \quad (5.8)$$

holds for a general interaction beyond the core.

The transformation (5.1) \rightarrow (5.2) involved integration by parts. If we were to reverse this procedure for

$$(\gamma^2 + k_0^2) \int_c^\infty \mathcal{J}_L \chi_L dr,$$

nonvanishing boundary terms would now appear. Instead, we compare the three differential equations

$$\left[\frac{d^2}{dr^2} - \frac{L(L+1)}{r^2} + k_0^2 \right] \mathcal{J}_L = 0, \quad (5.9)$$

$$\left[\frac{d^2}{dr^2} - \frac{L(L+1)}{r^2} - \gamma^2 \right] \mathcal{K}_L = 0, \quad (5.10)$$

$$\left[\frac{d^2}{dr^2} - \frac{L(L+1)}{r^2} - \gamma^2 \right] \chi_L = -v u_L. \quad (5.11)$$

We multiply (5.9) by χ_L , (5.11) by \mathcal{J}_L , subtract, and integrate to obtain

$$\begin{aligned} &(\gamma^2 + k_0^2) \int_c^\infty \mathcal{J}_L \chi_L dr \\ &= \left(\chi_L \frac{d}{dr} \mathcal{J}_L - \mathcal{J}_L \frac{d}{dr} \chi_L \right) \Big|_c + \int_c^\infty \mathcal{J}_L v u_L dr. \end{aligned} \quad (5.12)$$

Combining (5.10) and (5.11) similarly gives

$$\left(\mathcal{K}_L \frac{d}{dr} \chi_L - \chi_L \frac{d}{dr} \mathcal{K}_L \right) \Big|_c = \int_c^\infty \mathcal{K}_L v u_L dr. \quad (5.13)$$

Thus we find, using (5.8),

$$\begin{aligned} \int_0^\infty \mathcal{J}_L v u_L dr &= (\gamma^2 + k_0^2) \int_0^c \mathcal{J}_L^2 dr + \mathcal{J}_L (\mathcal{J}_L' - \mathcal{K}_L') \Big|_c \\ &\quad + \int_c^\infty (\mathcal{J}_L - \mathcal{K}_L) v u_L dr. \end{aligned} \quad (5.14)$$

All the effect of the outer potential is contained in the last integral, so that an exact separation into "core" and "outer" terms has been achieved. The meaning of the derivative terms becomes apparent when we try to derive (5.14) by means of (5.1) and (5.11) without using integration by parts. Inside the core, $v u_L$ has the indeterminate form $\infty \times 0$, but we know²⁰ that this must include a term of the form $\lambda \delta(r-c)$, which comes from the discontinuous change in slope of χ_L at $r=c$. Accord-

ing to (5.13), the slope of χ_L at $r=c+\epsilon$ is $\mathcal{K}_L'(c)$, the result for a pure hard core, plus a correction due to the outer potential, namely

$$[\mathcal{J}_L(c)]^{-1} \int_c^\infty \mathcal{K}_L v u_L dr.$$

The slope of χ_L at $r=c-\epsilon$ is $\mathcal{J}_L'(c)$, thus if the outer potential were absent, the change in slope would be $\mathcal{K}_L' - \mathcal{J}_L'$.

There is a simple interpretation for the outer integral in (5.14). For a pure hard core, $u_L(r>c) = \mathcal{J}_L - \mathcal{K}_L$ so that this term has the familiar form

$$\int (\text{unperturbed } u_L)(\text{perturbing } v)(\text{exact } u_L) dr. \quad (5.15)$$

This separation formula, (5.14), is actually the partial-wave decomposition of a general reaction-matrix identity which is derived in Appendix A (Eq. A16).

Core Contribution

We may use several spherical Bessel function identities to obtain the total core contribution to (5.1) in closed form. These identities follow immediately from the usual partial-wave expansion.³⁶

$$\sum_L (2L+1) j_L^2(k_0 r) = (4\pi)^{-1} \int d^2 \hat{r} e^{-i\mathbf{k}_0 \cdot \mathbf{r}} e^{i\mathbf{k}_0 \cdot \mathbf{r}} = 1, \quad (5.16)$$

$$\begin{aligned} \sum_L (2L+1) j_L(k_0 r) \frac{d}{dr} j_L(k_0 r) \\ = (4\pi)^{-1} \int d^2 \hat{r} e^{-i\mathbf{k}_0 \cdot \mathbf{r}} \frac{\partial}{\partial r} e^{i\mathbf{k}_0 \cdot \mathbf{r}} \\ = (4\pi)^{-1} \int d^2 \hat{r} (i\mathbf{k}_0 \cdot \mathbf{r}) = 0, \end{aligned} \quad (5.17)$$

$$\begin{aligned} \sum_L (2L+1) j_L(k_0 r) r^2 \frac{d^2}{dr^2} j_L(k_0 r) \\ = (4\pi)^{-1} \int d^2 \hat{r} (i\mathbf{k}_0 \cdot \mathbf{r})^2 \\ = -\frac{1}{3} (k_0 r)^2. \end{aligned} \quad (5.18)$$

The symbol $d^2 \hat{r}$ is used here to indicate integration over the entire solid angle. As a simple illustration, we note that

$$4\pi \sum_L (2L+1) \int_0^c j_L^2(k_0 r) r^2 dr = \frac{4\pi}{3} c^3, \quad (5.19)$$

which is just the hard-core volume. These identities

³⁶These sum rules may all be obtained, either directly or by differentiation, from Gegenbauer's addition theorem. See, e.g., G. N. Watson, *Theory of Bessel Functions* (Cambridge University Press, New York, 1952), 2nd ed., Sec. 11.4.

have a useful corollary.

$$\begin{aligned} \sum_L (2L+1) j_L^2(k_0 r) L(L+1) \\ = r \sum_L (2L+1) j_L(k_0 r) [L(L+1)/r^2] r j_L(k_0 r) \\ = r \sum_L (2L+1) j_L(k_0 r) \left[\frac{d^2}{dr^2} + k_0^2 \right] r j_L(k_0 r) \\ = \sum_L (2L+1) \left[j_L r^2 \frac{d^2}{dr^2} j_L + 2j_L r \frac{d}{dr} j_L + (k_0 r)^2 j_L^2 \right] \\ = \frac{2}{3} (k_0 r)^2. \end{aligned} \quad (5.20)$$

Now consider

$$\mathcal{J}H_L' \Big|_c = \mathcal{J}_L^2(c) (d/dr) \ln H_L^{(-)}(\gamma r) \Big|_c. \quad (5.21)$$

The logarithmic derivative of $H_L^{(-)}$ is a rational function, and for $(\gamma r)^2 \gg L(L+1)$ this may be expanded in an asymptotic series. But $(\gamma r)^2 \gg L(L+1)$ is just the region of validity for the WKB approximation to $H_L^{(-)}$. The WKB result for the logarithmic derivative is

$$-\gamma [1 + L(L+1)/(\gamma r)^2]^{1/2}. \quad (5.22)$$

Expanding this, we see that the leading terms in the asymptotic expansion must be

$$-\gamma [1 + L(L+1)/2(\gamma r)^2]. \quad (5.23)$$

Now thanks to the \mathcal{J}_L^2 factor, we are only interested in the first few L 's, those where $L \lesssim k_0 c$. We show in Sec. 7 that $k_0^2 \ll \gamma^2$, so that the ratio of the second term to the first is of order $\lesssim k_0^2/2\gamma^2$, which is considerably less than unity. The first term is what would be obtained if $H_L^{(-)}$ were replaced by $H_0^{(-)}$, that is if $H_L^{(-)}$ were a simple exponential. The WKB result suggests that the second term in the asymptotic expansion overestimates the correction, which is really quite small. It is reasonable then to group the leading "exponential" terms together, by means of the Bessel sum rules given above, and leave the remaining small corrections to be approximated in some manner. Using (5.16) and (5.17) to sum over L 's, and remembering the normalization from (5.1), Eq. (5.14) then gives

$$\begin{aligned} \langle k_0 | G^R | k_0 \rangle_{\text{core}} &= 4\pi \left\{ \frac{1}{3} (\gamma^2 + k_0^2) c^3 + c(1 + \gamma c) \right. \\ &\quad \left. + \sum_L (2L+1) c^2 j_L^2(k_0 c) \left[-\gamma - \frac{d}{dr} \ln H_L^{(-)} \Big|_c \right] \right\}. \end{aligned} \quad (5.24)$$

This result is not too surprising. It is possible to find the "inner boundary" term (the sum of the $\mathcal{J}_L \mathcal{J}_L'$ terms) and the "core volume" term in (5.24) without making a partial-wave expansion at all. This is true also for the "outer-boundary" terms provided that we approximate \mathcal{K}_L by an exponential, which amounts to assuming

$$(\partial/\partial r)(r\xi) \Big|_{c+\epsilon} \approx -\gamma c \xi(c). \quad (5.25)$$

Now we claim that a suitable approximation for the correction term is

$$[-\gamma - (d/dr) \ln \mathcal{C}_L^{(-)}]_c \approx \gamma L(L+1)[2\gamma c(\gamma c + 1)]^{-1}. \quad (5.26)$$

This is justified in connection with Eq. (5.34). This was chosen to be exact for $L=0$ and 1, and to have the correct WKB limit. Then (5.20) gives

$$\sum_L (2L+1)c^2 j_L^2(k_0 r) \left[-\gamma - \frac{d}{dr} \ln H_L^{(-)} \right]_c \approx c(k_0 r)^2 [3(\gamma c + 1)]^{-1}, \quad (5.27)$$

and finally

$$\langle k_0 | G^R | k_0 \rangle_{\text{core}} \approx 4\pi \left\{ (\gamma^2 + k_0^2) \frac{c^3}{3} + c \left[1 + \gamma c + \frac{(k_0 r)^2}{3(\gamma c + 1)} \right] \right\}. \quad (5.28)$$

Core Statistics

The result, for the core contribution, of including the exchange matrix element of G^R and averaging over the spins and isospins of the interacting pair, is to multiply the even states by 3/4 and the odd states by 5/4.

$$\begin{aligned} & \langle ab | G^R | ab \rangle - \langle ab | G^R | ba \rangle \}_{\text{core, spin average}} \\ &= 4\pi \left\{ \frac{3}{4} \sum_{\text{even } L} + \frac{5}{4} \sum_{\text{odd } L} \right\} (2L+1) \\ & \times \left\{ (\gamma^2 + k_0^2) \int_0^c j_L^2(k_0 r) r^2 dr + k_0^{-2} \mathcal{J}_L (\mathcal{J}_L' - \mathcal{C}_L') \right\}_c. \end{aligned} \quad (5.29)$$

That these are the correct statistical weights may be seen as follows: Given the momentum states $\mathbf{k}_a, \mathbf{k}_b$, 3/4 of the time the (spin, isospin) states of the two particles differ, allowing both even and odd spatial wave functions to contribute. The exchange term vanishes because the spin states are orthogonal. The remaining 1/4 of the time the (spin, isospin) states coincide, only odd states exist, but there is a factor of two since the direct and exchange terms both contribute.

Identities corresponding to (5.16), (5.17), (5.18), and (5.20) exist for sums over even states only, as can be seen by replacing

$$e^{i\mathbf{k}_0 \cdot \mathbf{r}} \quad \text{by} \quad \frac{1}{2}(e^{i\mathbf{k}_0 \cdot \mathbf{r}} + e^{-i\mathbf{k}_0 \cdot \mathbf{r}}),$$

at the appropriate steps in the derivations.

$$\begin{aligned} & \sum_{\text{even } L} (2L+1) j_L^2(k_0 r) \\ &= \frac{1}{2} (4\pi)^{-1} \int d^2 \hat{\mathbf{r}} e^{-i\mathbf{k}_0 \cdot \mathbf{r}} (e^{i\mathbf{k}_0 \cdot \mathbf{r}} + e^{-i\mathbf{k}_0 \cdot \mathbf{r}}) \\ &= \frac{1}{2} + \frac{1}{2} (4\pi)^{-1} \int d^2 \hat{\mathbf{r}} P_0(\hat{\mathbf{k}}_0 \cdot \hat{\mathbf{r}}) e^{-2i\mathbf{k}_0 \cdot \mathbf{r}} \\ &= \frac{1}{2} [1 + j_0(2k_0 r)], \quad (5.30) \end{aligned}$$

$$\begin{aligned} & \sum_{\text{even } L} (2L+1) j_L(k_0 r) \frac{d}{dr} j_L(k_0 r) \\ &= \frac{1}{2} (4\pi)^{-1} \int d^2 \hat{\mathbf{r}} e^{-i\mathbf{k}_0 \cdot \mathbf{r}} (i\mathbf{k}_0 \cdot \mathbf{r} e^{i\mathbf{k}_0 \cdot \mathbf{r}} - i\mathbf{k}_0 \cdot \mathbf{r} e^{-i\mathbf{k}_0 \cdot \mathbf{r}}) \\ &= -\frac{1}{2} ik_0 r (4\pi)^{-1} \int d^2 \hat{\mathbf{r}} P_1(\hat{\mathbf{k}}_0 \cdot \hat{\mathbf{r}}) e^{-2i\mathbf{k}_0 \cdot \mathbf{r}} \\ &= -\frac{1}{2} k_0 r j_1(2k_0 r), \end{aligned} \quad (5.31)$$

$$\begin{aligned} & \sum_{\text{even } L} (2L+1) j_L(k_0 r) \frac{d^2}{dr^2} j_L(k_0 r) \\ &= -\frac{1}{2} (4\pi)^{-1} \int d^2 \hat{\mathbf{r}} e^{-i\mathbf{k}_0 \cdot \mathbf{r}} (\mathbf{k}_0 \cdot \mathbf{r})^2 (e^{i\mathbf{k}_0 \cdot \mathbf{r}} + e^{-i\mathbf{k}_0 \cdot \mathbf{r}}) \\ &= -\frac{1}{6} (k_0 r)^2 \left\{ 1 + (4\pi)^{-1} \int d^2 \hat{\mathbf{r}} \right. \\ & \quad \left. \times [2P_2(\hat{\mathbf{k}}_0 \cdot \hat{\mathbf{r}}) + P_0(\hat{\mathbf{k}}_0 \cdot \hat{\mathbf{r}})] e^{-2i\mathbf{k}_0 \cdot \mathbf{r}} \right\} \\ &= \frac{1}{6} (k_0 r)^2 [2j_2(2k_0 r) - j_0(2k_0 r) - 1] \\ &= \frac{1}{2} k_0 r j_1(2k_0 r) - \frac{1}{2} (k_0 r)^2 j_0(2k_0 r) - \frac{1}{6} (k_0 r)^2. \end{aligned} \quad (5.32)$$

In the last step here we have exploited the recurrence relation

$$\begin{aligned} & 3z^{-1} j_1(z) = j_0(z) + j_2(z). \\ & \sum_{\text{even } L} (2L+1) j_L^2(k_0 r) L(L+1) \\ &= \sum_{\text{even } L} (2L+1) \left[j_{L'}^2 \frac{d^2}{dr^2} j_L + 2j_{L'} \frac{d}{dr} j_L + (k_0 r)^2 j_L^2 \right] \\ &= \frac{1}{3} (k_0 r)^2 - \frac{1}{2} k_0 r j_1(2k_0 r). \end{aligned} \quad (5.33)$$

The analogous identities for odd states are easily found by subtracting these results from the previous results for all L 's. Corresponding to (5.28),

$$\begin{aligned} & \langle k_0 | G^R | k_0 \rangle_{\text{core, spin average}} \\ &= 4\pi \left\{ (5/4) \sum_{\text{all } L} -\frac{1}{2} \sum_{\text{even } L} \right\} (2L+1) \\ & \times \left\{ (\gamma^2 + k_0^2) \int_0^c j_L^2(k_0 r) r^2 dr \right. \\ & \quad \left. + c j_L(k_0 r) [c(d/dr) j_L(k_0 r)]_c + j_L(k_0 c) \right\} \\ &+ c^2 j_L^2(k_0 c) \gamma + c^2 j_L^2(k_0 c) [-\gamma - (d/dr) \ln H_L^{(-)}]_c \\ &\approx 4\pi c \left\{ \frac{1}{3} (x^2 + y^2) - \frac{1}{4} c^{-1} (x^2 + y^2) \int_0^c j_0(2k_0 r) r^2 dr \right. \\ & \quad \left. + \frac{1}{4} x j_1(2x) + (1+y)[1 - \frac{1}{4} j_0(2x)] \right\} \\ &+ 4\pi c [2(y+1)]^{-1} \left\{ (5/4) \sum_{\text{all } L} -\frac{1}{2} \sum_{\text{even } L} \right\} \\ & \quad \times (2L+1) j_L^2(x) L(L+1) \\ &= 4\pi c \left\{ \frac{1}{3} (x^2 + y^2) + \frac{1}{8} x (1 - y^2/x^2) j_1(2x) \right. \\ & \quad \left. + (1+y)[1 - \frac{1}{4} j_0(2x)] \right\} \\ &+ (1+y)^{-1} [\frac{1}{3} x^2 + \frac{1}{8} x j_1(2x)], \quad (5.34) \end{aligned}$$

where

$$x \equiv k_0 c, \quad y \equiv \gamma c.$$

We have made a detailed calculation of this core term both by means of (5.34), and by evaluating the correction terms in (5.26) without approximation for $L=1, 2$, and 3. The approximation is worst for large values of k_0 where $L's > 1$ are important. We used the parameters $\Delta = 0.75$, $c = 0.4$ F, $k_F = 1.5$ F⁻¹, as discussed in Secs. 7 and 8. In the region from $k_b = k_F$ to $k_b = 5k_F$, the correction term was $\lesssim 3\%$ of the total core term, while the error in the correction due to this approximation was $\lesssim 2\%$. Thus, the over-all error in (5.34) is $\lesssim 0.06\%$, which leads to an error of $\lesssim 0.1$ MeV in the calculation of $U(b)$ (Sec. 8).

Outer Contribution

Referring to (5.1) and (5.14),

$$\begin{aligned} & \{\langle ab | G^R | ab \rangle - \langle ab | G^R | ba \rangle\}_{\text{outer, spin average}} \\ &= 4\pi \sum_{L,S} (2L+1)\nu(L,S) \int_c^\infty (\mathcal{J}_L - \mathcal{K}_L) \\ & \quad \times k_0^{-2} v(L,S) u(L,S) dr. \end{aligned} \quad (5.35)$$

In general, the statistical weights, $\nu(LS)$, are more complicated than for the core terms. An exception is the simplified interaction used in Sec. 9. Equation (5.35) also neglects the additional complications due to tensor forces. These matters are discussed in detail in Sec. 6.

From the definition of χ_L (index S suppressed), we may write

$$u_L = (\mathcal{J}_L - \mathcal{K}_L) + (\mathcal{K}_L - \chi_L). \quad (5.36)$$

Then (5.10) and (5.11) are combined to give

$$\begin{aligned} & \left[\frac{d^2}{dr^2} - \frac{L(L+1)}{r^2} - \gamma^2 \right] (\mathcal{K}_L - \chi_L) \\ &= v[(\mathcal{J}_L - \mathcal{K}_L) + (\mathcal{K}_L - \chi_L)], \end{aligned} \quad (5.37)$$

and

$$\begin{aligned} & [\mathcal{K}_L(r) - \chi_L(r)] = \int_c^\infty \mathcal{G}_L(r|r') v(r') \\ & \times \{[\mathcal{J}_L(r') - \mathcal{K}_L(r')] + [\mathcal{K}_L(r') - \chi_L(r')]\} dr', \end{aligned} \quad (5.38)$$

where \mathcal{G}_L is the Green's function corresponding to the operator on the left of (5.37).

Equation (5.38) may be formally solved by iteration to generate a modified Born series. It is shown in Secs. 8 and 9 that this series actually converges fairly rapidly, so that a form of perturbation theory is possible even in the case of a hard core. The first few terms of this series form what we call a modified Born approximation (MBA). In first MBA, the "unperturbed" wave function is $u_{L(0)} = \mathcal{J}_L - \mathcal{K}_L$. The Green's function is determined by the boundary conditions that $\mathcal{K}_L - \chi_L = 0$ at

$r=c$ and ∞ . Using the definition (5.6), the result is

$$\begin{aligned} \mathcal{G}_L(r|r') = & \frac{1}{2\gamma} \left[\frac{H_L^{(+)}(\gamma c)}{H_L^{(-)}(\gamma c)} H_L^{(-)}(\gamma r) H_L^{(-)}(\gamma r') \right. \\ & \left. - H_L^{(+)}(\gamma r) H_L^{(-)}(\gamma r') \right] \end{aligned} \quad (5.39)$$

for $r < r'$.

Equation (5.38) is quite useful for qualitative discussions. Writing

$$\begin{aligned} u_L &= (\mathcal{J}_L - \mathcal{K}_L) + (\mathcal{K}_L - \chi_L)_{(1)} + (\mathcal{K}_L - \chi_L)_{(2)} + \dots \\ &= u_{L(0)} + u_{L(1)} + u_{L(2)} + \dots \end{aligned} \quad (5.40)$$

one sees that the first MBA correction, $u_{L(1)}$, is inversely proportional to γ^2 , at least in the region of large γ . One factor of γ^{-1} comes from the coefficient in \mathcal{G}_L , while the second comes as a result of the integration. The γ dependence is perhaps clearer when \mathcal{G}_L is expressed in a form suitable for momentum-space calculations.

$$\begin{aligned} \mathcal{G}_L(r|r') = & -\frac{2}{\pi} rr' \int_0^\infty \left[j_L(kr) - j_L(kc) \frac{H_L^{(-)}(\gamma r)}{H_L^{(-)}(\gamma c)} \right] \\ & \times \frac{j_L(kr')}{\gamma^2 + k^2} k^2 dk. \end{aligned} \quad (5.41)$$

If the Fourier-Bessel transform of u_L is such that $\langle k^2 \rangle_{av} \gtrsim \gamma^2$, then the first MBA correction varies more slowly with γ than γ^{-2} .

It appears now that γ has two effects. It defines a "healing distance"²² of order γ^{-1} , through the "pure-core" term ($\mathcal{J}_L - \mathcal{K}_L$). It also tends to stiffen the wave function so that, for nuclear matter, it is not very different from the case of a pure hard core. Brueckner and Gammel⁴ have noted the latter effect; compare the curves labeled $U(r)$ and $S(r)$ in their Fig. 5.

When the tensor force is considered, vu_L must be replaced by $\sum_{L'} v_{LL'} u_{L'}$. It is well known that the tensor force vanishes in S states so that in the deuteron state its effect first appears in the second Born term. The tensor force is quite strong, causing a large admixture of D state within the range of the force. A short-range admixture of D state corresponds to a moderately large k^2 . It turns out that the fractional difference between $\langle k^2 \rangle_{av} + \gamma^2$, and $\langle k^2 \rangle_{av} - k_0^2$ [the corresponding denominator in (5.41) for free-particle scattering] is not large, so that the effect of the tensor force, relative to a central force, is only moderately reduced by γ .³⁷ However, it turns out (Sec. 7) that γ increases about as k_F , so that at higher densities the tensor force is considerably less effective. There is another reason why the tensor force appears to be weakened by the presence of nuclear matter. This is a consequence of the effective mass being less than unity, and is discussed in Sec. 7. These effects are both important in obtaining saturation at the observed density.

³⁷ E. J. Irwin (private communication).

For a detailed numerical calculation it is doubtful whether (5.38) is very useful. (A computer could be programmed to iterate this equation several times, in effect generating the MBA series.) It is probably simpler to solve (5.11) directly. In the case of tensor forces, there are pairs of coupled differential equations.

We have only discussed the diagonal elements of G^R . These are the most important, but for evaluating $G^N - G^R$ and for higher order clusters it is also necessary to know the off-diagonal elements. The procedure is straightforward, as we show in the next section.

6. TRIPLET STATES, $G^N - G^R$ CORRECTION TERM

The detailed treatment of the coupled triplet states was not discussed in the last section for the sake of clarity. There are 16 different (S, S_3, T, T_3) states, available with equal probability, for a pair of particles in momentum states $\mathbf{k}_a, \mathbf{k}_b$. What is actually needed for a lowest order calculation of the ground-state energy, or for the single-particle potential, is the average over these 16 states of the matrix element of (3.19),

$$\begin{aligned} & \langle ab | G^N | ab - ba \rangle \\ &= \left\langle \frac{ab - ba}{\sqrt{2}} \middle| G^R + G^{R\dagger} \left(\frac{1}{e^R} - \frac{Q}{e^N} \right) G^N \middle| \frac{ab - ba}{\sqrt{2}} \right\rangle. \end{aligned} \quad (6.1)$$

The simple arguments which gave the statistical average over the core contributions do not apply to the outer terms. To properly treat the triplet states, we follow the method described by Brueckner and Gammel.⁴ We present their method in some detail, instead of merely quoting their result for the diagonal element of G^R because we need also the nondiagonal elements of G^R in order to obtain G^N , see Eq. (3.20).

Consider the 3 states ($S=1, M=0, \pm 1, T=0$). We replace the spin projection by M , since the interaction can induce "local spin flips." M and S_3 coincide beyond the "healing distance." The free-particle wave functions are

$$\begin{aligned} & \left\langle \frac{ab - ba}{\sqrt{2}} \right\rangle_{(S=1, M, T=0)} \equiv \phi_{1,0}^M \\ &= \sqrt{2}(k_0 r)^{-1} \sum_{\text{even } L} [4\pi(2L+1)]^{1/2} i^L \mathcal{J}_L Y_L^0 \chi_{S=1}^M \lambda_{T=0}^0 \\ &= (8\pi)^{1/2} (k_0 r)^{-1} \sum_{\text{even } L} \sum_J i^L (2L+1)^{1/2} \\ & \quad \times C(L1J; 0MM) \mathcal{J}_L | \psi_{L,J}^M \rangle \lambda_0^0. \end{aligned} \quad (6.2)$$

The nuclear matter "reference" wave functions are

$$\begin{aligned} \psi_{1,0}^M &= (8\pi)^{1/2} (k_0 r)^{-1} \sum_{\text{even } L} \sum_J i^L (2L+1)^{1/2} \\ & \quad \times C(L1J; 0MM) u_{L,J}^M | \psi_{L,J}^M \rangle \lambda_0^0. \end{aligned} \quad (6.3)$$

There is a physical reason why the u 's should depend on

M ; this is discussed in connection with (6.11). Thus,

$$\begin{aligned} & \langle \phi_{1,0}^M | G^R | \phi_{1,0}^M \rangle = \langle \phi_{1,0}^M | v | \psi_{1,0}^M \rangle \\ &= 8\pi \sum_{\text{even } L, L'} \sum_J i^{(L'-L)} (2L+1)^{1/2} (2L'+1)^{1/2} \\ & \quad \times C(L1J; 0MM) C(L'1J; 0MM) \\ & \quad \times k_0^{-2} \int_0^\infty \mathcal{J}_L v_{L,L'}^J u_{L',J}^M dr. \end{aligned} \quad (6.4)$$

We have defined

$$v_{L,L'}^J \equiv \langle \psi_{L,J}^M | v | \psi_{L',J}^M \rangle, \quad (6.5)$$

which is independent of M .³⁸ In terms of

$$\begin{aligned} \xi_{1,0}^M &= \phi_{1,0}^M - \psi_{1,0}^M \\ &= (8\pi)^{1/2} (k_0 r)^{-1} \sum_{\text{even } L} \sum_J i^L (2L+1)^{1/2} \\ & \quad \times C(L1J; 0MM) \chi_{L,J}^M | \psi_{L,J}^M \rangle \lambda_0^0, \end{aligned} \quad (6.6)$$

the differential equation for the coupled states is

$$\begin{aligned} & \left[\frac{d^2}{dr^2} - \frac{L(L+1)}{r^2} - \gamma^2 \right] f_{L,J}^M \chi_{L,J}^M \\ &= - \sum_{L'} v_{L,L'}^J f_{L',J}^M u_{L',J}^M, \end{aligned} \quad (6.7)$$

where

$$f_{L,J}^M \equiv i^L (2L+1)^{1/2} C(L1J; 0MM). \quad (6.8)$$

In order to conveniently sum (6.4) over $M=0, \pm 1$, we follow Brueckner and Gammel⁴ by introducing radial functions for the "entrance channel" description which satisfy

$$\begin{aligned} & \left[\frac{d^2}{dr^2} - \frac{L'(L'+1)}{r^2} - \gamma^2 \right] (\delta_{L,L'} \mathcal{J}_L - u_{L',J}^{(L)}) \\ &= - \sum_{L''} v_{L',L''}^J u_{L'',J}^{(L)}, \end{aligned} \quad (6.9)$$

subject to

$$u_{L',J}^{(L)}(c) = 0, \quad u_{L',J}^{(L)} \rightarrow \delta_{L,L'} \mathcal{J}_L \quad \text{as } r \rightarrow \infty.$$

(Our notation and normalization differ from Brueckner and Gammel.) The primes in (6.9) have been placed so that L refers to the dominant wave, or entrance channel, while $L' \neq L$ or $L'' \neq L$ denotes the subsidiary wave. Now we multiply (6.9) by $f_{L,J}^M$ and sum over L . This results in Eq. (6.7) when we make the identification

$$f_{L',J}^M u_{L',J}^M = \sum_L f_{L,J}^M u_{L',J}^{(L)}. \quad (6.10)$$

In terms of these new radial functions, the sum over M takes on a rather simple form with the (L,J) channels

³⁸ The appropriate matrix elements of the tensor operator S_{12} are tabulated in J. Ashkin and Ta-You Wu, Phys. Rev. **73**, 973 (1948).

uncoupled,

$$\begin{aligned} & \sum_{M=-1}^1 \langle \phi_{1,0}^M | G^R | \phi_{1,0}^M \rangle \\ &= 8\pi \sum_{J \text{ even}} \sum_{L,L',L''} \sum_M f_{L,J}^M f_{L'',J}^M k_0^{-2} \\ & \quad \times \int_0^\infty \mathcal{J}_L v_{L,L',J} u_{L',J}^{(L'')} dr \quad (6.11) \\ &= 8\pi \sum_J (2J+1) \sum_{L,L'} k_0^{-2} \int_0^\infty \mathcal{J}_L v_{L,L',J} u_{L',J}^{(L)} dr, \end{aligned}$$

thanks to the Clebsch-Gordan identity³⁹

$$\begin{aligned} & \sum_M C(LSJ; 0MM) C(L''SJ; 0MM) \\ &= \delta_{L,L''} \frac{2J+1}{2L+1}. \quad (6.12) \end{aligned}$$

Note that for each value of L (except $L=0$) there are three values of J to consider in (6.11). This result is the same as Brueckner and Gammel's Eq. (63), except for a factor of two and the restriction to even states, which occur because we have included the exchange term.

In the original M description, the wave functions depend on M because they describe physically different

situations. $M=0$ refers to the interaction of a pair whose resultant spin is perpendicular to the relative momentum, while $M=\pm 1$ describes collisions with spin parallel to the momentum. The dependence on M is given explicitly by (6.10). We have made a canonical transformation to the entrance-channel description, where each (L,J) channel has the relative weight $(2J+1)$ and includes an appropriate mixture of M states.

As in Sec. 5, we separate the core and outer terms by using (5.9), (5.10), and (6.9).

$$\begin{aligned} & \sum_{L'} \int_0^\infty \mathcal{J}_L v_{L,L',J} u_{L',J}^{(L'')} dr \\ &= \delta_{L,L''} \left[(\gamma^2 + k_0^2) \int_0^c \mathcal{J}_L^2 dr + \mathcal{J}_L (\mathcal{J}_{L'} - \mathcal{J}_{L''})|_c \right] \\ & \quad + \int_c^\infty (\mathcal{J}_L - \mathcal{J}_{L''}) \sum_{L'} v_{L,L',J} u_{L',J}^{(L'')} dr. \quad (6.13) \end{aligned}$$

We only need this result for the case $L''=L$.

Now that we have described the sum of diagonal elements of G^R for the triplet-even states, the result for the other (S,T) states is obvious. The statistical average for the G^R diagonal element is

$$\begin{aligned} & \frac{1}{16} \sum_{(S,M,T,T_S)} \langle \phi_{S,T}^M | G^R | \phi_{S,T}^M \rangle \\ &= 8\pi \left[\frac{1}{16} \sum_{\text{odd } L} (2L+1) k_0^{-2} \int_0^\infty \mathcal{J}_L v(s=0, T=0) u_L dr + \frac{3}{16} \sum_{\text{even } L} (2L+1) k_0^{-2} \int_0^\infty \mathcal{J}_L v(s=0, T=1) u_L dr \right. \\ & \quad \left. + \frac{1}{16} \sum_{\text{even } L, L'} \sum_J (2J+1) k_0^{-2} \int_0^\infty \mathcal{J}_L v_{L,L',J}(S=1, T=0) u_{L',J}^{(L)} dr \right. \\ & \quad \left. + \frac{3}{16} \sum_{\text{odd } L, L'} \sum_J (2J+1) k_0^{-2} \int_0^\infty \mathcal{J}_L v_{L,L',J}(S=1, T=1) u_{L',J}^{(L)} dr \right] \quad (6.14a) \end{aligned}$$

$$\begin{aligned} &= 4\pi \left[\left\{ \frac{3}{4} \sum_{\text{even } L} + (5/4) \sum_{\text{odd } L} \right\} (2L+1) k_0^{-2} \left\{ (\gamma^2 + k_0^2) \int_0^c \mathcal{J}_L^2 dr + \mathcal{J}_L (\mathcal{J}_{L'} - \mathcal{J}_{L''})|_c \right\} \right. \\ & \quad \left. + \frac{1}{8} \sum_{\text{odd } L} (2L+1) k_0^{-2} \int_c^\infty (\mathcal{J}_L - \mathcal{J}_{L''}) v(s=0, T=0) u_L dr + \frac{3}{8} \sum_{\text{even } L} (2L+1) k_0^{-2} \int_c^\infty (\mathcal{J}_L - \mathcal{J}_{L''}) v(s=0, T=1) u_L dr \right. \\ & \quad \left. + \frac{1}{8} \sum_{\text{even } L, L'} \sum_J (2J+1) k_0^{-2} \int_c^\infty (\mathcal{J}_L - \mathcal{J}_{L''}) v_{L,L',J}(S=1, T=0) u_{L',J}^{(L)} dr \right. \\ & \quad \left. + \frac{3}{8} \sum_{\text{odd } L, L'} \sum_J (2J+1) k_0^{-2} \int_c^\infty (\mathcal{J}_L - \mathcal{J}_{L''}) v_{L,L',J}(S=1, T=1) u_{L',J}^{(L)} dr \right]. \quad (6.14b) \end{aligned}$$

Use of (6.13) has permitted us to group the core terms together. Of course, the result is the same as (5.29), obtained by simpler arguments. Note that since we are leaving a factor $\hbar^2 M^{-1}$ understood, the quantity $k_0^{-2} v$ is dimensionless.

³⁹ See M. E. Rose, *Elementary Theory of Angular Momentum* (John Wiley & Sons, Inc., New York, 1957), Chap. 3. The relevant equations are (3.17a) and (3.7).

$G^N - G^R$ Correction

In order to calculate the correction term, we use (3.6) in the form

$$1 - \Omega^R = \frac{1}{e^R} G^R \quad (6.15)$$

to simplify the expression,⁴⁰ see (3.19),

$$G^N - G^R = G^{R\dagger} \left(\frac{1}{e^R} - \frac{Q}{e^N} \right) G^R \approx G^{R\dagger} \left(\frac{1}{e^R} - \frac{Q}{e^N} \right) G^R. \quad (6.16)$$

Thus for a given (S, M, T, T_3) state,

$$\begin{aligned} & \langle \phi_{S,T^M} | G^N - G^R | \phi_{S,T^M} \rangle \\ & \approx \langle \phi_{S,T^M} | (1 - \Omega^R)^\dagger (e^N - Qe^R) (e^R/e^N) (1 - \Omega^R) | \phi_{S,T^M} \rangle \\ & = \sum_{\mathbf{k}', M'} \langle \mathbf{k}', M' | (e^N - Qe^R) (e^R/e^N) | \mathbf{k}', M' \rangle \\ & \quad \times |\langle \mathbf{k}', M' | (1 - \Omega^R) | \phi_{S,T^M} \rangle|^2. \end{aligned} \quad (6.17)$$

From here on, we restrict the discussion to the case where the center-of-mass momentum \mathbf{P} is zero. Then

$$\begin{aligned} & \left\langle \phi_{S,T^M} \left| G^{R\dagger} \left(\frac{1}{e^R} - \frac{Q}{e^N} \right) G^R \right| \phi_{S,T^M} \right\rangle \\ & = \int_0^\infty \mathcal{E}(k') \mathfrak{F}_{S,T^M}(k') dk', \end{aligned} \quad (6.18)$$

where

$$\mathcal{E}(k') \equiv \langle \mathbf{k}', M' | (e^N - Qe^R) e^R / e^N | \mathbf{k}', M' \rangle, \quad (6.19)$$

$$\begin{aligned} \mathfrak{F}_{S,T^M}(k') & \equiv \sum_{M'} (2\pi)^{-3} \int d^3 \hat{\mathbf{k}}' \\ & \quad \times k'^2 |\langle \mathbf{k}', M' | (1 - \Omega^R) | \phi_{S,T^M} \rangle|^2. \end{aligned} \quad (6.20)$$

The natural quantization axis to use for the intermediate states is $\hat{\mathbf{k}}'$. These states are plane waves in relative-coordinate space, so $M_L' = 0$ and therefore $M' = M_s'$. These states must have the same (S, T, T_3) as the original ϕ , thus in general one must consider all $2S+1$ possible values for M' . It is only for the special case where $\hat{\mathbf{k}}' = \pm \hat{\mathbf{k}}_0$ that M' is definite, when it is clear that $M' = \pm M$.

The intermediate states $|\mathbf{k}', S, M', T, T_3\rangle$ are not (and need not be) antisymmetrized. They may be expanded in terms of products of simple one-particle states. Each of these one-particle states has an energy which depends only on its total momentum magnitude, hence the matrix element in (6.19) is independent of (S, M', T, T_3) . Assuming $\mathbf{P}=0$, it is also independent of $\hat{\mathbf{k}}'$. In this case

$$\begin{aligned} \mathcal{E}(k') & = e^R, \quad k' < k_F \\ & = (e^N - e^R) e^R / e^N, \quad k' > k_F, \end{aligned} \quad (6.21)$$

⁴⁰ In this section we use $e^N = e$ to clearly distinguish the correct “nuclear” energies from the “reference” energies.

and the integral in (6.18) divides naturally into two regions, which we call the “Pauli” and “spectral” corrections. Also in this case

$$e^{R,N} = 2[T(k') + U^{R,N}(k') - T(k_0) - U^N(k_0)]. \quad (6.22)$$

The use of $U^N(k_0)$ for e^R is explained in Secs. 3 and 7. Then to find the statistical average of (6.16), it is sufficient to average over the quantity \mathfrak{F}_{S,T^M} .

The singlet-odd state is quite straightforward. $M'=0$, and

$$\begin{aligned} |\mathbf{k}', M'\rangle & = (4\pi)^{1/2} \sum_{\text{all } L} i^L (2L+1)^{1/2} \\ & \quad \times j_L(k'r) Y_L^0(\hat{\mathbf{k}}' \cdot \hat{\mathbf{r}}) \chi_0^0 \lambda_0^0, \end{aligned} \quad (6.23)$$

$$\begin{aligned} (1 - \Omega^R) |\phi_{0,0}^0\rangle & = \zeta_{0,0}^0 = (8\pi)^{1/2} (k_0 r)^{-1} \sum_{\text{odd } L} i^L (2L+1)^{1/2} \\ & \quad \times \chi_L Y_L^0(\hat{\mathbf{k}}_0 \cdot \hat{\mathbf{r}}) \chi_0^0 \lambda_0^0. \end{aligned} \quad (6.24)$$

The familiar addition theorem for spherical harmonics gives

$$\begin{aligned} & \langle \mathbf{k}', M' | (1 - \Omega^R) | \phi_{0,0}^0 \rangle \\ & = 4\pi \sum_{\text{odd } L} [8\pi(2L+1)]^{1/2} k_0^{-1} \int_0^\infty j_L(k'r) \\ & \quad \times \chi_L r dr Y_L^0(\hat{\mathbf{k}}' \cdot \hat{\mathbf{k}}_0), \end{aligned} \quad (6.25)$$

$$\begin{aligned} \mathfrak{F}_{0,0}^0(k') & = 2 \left(\frac{4\pi}{2\pi} \right)^3 \sum_{\text{odd } L} (2L+1) \\ & \quad \times \left[k_0^{-1} \int_0^\infty k'r j_L(k'r) \chi_L dr \right]^2. \end{aligned} \quad (6.26)$$

Note the occurrence of the factor 2. This has come from taking $|\phi\rangle$ to be antisymmetrized and $|\mathbf{k}'\rangle$ unsymmetrized. The same result would be obtained by taking $|\phi\rangle$ unsymmetrized, $= |ab\rangle$, computing $\langle ab | G(\) G | ab \rangle$ for given (S, M, T, T_3) , then finding the corresponding exchange term and subtracting.

For the triplet-even states we have

$$\begin{aligned} |\mathbf{k}', M'\rangle & = (4\pi)^{1/2} \sum_{\text{all } L} \sum_J i^L (2L+1)^{1/2} C(L1J; 0M'M') \\ & \quad \times j_L(k'r) |\mathcal{Y}_{L,J,k'}^M\rangle \lambda_0^0 \end{aligned} \quad (6.27)$$

$$= (4\pi)^{1/2} \sum_{\text{all } L} \sum_J f_{L,J,M'} j_L(k'r) |\mathcal{Y}_{L,J,k'}^M\rangle \lambda_0^0,$$

and

$$\begin{aligned} (1 - \Omega^R) |\phi_{1,0}^M\rangle & = \zeta_{1,0}^M = (8\pi)^{1/2} (k_0 r)^{-1} \\ & \quad \times \sum_{\text{even } L, L'} \sum_J f_{L,J,M} \chi_{L',J}^{(L)} |\mathcal{Y}_{L',J,k_0}^M\rangle \lambda_0^0. \end{aligned} \quad (6.28)$$

We have used (6.6), (6.10), and the obvious definition

$$\chi_{L',J}^{(L)} = \delta_{L,L'} \mathcal{J}_L - u_{L',J}^{(L)}. \quad (6.29)$$

The axes of quantization, \mathbf{k}_0 and \mathbf{k}' , are shown explicitly

for the total angular momentum eigenstates. Thus

$$\begin{aligned} \langle \mathbf{k}', M' | (1 - \Omega^R) | \phi_{1,0}^M \rangle &= 4\pi\sqrt{2} \sum_{\text{even } L, L'} \sum_J f_{L', J} M'^* f_{L, J} M \\ &\times \langle \mathcal{Y}_{L', J, \mathbf{k}'}^M | \mathcal{Y}_{L, J, \mathbf{k}_0}^M \rangle \\ &\times k_0^{-1} \int_0^\infty j_{L'}(k'r) \chi_{L', J}^{(L)} r dr. \end{aligned} \quad (6.30)$$

Note that

$$\begin{aligned} \langle \mathcal{Y}_{L', S', \mathbf{k}'^M} | \mathcal{Y}_{L, S, J, \mathbf{k}_0}^M \rangle &= \delta_{L, L'} \delta_{S, S'} \delta_{J, J'} \mathcal{D}_J^{M', M}(\hat{k}_0 \rightarrow \hat{k}'). \end{aligned} \quad (6.31)$$

We may regard (6.31) as a definition of the \mathcal{D} 's, which are called rotation matrices. Obviously one interpretation of the \mathcal{D} 's is that they describe the canonical transformations of total angular momentum eigenstates which arise from rotation of the coordinate system. Although the matrix elements conserve L , the resulting rotation matrices are L independent.⁴¹ Now we use the identity

$$\begin{aligned} \int d^2 \hat{k}' [\mathcal{D}_{J', \mu', \mu}(\hat{k}_0 \rightarrow \hat{k}')]^* \mathcal{D}_{J}^{M', M}(\hat{k}_0 \rightarrow \hat{k}') \\ = \delta_{\mu', M'} \delta_{\mu, M} \delta_{J', J} 4\pi (2J+1)^{-1} \end{aligned} \quad (6.32)$$

to write

$$\begin{aligned} (2\pi)^{-3} \int d^2 \hat{k}' k'^2 | \langle \mathbf{k}', M' | (1 - \Omega^R) | \phi_{1,0}^M \rangle |^2 \\ = 2(4\pi/2\pi)^3 \sum_{\text{even } L, L', L'', L'''} \sum_J (2J+1)^{-1} \\ \times f_{L''', J} M' f_{L'', J} M'^* f_{L', J} M'^* f_{L, J} M \\ \times \left[k_0^{-1} \int_0^\infty k'r j_{L'''}(k'r) \chi_{L''', J}^{(L''')} dr \right] \\ \times \left[k_0^{-1} \int_0^\infty k'r j_{L'}(k'r) \chi_{L', J}^{(L)} dr \right]. \end{aligned} \quad (6.33)$$

The sum over M and M' is now only a matter of applying the identity (6.12) twice.

$$\begin{aligned} \sum_M \langle \mathbf{k}', M' | (1 - \Omega^R) | \phi_{1,0}^M \rangle &= \sum_{M, M'} (2\pi)^{-3} \int d^2 \hat{k}' k'^2 | \langle \mathbf{k}', M' | (1 - \Omega^R) | \phi_{1,0}^M \rangle |^2 \\ &= 16 \sum_{\text{even } L, L'} \sum_J (2J+1) \\ &\times \left[k_0^{-1} \int_0^\infty k'r j_{L'}(k'r) \chi_{L', J}^{(L)} dr \right]^2. \end{aligned} \quad (6.34)$$

⁴¹ This, and the identity (6.31) are discussed in reference 39, Chap. 4 and Appendix II.

In view of the form of (6.26) and (6.34), it is convenient to define

$$F_L(k') = k_0^{-1} \int_0^\infty k'r j_L(k'r) \chi_L dr, \quad (6.35)$$

$$F_{L', J}^{(L)}(k') = k_0^{-1} \int_0^\infty k'r j_{L'}(k'r) \chi_{L', J}^{(L)} dr. \quad (6.36)$$

Then the desired statistical average of $\mathfrak{F}_{S, T}^M$ becomes simply

$$\begin{aligned} \mathfrak{F}(k')_{\text{spin average}} &= \frac{1}{16} \sum_{(S, M, T, T_3)} \mathfrak{F}_{S, T}^M(k') \\ &= \sum_{\text{odd } L} (2L+1) F_L^2(k') + 3 \sum_{\text{even } L} (2L+1) F_L^2(k') \\ &\quad + \sum_{\text{even } L, L'} \sum_J (2J+1) F_{L', J}^{(L)2}(k') \\ &\quad + 3 \sum_{\text{odd } L, L'} \sum_J (2J+1) F_{L', J}^{(L)2}(k'). \end{aligned} \quad (6.37)$$

Note that the F 's have the dimension [length]². F_0 is simply the Fourier sine transform of $k_0^{-1} \chi_0$. Continuity of χ_0 , and the fact that its first derivative is discontinuous, imply that $F_0 \sim k'^{-2}$ in the asymptotic region of large k' . All other F 's behave similarly because $k'r j_L(k'r)$ asymptotically approaches a sine wave.

The structure of (6.14a) and (6.37) is a reflection of the fact that when the center-of-mass momentum, \mathbf{P} , is zero, J is a good quantum number. Thus each of these quantities is a sum over separate terms for the scattering eigenstates belonging to each (S, T, J) . Because of this feature, it is also possible to introduce a Moszkowski-Scott separation in any of these (S, T, J) states without altering the formalism for the remaining states.

Of course, formulas (6.18), (6.21), and (6.37) are only valid when $\mathbf{P}=0$. There are three effects to consider when this is not true:

(1) The region of relative-momentum space excluded by the Q operator is no longer spherical. (Note that the region is not a displaced sphere, but has a “dumbbell” shape.) In the G^N-G^R calculation, the various J 's in each (S, T) state are coupled together.⁴²

(2) e^N is, in general, a function of \mathbf{P} , $\hat{\mathbf{P}} \cdot \hat{\mathbf{k}}_0$, and $\hat{\mathbf{P}} \cdot \hat{\mathbf{k}}'$, but e^R is unaffected.

(3) The volume of relative-momentum space excluded by the Q operator increases. The result is qualitatively the same as using a larger “effective k_F ” in (6.21).

Note that calculations with G^R are unaffected.

7. REFERENCE SPECTRUM PARAMETERS

Our goal is to achieve a sort of self-consistency for the reference spectrum. The choice of U^R should lead

⁴² See, for example, E. Werner, Nuclear Phys. **10**, 688 (1959).

to a U which is well approximated by the original U^R . This only needs to be true for $k_b > k_F$, as shown in the beginning of Sec. 3 where the reference spectrum is introduced. It turns out that there is a large quadratic term in $U(b)$ for $k_b \gg k_F$, as shown in Sec. 4, so that U indeed has approximately the form assumed in (3.2) for U^R . The quadratic term is easily combined with the kinetic energy by defining an effective mass, $m^* = M^*/M$. Then the reference spectrum may be written

$$\begin{aligned} U^R &= A_2 + Bk^2, \\ T(k) + Bk^2 &= T(k)/m^*. \end{aligned} \quad (7.1)$$

This form for U^R is valid for all k , by definition of the reference spectrum, but it approximates the actual $U(k)$ only for certain $k_b \gg k_F$, and in any case not for $k_m < k_F$. We now define, for simplicity, an *approximate* (not reference) spectrum E^0 for states in the Fermi sea, and we assume that the same effective mass m^* applies to this as to the reference spectrum, thus

$$U^0(m) = A_1 + Bk_m^2, \quad (7.2)$$

with the same B as in (7.1). The energy denominators e^R contain $U^R(b) - U^0(m)$ and hence

$$A_2 - A_1 \equiv (\hbar^2 k_F^2 / M m^*) \Delta. \quad (7.3)$$

Clearly the reference energy denominators e^R are determined by the two parameters Δ and m^* . Note the distinction between our approach and that of previous authors: We define m^* by the behavior of U for $k_b \gg k_F$, while the usual practice has been to do this for $k_m \lesssim k_F$.

The approximate potential energy, $U^0(m)$, is obviously not equal to the actual potential energy, $U(m)$, for states in the Fermi sea because of our assumption that B is the same for m states as for b states. However, we believe that this assumption is a fair approximation for several reasons: (1) Several previous works have shown that $U(m)$ is very nearly quadratic, and that the corresponding m^* is not too different from what we find below for the b states. (2) We are mainly interested in calculating $U(b)$, and although the energies $E(m)$ for particles in the sea enter the calculation of $U(b)$, they are less important than the reference energy $E^R(b)$, and, in addition, they enter only in an average manner. It is, of course, easy to make $U^0(m)$ exactly equal to $U(m)$ for an "average" state, which we may symbolize by \bar{m} . Assuming only that $U(m)$ is roughly quadratic in k_m , an "average" state is one whose momentum is given by $k_{\bar{m}}^2 = 0.6k_F^2$. In this case we need only assume that

$$A_1 = U(\bar{m}) - 0.6k_F^2 B, \quad (7.4)$$

and the detailed form of $U(m)$, i.e., the appropriate value of m^* for states in the Fermi sea, becomes unimportant for calculations of $U(b)$. (3) When we actually make the final and detailed calculation of $U(m)$, i.e., the G matrix elements involved in it, we are free to use the *exact* starting energy by substituting the correct values in (2.5), in effect associating a different value of

Δ with each state m ; therefore, we only need to use the reference energies for intermediate states above the sea. These three points are also the reasons why we have chosen to determine m^* from the behavior of U for reasonably large k_b rather than for $k_m \lesssim k_F$.

For the purpose of this exposition, we use the further two approximations

$$\begin{aligned} U(b) &\approx \sum_{k_n < k_F} \langle bn | G^R | bn - nb \rangle \\ &\approx \rho \langle \langle bn | G^R | bn - nb \rangle \rangle_{\text{spin average}}. \end{aligned} \quad (7.5)$$

The first near equality amounts to neglecting the difference $G^N - G^R$, while the second consists of multiplying an "average matrix element" by the number of states in the Fermi sea. Since the G -matrix elements have been multiplied by the volume, for convenience in passing to the limit of infinite volume, the "number of states" is replaced by the density, Eq. (4.20). To find the "average matrix element" we will average over all hole states, partly for simplicity and partly for the reasons given in Sec. 4. Referring to Fig. 4, we have seen that it is necessary to average over the states l and m , but to average over n is a new approximation. Both of these approximations in (7.5) are reasonable for $k_b \gg k_F$, but they would not be satisfactory for a calculation of $U(m)$. For a general orientation, however, it is useful to also begin the discussion of $U(m)$ with these same approximations. In this section we do not discuss Rajaraman's suggestion²⁶; that is we ignore the diagrams in Fig. 3.

To calculate $U(m)$ and $U(b)$, we must know γ_m^2 and γ_b^2 . As discussed in Sec. 4, these parameters are defined differently. The Goldstone diagram for the calculation of $\langle mn | G^R_2 | mn \rangle$ is shown in Fig. 9. (We have now added the subscript 2 to indicate that two particle-hole pairs are involved in the intermediate states.) Assuming (7.1), (7.2), and (7.3), the energy denominator at the level of intermediate states a, b is

$$\begin{aligned} e^{R_2} &= E^R(a) + E^R(b) - E^0(m) - E^0(n) \\ &= (m^*)^{-1} (k_{ab}^2 - k_{mn}^2 + 2\Delta k_F^2) \\ &= (m^*)^{-1} (\gamma_m^2 - \nabla^2), \end{aligned} \quad (7.6)$$

where

$$k_{ab}^2 \rightarrow -\nabla^2, \quad \gamma_m^2 = 2\Delta k_F^2 - k_0^2, \quad (7.7)$$

and

$$k_0^2 = k_{mn}^2 = \frac{1}{4} (k_m^2 + k_n^2 - 2\mathbf{k}_m \cdot \mathbf{k}_n). \quad (7.8)$$

For simplicity we average over k_n ; then the scalar product vanishes and $k_n^2 \rightarrow 0.6k_F^2$. This averaging is somewhat justified because often the dominant terms in U are quadratic functions of k , as seen, for example, from a power-series expansion of (5.34), our expression for $\langle G^R \rangle$ due to the core. Thus we use

$$k_0^2 = \frac{1}{4} (k_m^2 + 0.6k_F^2). \quad (7.9)$$

To calculate the average potential energy $U(\bar{m})$ we set $k_{\bar{m}}^2 = 0.6k_F^2$ so $\langle k_0^2 \rangle_{\text{av}} = 0.3k_F^2$. We note also that

$\langle P^2 \rangle_{av} = 0.3k_F^2$ for pairs of particles in the sea, but in this section we are consistently ignoring all $P \neq 0$ corrections since they may be considered as part of the $G^N - G^R$ correction (Sec. 6).

The corresponding diagram for $\langle bn|G_3^R|bn\rangle$, which determines $U(b)$, is shown in Fig. 4. At the level of intermediate states c, d ,

$$\begin{aligned} e^R_3 &= E^R(a) + E^R(c) + E^R(d) - E^0(l) - E^0(m) - E^0(n), \\ &= (m^*)^{-1}(k_{ab}^2 - k_{lm}^2 + k_{cd}^2 - k_{bn}^2 + 3\Delta k_F^2), \\ &= (m^*)^{-1}(\gamma_b^2 - \nabla^2), \end{aligned} \quad (7.10)$$

where

$$\begin{aligned} k_{cd}^2 &\rightarrow -\nabla^2, \\ \gamma_b^2 &= k_{ab}^2 - k_{bn}^2 - k_{lm}^2 + 3\Delta k_F^2, \end{aligned} \quad (7.11)$$

and the initial relative momentum is

$$k_0^2 = k_{bn}^2 \rightarrow \frac{1}{4}(k_b^2 + 0.6k_F^2). \quad (7.12)$$

Note that (7.12) is similar to (7.9), so k_0 is a continuous function of the single-particle momentum.

Clearly, (7.11) depends strongly on k_a which is given by (4.7). Inserting this into (7.11),

$$\begin{aligned} k_{ab}^2 - k_{bn}^2 - k_{lm}^2 &= \frac{3}{4}k_b^2 - \mathbf{k}_b \cdot (\mathbf{k}_l + \mathbf{k}_m - \frac{1}{2}\mathbf{k}_n) \\ &\quad + \mathbf{k}_l \cdot \mathbf{k}_m - \frac{1}{4}k_n^2. \end{aligned} \quad (7.13)$$

Averaging again over directions for l, m , and n , and finally over the magnitude of k_n , we get

$$\gamma_b^2 = 3\Delta k_F^2 + \frac{3}{4}k_b^2 - 0.15k_F^2 = 3k_0^2 + (3\Delta - 0.6)k_F^2. \quad (7.14)$$

This averaging is, of course, not really justified, especially if k_b is close to k_F . In this case the state a is more likely to be outside the Fermi sea if $\mathbf{k}_b \cdot (\mathbf{k}_l + \mathbf{k}_m)$ is negative, thus increasing (7.13) to a value greater than (7.14). Conversely, for large k_b , the matrix element $\langle ab|G|lm\rangle$, which in Fig. 4 creates the state b , will be larger if $k_a < k_b$. For “average” k_b ’s, i.e., those which give the greatest contribution to Fig. 8, (7.14) should be about right.

The first point to observe in (7.14) is the strong quadratic dependence of γ_b^2 on k_b . This leads, largely through the core-volume term in (5.14), to a large quadratic term in $U(b)$, and, therefore, to the term Bk_b^2 in (7.1). Thus the term $\frac{3}{4}k_b^2$ in (7.14) is the main reason why $m^* \neq 1$ even for large k_b . Secondly, we may compare (7.14) for $k_b = k_F + \epsilon$ with (7.7) and (7.9) for $k_m = k_F - \epsilon$ to see that

$$\gamma_b^2(k_F + \epsilon) - \gamma_m^2(k_F - \epsilon) = (1 + \Delta)k_F^2. \quad (7.15)$$

Therefore, γ^2 makes a considerable jump at the Fermi surface. This is due to the extra pair l, a which contributes to γ_b^2 . Brueckner expresses this by saying that G_3 is “off the energy shell,” while by definition, G_2 is “on the energy shell.” This jump in γ^2 in turn causes a jump in U , and thus it contributes in some measure to Δ . Since the jump (7.15) contains Δ as a major contribution, Δ is to some extent self-generating. To be

sure that this is not a circular argument, we must investigate the other contributions to Δ .

The Δ defined in (7.3) represents an “averaged” feature of $U(b)$. It is too much to expect that $U(b)$ has just the form assumed for $U^R(b)$ for all $k_b > k_F$. All we can hope to achieve is to have U^R approximate U in some range of k_b . Before discussing Δ , then, we must first determine the range of k_b for which it is most important that $U^R \approx U$.

The intermediate state energies are mainly needed in order to calculate the lowest order diagram, Fig. 1(a), or in other words to calculate $U(m)$. The criterion for determining the “important region” of k_b , then, is to obtain the best accuracy for $U(m)$, or more specifically to minimize the “Pauli” and “spectral” corrections of Sec. 6. If the “Pauli” correction turns out to be large, this may be held within bounds by means of an MS separation, as is shown in greater detail in Sec. 10, so that we should use the freedom of choice of $U^R(b)$ to minimize the “spectral” correction to $U(m)$.

We see then that according to Sec. 6, especially Eq. (6.37), the “important” range is determined by the statistical average of the square of (k' times the Fourier transform of ξ). For a pair of particles m, n in the Fermi sea, the relative momentum, $k_0 = \frac{1}{2}|\mathbf{k}_m - \mathbf{k}_n|$, is rather small, therefore only the S -state component of ξ_{mn} is important. Thus, we are mainly interested in

$$F_0(k') = k_0^{-1} \int_0^\infty \sin k' r \chi_0(r) dr. \quad (7.16)$$

Inside the core, $\chi_0 = \mathcal{J}_0 - u_0$ is large because $u_0 = 0$, and k_0 is small enough so that $\chi_0/k_0 \approx r$. Outside the core, χ_0 decreases rapidly, becoming very small beyond the healing distance of order γ_{mn}^{-1} , or beyond the MS separation distance. Therefore, χ_0 has approximately a triangular shape, peaking at $r = c$ (see Fig. 13). We expect then that the maximum of (7.16) as a function of k' occurs near that value of k' which makes the crest of the sine function come at the same point as the peak of the triangle, or

$$k_b \approx k_{ab} = k' \approx \pi/2c, \quad (7.17)$$

because k' corresponds to the relative momentum of the intermediate state in Fig. 9. Assuming $c = 0.4 F$, this gives $k_b \approx 4 F^{-1} \approx 2.6k_F$. Further calculations, which include the D -wave part of the 3S_1 (deuteron) state, bear this out.

We thus try to choose A_2 and B in (7.1) in such a way as to approximate $U(b)$ near $k_b = 2.6k_F$, or in the range, say, of $2k_F$ to $4k_F$. [$U(b)$ is bound to deviate from the reference spectrum form for $k_b \gtrsim 2k_F$, due to the importance of second MBA terms, to the “Serber effect,” as is explained below, and to the breakdown of the approximations in (7.5).] These are rather large momenta, and the main contribution to $\langle bn|G|bn\rangle$ comes from the core terms, (5.34). These core terms are well represented by the quadratic form assumed for the

reference spectrum, and this is an important reason for our confidence in this method.

Now to return to the question posed above concerning the various sources of Δ . One source is the core term (5.34) which has a jump at k_F because of the jump of γ^2 , (7.15). This term which is due to "going off the energy shell" has been found to contribute only about 20% of the total Δ so that there is no real problem from the "positive feedback" of Δ onto itself. The major part (80%) of Δ arises from the outer, mostly attractive, potential and it is sufficient, for an understanding of Δ , to treat this by the MBA expansion of Sec. 5. We begin with the first MBA terms.

Let us consider a hypothetical case where $v=v$ (outer) only, i.e., $v=0$ for $r < c$, and where v is a central Serber force (interaction in even states only) with, say, a Yukawa shape with the range appropriate for the exchange of two pions (TPEP). We may use (5.30) to find the sum of the (conventional) first Born terms for all L 's.

$$\begin{aligned} \sum_{\text{even } L} (2L+1) \int_c^\infty V_0(\mu r)^{-1} e^{-\mu r} j_L^2(k_0 r) r^2 dr \\ = \frac{1}{2} V_0 \int_c^\infty (\mu r)^{-1} e^{-\mu r} [1 + j_0(2k_0 r)] r^2 dr. \end{aligned} \quad (7.18)$$

When both members of an interacting pair of particles are in the Fermi sea, k_0 is small enough so that $j_0(2k_0 r)$ is large within the range of the force. The interaction occurs mostly through the S state, and the Serber character of the potential is not very evident. But for $k_b \gg k_F$, $j_0(2k_0 r) \approx 0$ and the first Born terms are considerably decreased. For example, with the Gammel-Thaler potential discussed in Sec. 8 the first Born terms in U would be roughly 2/3 as large for high k_b 's as for an average state in the Fermi sea. We may call this decrease the "Serber effect." As k_0 increases, the

Serber effect rapidly "saturates" to simply give a factor of 1/2 for a Serber force as compared to an ordinary nonexchange force. This "saturation" is essentially complete for $k_b \gtrsim 2.0k_F$ (see Table I in Sec. 8). It might seem that this is the major source of Δ , but such is not the case. In nuclear matter, the Serber effect is very nearly compensated by the effect of the core on the wave function, that is, the effect of replacing \mathcal{J}_L by $\mathcal{J}_L - \mathcal{J}\mathcal{C}_L$ in the modified Born approximation. The effect of the hard core in the case of a weak outer potential (first MBA) is to make the wave function vanish at $r=c$, and to approach the free-particle wave function roughly exponentially, with decay constant γ . Thus a small value of γ greatly reduces the wave function in the region where the outer potential is strongest, while, on the other hand, this effect vanishes as $\gamma \rightarrow \infty$.

We briefly describe a method we have used to estimate this effect. The object is to replace $H_L^{(-)}$ by a simple exponential with a suitable average inverse range $\bar{\gamma}$ chosen to be the same for all L 's. As discussed in Sec. 5, the WKB method gives

$$(d/dr) \ln H_L^{(-)}(\gamma r) \approx -\gamma [1 + L(L+1)/(\gamma r)^2]^{1/2}. \quad (7.19)$$

Now we use (5.20) and (5.16) to define a suitable average value of L ,

$$\langle L(L+1) \rangle_{\text{av}} = \frac{2}{3} (k_0 r)^2. \quad (7.20)$$

Inserting this in (7.19) we obtain

$$\begin{aligned} \bar{\gamma} &\equiv \gamma [1 + \langle L(L+1) \rangle_{\text{av}} / (\gamma r)^2]^{1/2} \\ &= \gamma [1 + \frac{2}{3} (k_0/\gamma)^2]^{1/2}. \end{aligned} \quad (7.21)$$

Note that the resulting $\bar{\gamma}$ is independent of r . For any particular L , increasing r decreases the effective γ_L . However, increasing r shifts the weighted average of L toward larger L 's. Thus to take account of the core wave function effect, we replace the factor of $\frac{1}{2}[1+j_0]$ in (7.18) by the kernel

$$\begin{aligned} K_1^{(+)}(r) &\equiv \sum_{\text{even } L} (2L+1)(k_0 r)^{-2} (\mathcal{J}_L - \mathcal{J}\mathcal{C}_L)^2 \approx \sum_{\text{even } L} (2L+1) \{ j_L(k_0 r) - j_L(k_0 c) (c/r) \exp[-\bar{\gamma}(r-c)] \}^2 \\ &= \frac{1}{2} [1 + j_0(2k_0 r)] - (c/r) \exp[-\bar{\gamma}(r-c)] \{ j_0[k_0(r-c)] + j_0[k_0(r+c)] \} \\ &\quad + \frac{1}{2} (c/r)^2 \exp[-2\bar{\gamma}(r-c)] [1 + j_0(2k_0 c)]. \end{aligned} \quad (7.22)$$

By making a few fairly obvious approximations, one may obtain analytic results for exponential and Yukawa potentials. In this way we estimate that for the case of the Gammel-Thaler potential, first MBA terms contribute only about 10% of the total value of Δ , due to a near cancellation between the "Serber" and the " $\mathcal{J}-\mathcal{J}\mathcal{C}$ " effects.

This leaves, as the main contribution to Δ , the second and higher MBA terms. These depend strongly on the momentum. It is well known that in free-particle scattering, the ratio of higher Born terms to first Born decreases with increasing k_0 . This decrease is stronger within nuclear matter since the scattering is now off the

energy shell by a rapidly increasing amount, $(k_0^2 + \gamma^2)$. On the other hand, the second MBA is reduced even for states within the sea by γ_m and, in addition, the second MBA term in Δ contains a factor m^{*2} . One factor of m^* comes from the definition of Δ , (7.3), the other is contained in the second MBA, as we show below. These two effects make the second MBA contribution to $U(\bar{m})$ only of order -20 MeV for a purely central potential, such as assumed by Moszkowski and Scott (Sec. 9). Even if the corresponding quantity for $U(b)$ is reduced by a large factor, the resulting contribution to Δ would be quite small. On the other hand, a tensor force leads to much larger second Born terms.

Indeed, the first-order effect of the tensor force is zero—the binding energy of the deuteron, for example, arises mostly from the second (and higher) orders of the tensor force. We conclude that the strong tensor force in triplet-even states is one of the main sources of Δ . This suggests that actual calculations with nuclear matter should be quite sensitive to the relative amounts of central and tensor force in the triplet-even states.⁴³

Having discussed the origin of Δ , we now consider the consequences of the fact that $m^* < 1$. An elementary discussion of this was given in Sec. 4. In Secs. 5 and 6, we only treated the case where $m^* = 1$. Actually, the effective potential that enters everywhere in these sections should be m^*v , as seen from Eq. (3.10). We recall that we decided to leave the factor \hbar^2/M understood in all energy quantities. Now the corresponding factor is \hbar^2/Mm^* , or in terms of our original convention we should make the replacement

$$\begin{aligned} \langle\phi|G(m^*=1)|\phi\rangle &= \langle\phi|v|\psi(m^*=1)\rangle \rightarrow \\ (m^*)^{-1}\langle\phi|m^*v|\psi(m^*)\rangle. \end{aligned} \quad (7.23)$$

The pure core wave function is not altered by m^* , either inside or beyond the core (for a given γ). The quantity $m^*\psi$, as defined in the core interior by the differential equation (3.10), is similarly unaffected by m^* . The result is that the entire core term (5.34) is simply increased by the factor $(m^*)^{-1}$, as was also shown in Sec. 4, Eq. (4.17). The differential equation, (3.10), shows that the outer portion of ψ deviates less strongly from the pure core wave function when $m^* < 1$. In first MBA, it is assumed that ψ is just the pure core wave function. Then the m^* factors in the right-hand side of (7.23) cancel, and the first MBA is independent of m^* . A glance at (5.38), which defines the MBA expansion, shows, however, that higher order MBA terms contain increasing powers of m^* . To summarize then, the core term scales as $(m^*)^{-1}$, the first MBA term is unchanged, while the second MBA scales as m^* , third MBA as m^{*2} , etc.

This has an interesting and important result. The second MBA term is attractive, while the core term is repulsive. Both terms vary so as to make the G -matrix element more repulsive as m^* decreases. From the elementary discussion in Sec. 4, we see that $1-m^*$ must be roughly proportional to the density. As the density increases beyond its equilibrium value, the binding energy per particle must decrease and eventually become negative. According to this simplified picture (since only low-order diagrams are being considered) the core repulsion increases rapidly and becomes infinite for a rather modest value of ρ . This comes about entirely from the action of the core, although the detailed mechanism is somewhat involved. It is a two-stage process, where the core first leads to a large quadratic term in $U(b)$ because the appropriate matrix ele-

ments are far off the energy shell, and secondly, the resulting m^* increases the repulsive core contribution to $U(m)$ and therefore to the binding energy. This demonstrates two things. It has often been stated that the hard core is important in understanding saturation, since obviously the classical picture of a box of nucleons with the cores all touching would require infinite energy.⁴⁴ Numerical calculations with various core radii have shown that larger cores do in fact lead to saturation at a lower density. We have shown this by an explicit qualitative argument. Secondly, we have shown that the use of proper single-particle energies for states above the Fermi sea, or alternatively, the calculation of certain higher order diagrams, is not merely an added refinement but is quite necessary for an understanding of the basic features of nuclear matter.

We conclude that saturation is due to a combination of effects from the hard core, the Serber character of the outer potential, and the strong tensor force in triplet-even states. The core is ultimately responsible, but the rapid weakening of the tensor contribution as density increases (due to m^*) leads to saturation at a lower density than would be obtained with purely central forces. The Serber and tensor force effects lead to a large Δ and thus they justify the reference spectrum approach. Thanks to this large Δ , the Pauli exclusion operator, Q , is not needed to prevent real scattering, or even to provide the small healing distance. The “Pauli correction” due to Q is not negligible⁴⁵ but it no longer has any fundamental role in the process of saturation when the reference spectrum is used. A more careful study of the saturation process is in preparation and will be published separately.

8. ENERGY SPECTRUM FOR THE GAMMEL-THALER POTENTIAL

As an illustration of our general method, we estimate the “nuclear spectrum” and the associated “reference spectrum” for the version of the Gammel-Thaler potential used by Brueckner and Gammel.⁴⁶ This was chosen both for its analytical simplicity and to obtain a comparison with the IBM calculation of Brueckner and Gammel. In a detailed nuclear matter calculation the procedure would be to choose some values for Δ and m^* , calculate $U(m)$ and $U(b)$, approximate these by improved values of Δ and m^* , and iterate to achieve approximate self-consistency. The following estimates

⁴⁴ Gomez, Walecka and Weisskopf, reference 22. These authors did not anticipate such a strong saturation effect from the core, because they were unable to show how m^* varies with ρ .

⁴⁵ The Pauli correction is large enough so that for accurate calculations it must be included, and perhaps the modified Moszkowski-Scott separation technique of Sec. 10 may be necessary. However, it is small enough to be ignored in many qualitative arguments.

⁴⁶ Reference 4. See also the review articles by J. L. Gammel and R. M. Thaler, in *Progress in Elementary Particle and Cosmic Ray Physics* (North Holland Publishing Company, Amsterdam, 1960), Vol. 5, p. 99; and J. S. Bell and E. J. Squires, in *Advances in Physics*, edited by N. F. Mott (Taylor and Francis, Ltd., London, 1961), Vol. 10, p. 211, for comments on the validity of this potential.

⁴³ This was found, for example, by S. A. Moszkowski and B. L. Scott, *Ann. Phys. (New York)* 14, 107 (1961).

could be used, for example, in the first iteration, subject to the important correction due to Rajaraman, mentioned in Sec. 4.

It is a great simplification to assume that both the theory and the two-nucleon potential are valid, and then use the *observed* binding energy per nucleon to obtain $U(\bar{m})$. For the present, we take the "observed" nuclear matter parameters to be $B.E./A = 15.5$ MeV, $k_F = 1.5$ F⁻¹. Then

$$\begin{aligned} \bar{T} + \frac{1}{2}\bar{U} &= -15.5 \text{ MeV}, \\ \bar{T} &= 0.3\hbar^2 k_F^2 M^{-1} = 28.0 \text{ MeV}, \\ \bar{U} &= U(\bar{m}) = -87.0 \text{ MeV}, \\ \bar{E} &= \bar{T} + \bar{U} = -59.0 \text{ MeV} \\ &= A_1 + \bar{T} m^{*-1}. \end{aligned} \quad (8.1)$$

This argument is due to Weisskopf.⁴⁷ It has the advantage of being independent of the form assumed for the two-nucleon interaction.

In order to proceed, we must assume a value for Δ . Let $\Delta = 0.75$. Then the core contribution to $U(b)$ is easily calculated from (7.12), (7.14), and (5.34). In the approximation (7.5), this is multiplied by ρ . The result is shown in Fig. 10, for $c = 0.4$ F and $m^* = 1$, since the actual value of the core term differs only by the factor m^{*-1} . The result is remarkably well fit by the quadratic form

$$U_{\text{core}}(b) = (1/m^*)(A_c + B_c k_b^2). \quad (8.2)$$

Fitting this to the curve in Fig. 10 at the points $k_b = 1.5k_F$, $3.5k_F$, one obtains $A_c = 81.5$ MeV, $B_c = 4.74$ MeV-F². Deviations from this quadratic form over the region $k_b = k_F$ to $4k_F$ are $\lesssim 2\%$. Formally we should allow for the possibility that m^* may include a term from the outer contribution to $U(b)$, but actually this outer contribution to m^* is negligible for the Gammel-Thaler potential. Matching the coefficients of k_b^2 in

$$\frac{\hbar^2 k_b^2}{2M} \left(\frac{1}{m^*} - 1 \right) = \frac{B_c k_b^2}{m^*} \quad (8.3)$$

leads to $m^* = 0.77$. The quantity $(1-m^*)$ differs from its asymptotic value (end of Sec. 4) by about a factor of 2. The fractional amounts of the various contributions to $1-m^*$ mentioned in Sec. 4 are roughly: core volume, $\frac{1}{2}$; boundary terms, $\frac{3}{8}$; statistical weights, $\frac{1}{8}$.

In Fig. 10 we also show the results of considering only even angular momenta in the core term. The methods of Sec. 5 give as the analog of (5.34):

$$\begin{aligned} \langle k_0 | G^R | k_0 \rangle_{\text{core, spin average, even states}} &= 4\pi c \left\{ \frac{1}{8}(x^2 + y^2) \right. \\ &\quad + \frac{3}{16}[(y^2/x^2) - 1]xj_1(2x) + \frac{3}{8}(1+y)[1+j_0(2x)] \\ &\quad \left. + (1+y)^{-1}[\frac{1}{8}x^2 - \frac{3}{16}xj_1(2x)] \right\}. \quad (8.4) \end{aligned}$$

It is apparent that when the core volume terms are included, odd angular momenta must not be neglected (as was done in the calculation of Brueckner and

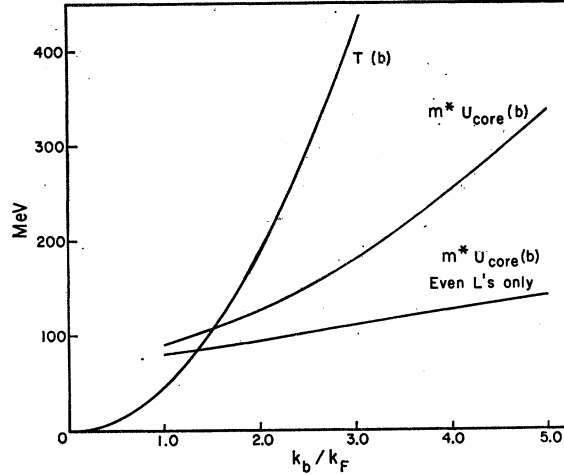


FIG. 10. Core contribution to the potential energy of intermediate states. Results are shown for all angular momenta, Eq. (5.34) and for even angular momenta only, Eq. (8.4). These results must be divided by m^* to obtain the correct values. The kinetic energy is shown for comparison.

Gammel). The result for even L alone is linear in k , not quadratic, so the effective mass concept is not so useful. Most of our quadratic core term, B_c , in the important region of k_b , is due to P states.

Our estimate of the outer potential term in $U(b)$ closely follows the discussion of the first MBA term in Sec. 7. In the asymptotic limit of large k_b , higher terms in the Born series may be neglected and the core wave function correction, the \mathcal{C} in $u_{(0)} = \mathcal{J} - \mathcal{C}$, vanishes so that $\text{MBA} \rightarrow$ ordinary first Born approximation. Because higher Born terms vanish in this asymptotic limit, tensor and spin-orbit forces contribute nothing, thanks to the identities,

$$\sum_{J=|L-S|}^{L+S} (2J+1) \left\langle LSJ \left| \left\{ \begin{array}{c} \mathbf{L} \cdot \mathbf{S} \\ S_{12} \end{array} \right\} \right| LSJ \right\rangle = 0. \quad (8.5)$$

Our first approximation to the outer term is, therefore,

$$U_{\text{out}}(k_b \rightarrow \infty)$$

$$\begin{aligned} &= 4\pi\rho \int_c^\infty (\frac{1}{16}{}^1V_c - + \frac{3}{16}{}^1V_c + + \frac{3}{16}{}^3V_c + + \frac{9}{16}{}^3V_c -) r^2 dr \\ &\equiv {}^1E^- + {}^1E^+ + {}^3E^+ + {}^3E^-. \end{aligned} \quad (8.6)$$

The Gammel-Thaler results are

$$\begin{aligned} {}^1E^- &= 21.8 \text{ MeV}, \quad {}^1E^+ = -67.7 \text{ MeV}, \\ {}^3E^+ &= -41.2 \text{ MeV}, \quad {}^3E^- = -21.2 \text{ MeV}. \end{aligned}$$

Note that the odd-parity terms are small and have opposite signs. This is a justification for the often-used Serber potential model for the nuclear force. The almost perfect cancellation, however, is a special feature of the Gammel-Thaler potential.

⁴⁷ V. Weisskopf, Nuclear Phys. 3, 423 (1957).

TABLE I. Parameters for the calculation of $U(b)$, as explained in Sec. 8. $R_1^{(+)}=1+\delta R_s-\delta R_c$.

k_b/k_F	$k_0 c$	γc	$\bar{\gamma} c$	δR_s	δR_c	$R_1^{(+)}$	$\bar{\gamma}_{Tc}$	$(\bar{\gamma}_{Tc} + {}^3\mu_T{}^+ c)^{-2}$
1.0	0.380	1.013	1.060	0.353	0.439	0.914	1.282	0.346
1.5	0.507	1.168	1.239	0.201	0.371	0.830	1.434	0.291
2.0	0.643	1.355	1.453	0.101	0.306	0.795	1.623	0.240
2.5	0.785	1.563	1.689	0.040	0.248	0.792	1.837	0.197
3.0	0.930	1.785	1.940	0.005	0.201	0.804	2.070	0.161
3.5	1.076	2.016	2.199	-0.015	0.162	0.823	2.314	0.134
4.0	1.222	2.253	2.464	-0.025	0.131	0.844	2.568	0.112
4.5	1.370	2.495	2.734	-0.028	0.108	0.864	2.828	0.095
5.0	1.518	2.740	3.007	-0.027	0.091	0.882	3.093	0.081

Apart from (7.5), there are 3 approximations to correct for in (8.6), namely, the neglect of higher MBA terms, and the Serber and core-wave-function effects at finite k_b . The small term ${}^1E^- + {}^3E^-$ is ignored, and the latter two corrections to ${}^1E^+ + {}^3E^+ = -108.9$ MeV are given by the factor

$$R_1^{(+)} = \left[\int_c^\infty K_1^{(+)}(r) ({}^1V_c^+ + {}^3V_c^+) r^2 dr \right] / \left[\frac{1}{2} \int_c^\infty ({}^1V_c^+ + {}^3V_c^+) r^2 dr \right], \quad (8.7)$$

in which $K_1^{(+)}(r)$ is approximated by (7.22). The resulting $R_1^{(+)}$ for a single Yukawa potential is roughly linear in the inverse range, so for simplicity we replace $({}^1V_c^+ + {}^3V_c^+)$ by a single Yukawa form with the weighted average $\bar{\mu} = 1.69$ F⁻¹. The Serber and core corrections vary with k in opposite directions, with the result that $R_1^{(+)}$ is nearly independent of k_b . This is shown in Table I. The notation there is $R_1^{(+)} = 1 + \delta R_s - \delta R_c$, where δR_s comes from the j_0 term in the first square bracket of (7.22), i.e., the Serber correction with core correction ignored, and δR_c comes from the exponential terms in (7.22), the core correction including the full Serber effect. $\bar{\gamma}$ is the average given by (7.21). This parameter is used both for the core correction and for the central force second MBA terms discussed below. The small difference between $\bar{\gamma}$ and γ suggests that this method of approximating the effect of \mathcal{J}_L is probably quite accurate.

The same methods may be applied to the second MBA terms. First we note that (8.5) and

$$\sum_{J=|L-S|}^{L+S} (2J+1) \langle LSJ | (\mathbf{L} \cdot \mathbf{S}) S_{12} | LSJ \rangle = 0 \quad (8.8)$$

imply that in second MBA the effects of central, tensor, and spin-orbit forces are uncoupled and may be treated independently. We first discuss the second MBA expression for the singlet-even central force,

which is

$${}^1(2^{\text{nd}}MBA)_c^+ = \frac{3}{8} 4\pi\rho M m^* \hbar^{-2} \int_c^\infty {}^1V_c^+(r) dr \int_c^\infty {}^1V_c^+(r') dr' \\ \times k_0^{-2} \sum_{\text{even } L} (2L+1) [\mathcal{J}_L(r) - \mathcal{J}\mathcal{C}_L(r)] \\ \times \mathcal{G}_L(r|r') [\mathcal{J}_L(r') - \mathcal{J}\mathcal{C}_L(r')], \quad (8.9)$$

where \mathcal{G}_L is the Green's function defined in (5.39). The procedure is quite analogous to our treatment of the first MBA. Considering the asymptotic limit of the Serber effect and neglecting the core correction, i.e., the $\mathcal{J}\mathcal{C}_L$ terms, we make the replacement

$$k_0^{-2} \sum_{\text{even } L} (2L+1) [\mathcal{J}_L(r) - \mathcal{J}\mathcal{C}_L(r)] \mathcal{G}_L(r|r') \\ \times [\mathcal{J}_L(r') - \mathcal{J}\mathcal{C}_L(r')] \rightarrow \frac{1}{2} rr' \mathcal{G}_{av}(r|r'), \quad (8.10)$$

by means of Eq. (5.30). In order to define the “average Green's function,” \mathcal{G}_{av} , we return to (5.39) which expresses \mathcal{G}_L in terms of $H_L^{(\pm)}(\gamma r)$ and use a more careful WKB estimate than the simple exponential assumed for $\mathcal{J}\mathcal{C}_L$, viz.,

$$H_L^{(\pm)}(\gamma r) \approx [1 + L(L+1)/(\gamma r)^2]^{-1/4} \\ \times \exp\{\pm \gamma r [1 + L(L+1)/(\gamma r)^2]\}. \quad (8.11)$$

Then the L 's are averaged as before to obtain

$$\langle H_L^{(\pm)}(\gamma r) \rangle_{av} \approx (\bar{\gamma}/\gamma)^{-1/2} \exp(\pm \bar{\gamma}r), \quad (8.12)$$

where $\bar{\gamma}$ is given again by (7.21). The resulting expression for \mathcal{G}_{av} is the same as \mathcal{G}_0 , with γ replaced everywhere by $\bar{\gamma}$.

$$\mathcal{G}_{av}(r|r') \\ = (2\bar{\gamma})^{-1} \{ \exp[-\bar{\gamma}(r-c)] \exp[-\bar{\gamma}(r'-c)] \\ - \exp[\bar{\gamma}(r_c - r')]\}. \quad (8.13)$$

With (8.10) and (8.13) the double integral in (8.9) becomes elementary. This procedure is easily modified for the other terms in the Gammel-Thaler potential. For the triplet-even central force, (8.9) is directly applicable. The singlet-odd central force requires a statistical weight factor of 1/8 instead of 3/8, and the triplet-odd central force requires 9/8 [see Eq. (6.14b)].

In the case of the triplet-even tensor force, the quantity

$$\sum_{J=|L-S|}^{L+S} (2J+1) |\langle LSJ | 1 | LSJ \rangle|^2 g_L = 3(2L+1) g_L, \quad (8.14)$$

which arises in the central force calculation, is replaced by

$$\begin{aligned} & \sum_{J=|L-S|}^{L+S} (2J+1) [|\langle LSJ | S_{12} | LSJ \rangle|^2 g_L] \\ & + (1-\delta_{LJ}) |\langle L'=2J-L, SJ | S_{12} | LSJ \rangle|^2 g_{L'} \\ & \approx \sum_{J=|L-S|}^{L+S} (2J+1) [|\langle LSJ | S_{12} | LSJ \rangle|^2 \\ & + (1-\delta_{LJ}) |\langle L'=2J-L, SJ | S_{12} | LSJ \rangle|^2] g_{av,T} \\ & = 24(2L+1) g_{av,T} \end{aligned} \quad (8.15)$$

The tensor force thus requires an additional factor of 8 compared to (8.9), this being the expectation value of S_{12}^2 . [The factor of 3 in (8.14) is included in (8.9) in the statistical weight factor of 3/8.] Equation (8.15) suggests that a different sort of averaged Green's function, $g_{av,T}$, is required for the tensor force. The identity

$$\begin{aligned} & \sum_{J=|L-S|}^{L+S} (2J+1) [|\langle LSJ | S_{12} | LSJ \rangle|^2 L(L+1) \\ & + (1-\delta_{LJ}) |\langle L'=2J-L, SJ | S_{12} | LSJ \rangle|^2 L'(L'+1)] \\ & = 24(2L+1)[L(L+1)+6], \end{aligned} \quad (8.16)$$

together with (5.16), (5.20), and the identity in (8.15), leads to

$$\langle L(L+1) \rangle_{av,T} = 6 + \frac{2}{3}(k_0 \bar{r})^2. \quad (8.17)$$

We use $c+\mu^{-1}$ for \bar{r} , where μ is the inverse range, 1.05 F⁻¹ for the triplet-even tensor force. The resulting $g_{av,T}$ is formally the same as before, but with \bar{r} replaced by

$$\bar{r}_T = \gamma \left[1 + \frac{2}{3} \left(\frac{k_0}{\gamma} \right)^2 + \frac{6}{\gamma^2(c+\mu^{-1})^2} \right]^{1/2} \quad (8.18)$$

Numerical values of \bar{r}_T are listed in Table I. It is easy to see that these modifications are correct in the limit $k_0 \rightarrow 0$. Then the only term in the sum over L and J is the deuteron state. This contains a factor of 8 from the square of the S_{12} matrix element, and $L(L+1)=6$ for the relevant D -state Green's function.

For the spin-orbit forces, we use the identity

$$\begin{aligned} & \sum_{J=|L-S|}^{L+S} (2J+1) |\langle LSJ | (\mathbf{L} \cdot \mathbf{S}) | LSJ \rangle|^2 \\ & = 2(2L+1)L(L+1). \end{aligned} \quad (8.19)$$

It is simpler to modify the above procedure to take advantage of the fact that the ${}^3V_{L,S^+}$ and ${}^3V_{L,S^-}$ are not too different in the Gammel-Thaler potential. (Actually ${}^3V_{L,S^+} \approx \frac{2}{3} {}^3V_{L,S^-}$.) Now we observe two features. The first is that thanks to the very short range, ($\mu=3.7$ F⁻¹ in both cases), even at the large values of k_0 important in $U(b)$ the spin-orbit interaction occurs mostly in the P states. At $k_b=2.6k_F$, D states contribute roughly 10% as much as P states, if the different statistical weights of P and D states are ignored by simply comparing $(2L+1)j_L^2(k_0 r)$. The second feature to note is that $\frac{2}{3}L(L+1) \times 3$ for P states is the same as $\frac{2}{3}L(L+1)$ for D states, the result being 4 in both cases. Thus we multiply (8.9) by 4, sum over all L 's, and subtract the S -state term explicitly. A weighted average strength of 97% of ${}^3V_{L,S^-}$ is used to allow for the small amount of D -state interaction. This treats S , P , and D states properly. Higher L 's are underestimated, but they are small and there is some evidence that a smaller ${}^3V_{L,S^-}$ should be used in F states anyway.⁴⁸

Results for all except the spin-orbit force may be expressed, for $k_b=2.6k_F$, as

$$\begin{aligned} & (2^{\text{nd}} \text{ MBA})_{c,T} \\ & = -m^* [R_2^{(+)} ({}^3V_{1T^+} + {}^1V_{c^+} + {}^3V_{2.5c^+}) \\ & + R_2^{(-)} ({}^3V_{1T^-} + {}^1V_{c^-} + {}^3V_{0.1c^-})] \text{ MeV.} \end{aligned} \quad (8.20)$$

Each term is labeled, by standard notation, to show the type of force from which it originates; the large numbers giving the energy in MeV. The R_2 factors are the analogs of R_1 , incorporating the core and Serber corrections. Since all terms are much smaller than the first MBA, it is reasonable, in addition to neglecting higher MBA terms, to make further approximations in calculating the R_2 's. The tensor terms are roughly 2.5 times as large as the central terms. To see how (8.20) scales with k_b , we lump all the terms together with ${}^3V_{T^+}$. Then we notice that the mean value of r which enters most prominently in the evaluation of $R_2^{(+)}$ is not very different from that for $R_1^{(+)}$. g_{av} by itself makes the second MBA wave function vanish at $r=c$, and so one might expect \bar{r} to be larger and hence the core correction to be smaller than for the first MBA. This is largely compensated by the fact that there are now two factors of $V(r)$ which reduce the weight of large r 's in the double integral of (8.9). It is a reasonable approximation then to replace $R_2^{(+)}$ by $R_1^{(+)}$. In addition, we find from the double integral that second MBA terms scale as $(\gamma+\mu)^{-2}$, when (8.10) is used. (Compare this with the discussion of the second MBA in Sec. 5.)

⁴⁸ R. A. Bryan, Nuovo Cimento **16**, 895 (1960); T. Hamada, Progr. Theoret. Phys. **24**, 1033 (1960); G. Breit (private communication).

TABLE II. Contributions (in MeV) to $U(b)$. U_1 and U_2 are the first and second MBA terms. The spin-orbit contribution in second MBA is listed separately as $U_2^{L,S}$. $U_{out} = U_1 + U_2^{S,T} + U_2^{L,S}$, and $U = U_{out} + U_{core}$. U^R , the best quadratic fit to U , is given by (7.1), (8.3), and (8.22) as $A_2 + [(m^*)^{-1} - 1]T(b)$, for $A_2 = -5.5$ MeV and $m^* = 0.77$.

k_b/k_F	$-U_1$	$-U_2^{C,T}$	$-U_2^{L,S}$	$-U_{out}$	U_{core}	U	U^R	$U - U^R$
1.0	99.5	30.5	3.9	133.9	117.5	-16.4	8.3	-24.7
1.5	90.4	23.3	6.1	119.8	136.7	16.9	25.6	-8.7
2.0	86.6	18.4	8.3	113.3	162.4	49.1	49.8	-0.7
2.5	86.2	15.0	10.0	111.2	194.2	83.0	80.9	2.1
3.0	87.5	12.5	10.7	110.7	231.8	121.1	118.9	2.2
3.5	89.6	10.6	10.9	111.1	274.9	163.8	163.8	0
4.0	91.9	9.1	10.7	111.7	323.3	211.6	215.6	-4.0
4.5	94.1	7.9	10.1	112.1	376.6	264.5	274.3	-9.8
5.0	96.1	6.9	9.1	112.1	434.5	322.4	340.0	-17.6

Finally then,

$$(2^{\text{nd}} \text{ MBA})_{C,T} \approx -m^* R_1^{(+)}(k_b) \times \left[\frac{\bar{\gamma}_T(2.6k_F) + {}^3\mu_T^+}{\bar{\gamma}_T(k_b) + {}^3\mu_T^+} \right]^2 \times 23.6 \text{ MeV.} \quad (8.21)$$

Results are shown in Table II and Fig. 11.

Referring to (7.1) and (8.1), and using $m^* = 0.77$, we find

$$A_2 = A_c/m^* + U_{out}(k_b = 2.6k_F) = -5.5 \text{ MeV,} \quad (8.22)$$

$$A_1 = \bar{E} - \bar{T}/m^* = -95.3 \text{ MeV,} \quad (8.23)$$

$$\Delta = (m^* M/h^2 k_F^2)(A_2 - A_1) = 0.743. \quad (8.24)$$

We conclude that $\Delta = 0.75$ leads to self-consistency within the accuracy of our estimates.

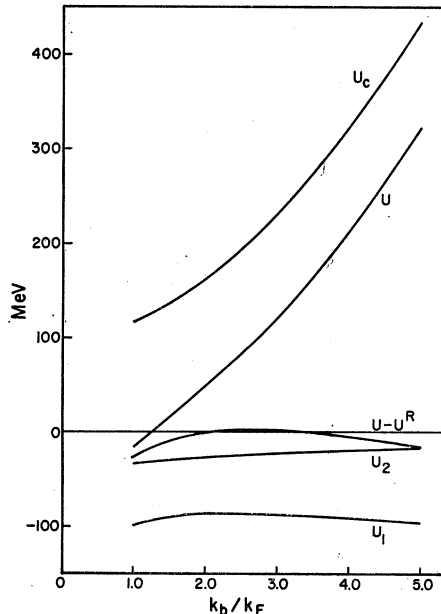


FIG. 11. Contributions to the “nuclear” potential for intermediate states $U(b)$. U_1 , U_2 , U_c , and U are the first MBA, second MBA, core, and total potentials, respectively. The difference between “nuclear” and “reference” potentials is also shown, where U^R is determined by $A_2 = -5.5$ MeV, $m^* = 0.77$.

There are two rather unexpected cancellations illustrated in Table II and Fig. 11. First, the various terms in U_{out} combine to give a result which is almost independent of k_b , and, second, the constant terms in U_{core} and U_{out} combine to give a very small A_2 , so that the total $U(b)$ can be qualitatively described by the effective mass alone, i.e., $U(b) \approx (1/m^* - 1)T(b)$.

The difference between U and U^R has been reduced about as far as is practical. There is little to be gained by allowing m^* to include some of the small variation in U_{out} . A further reduction in $U - U^R$ would be possible if the reference spectrum could contain a linear term, but this would prevent easy solution of the differential equation for ψ^R .

As mentioned at the beginning and end of Sec. 4, Rajaraman has pointed out that the particle energies for high k should be reduced due to the influence of the remaining third-order diagrams shown in Fig. 3. He finds that only the contribution of the even L states should be used, but with the full factor 1 rather than the statistical factor $3/4$ which we have used in (5.29) and thereafter. Thus $m^* U_{core}$ would be given by $4/3$ of the curve “Even L only” in Fig. 10. Rajaraman’s result holds if the initial interaction $lm \rightarrow ab$ is central; if it is a tensor force the potential in the intermediate state b seems to be approximately half the sum of the even and odd L state contributions. In any case, $1 - m^*$ at large k is reduced by a factor $1/2$, and at the important values of k_b , near $2.6k_F$, perhaps by an even larger factor, as seen from Fig. 10. On the other hand, there is at least at present no clear indication how A_2 and Δ should be changed.

We therefore assume that $1 - m^*$ is reduced to one-half and Δ is not changed. For the Gammel-Thaler potential this means $m^* = 0.88$ and $\Delta = 0.75$; these values are used in the next section. We note, however, that recent calculations on nuclear forces⁴⁹ favor a larger core radius than 0.4 F, and this again decreases m^* . The above result of 0.77 for m^* may be fairly realistic for these newer potentials.

We wish to point out that our m^* does not apply to

⁴⁹ T. Hamada, Progr. Theoret. Phys. **24**, 1033 (1960); **25**, 247 (1960); T. Hamada and I. D. Johnston, Nucl. Phys. **34**, 382 (1962); G. Breit (private communication).

states inside the Fermi sea, i.e., to $U(m)$. There is some evidence⁴⁷ that the effective mass for these states is considerably smaller. We expect to obtain such a result from the Serber and core-wave function effects in the calculation of $U_{\text{out}}(m)$, as well as from $U_{\text{core}}(m)$. $U_{\text{core}}(m)$ depends much more weakly on the single-particle momentum than does $U_{\text{core}}(b)$ but, on the other hand, the core-wave function (\mathcal{C}_L) effect now operates in the same direction as the Serber effect.

9. APPROXIMATE WAVE FUNCTIONS, PAULI AND SPECTRAL CORRECTIONS

The purpose of this section is (1) to discuss several approximation methods we have used for solving the wave equations, (2) to estimate some of the contributions to $U(\bar{m})$ and thus to $B.E./A$, and (3) to estimate the Pauli and spectral corrections. The MS separation technique is not used, both for simplicity and to estimate the accuracy obtainable without separation. For the calculations in this section we have chosen the parameters $m^*=0.88$, $\Delta=0.75$, and $A_2=-10$ MeV. The spectral correction is estimated by using the value of $U(b)-U^R(b)$ found in Sec. 8, without considering the Rajaraman correction. Our reasons for this choice are discussed at the end of the previous section. All energies quoted in this section refer to contributions to $U(\bar{m})$, therefore each term must be divided by two to obtain the corresponding contribution to $B.E./A$. We use the approximation that $U(\bar{m})$ equals the particle density, ρ , times an "average matrix element," as defined in Sec. 7. Parameters for this average element are $k_0=(0.3)^{1/2}k_F=0.822 \text{ F}^{-1}$, $\gamma=(1.2)^{1/2}k_F=1.643 \text{ F}^{-1}$, and $P=(0.3)^{1/2}k_F$.

In accord with the usual notation of perturbation theory, we define the zero-order wave function of the MBA expansion to be

$$u_{L(0)} = \mathcal{J}_L - \mathcal{C}_L \quad (9.1)$$

for the uncoupled states, and

$$u_{L',J(0)}^{(L)} = \delta_{L,L'} (\mathcal{J}_L - \mathcal{C}_L) \quad (9.2)$$

for the coupled states. (This notation is explained in Sec. 6.) The first-order corrections are labeled $u_{(1)}$, etc.; these yield the second-order MBA for the energy. It is also convenient to introduce

$$\theta_L = u_L - u_{L(0)} = \mathcal{C}_L - \chi_L, \quad (9.3)$$

so that θ is the distortion of a partial wave caused by the outer potential. (The corresponding θ for the coupled states has \mathcal{C}_L replaced by $\delta_{L,L'}\mathcal{C}_L$.)

We use the potential of Moszkowski and Scott¹⁴ to estimate the two S -state wave functions, namely the 1S_0 and 3S_1 (deuteron state) radial functions which are u_0 and $u_{01(0)}$ in our notation. (Our notation for the deuteron state D wave is $u_{21(0)}$.) We believe that $u_{01(0)} \approx u_0$ is a good approximation, as is explained in connection with (9.11), therefore it is reasonable to

use the same potential to calculate both wave functions. The Moszkowski-Scott potential is

$$\begin{aligned} V_{\text{MS}} &= +\infty, \quad r < c, \\ &= -260e^{-\mu(r-c)} \text{ MeV}, \quad r > c, \\ c &= 0.4 \text{ F}, \quad \mu = 2.083 \text{ F}^{-1}, \end{aligned} \quad (9.4)$$

which they obtained from effective-range theory. They used an average over the 1S_0 and 3S_1 data at low energies, together with a hard core having the Gammel-Thaler radius. For this potential the first and second MBA terms may be found analytically. The resulting $u_{0(0)} = \mathcal{J}_0 - \mathcal{C}_0$ and $u_{0(1)}$ (for $m^*=0.88$) are shown in Fig. 12, together with the shape of the potential. We find, by means of (6.14b), that 1S_0 and 3S_1 each contribute -52.1 MeV in first MBA, and -9.06 MeV in second MBA. Higher MBA terms may be estimated as follows. A glance at Fig. 12 shows that, within the range of the potential, $u_{0(1)}$ is roughly proportional to $u_{0(0)}$, and, therefore,

$$\epsilon = u_{0(1)}/u_{0(0)} \quad (9.5)$$

is a slowly varying function of r . If they were strictly proportional, that is, if ϵ were a constant, it would follow that all higher MBA corrections to $u_{0(0)}$ would have the same shape, and therefore

$$u_0 = (1-\epsilon)^{-1}u_{0(0)}. \quad (9.6)$$

We would simply find that

$$\int_c^\infty (\mathcal{J}_0 - \mathcal{C}_0)v u_0 dr = (1-\epsilon)^{-1} \int_c^\infty (\mathcal{J}_0 - \mathcal{C}_0)v u_{0(0)} dr. \quad (9.7)$$

Some sort of weighted average ϵ must be used in (9.7), since ϵ is actually a function of r . A reasonable average

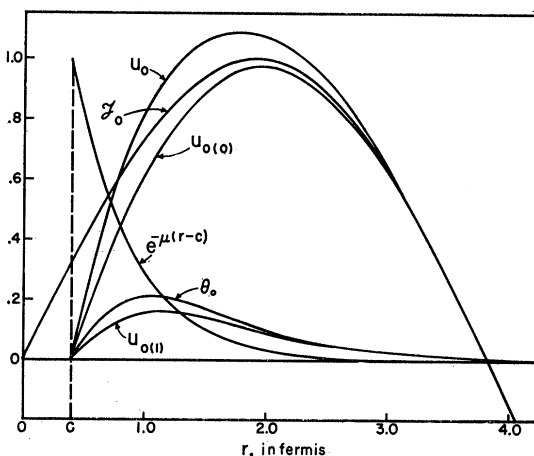


FIG. 12. Approximate S -state wave functions for an "average pair" in the Fermi sea, $k_0=(0.3)^{1/2}k_F=0.822 \text{ F}^{-1}$, $\gamma_m=(1.2)^{1/2}k_F=1.643 \text{ F}^{-1}$. \mathcal{J}_0 is $\sin k_0 r$, $u_{0(0)}$ is $\mathcal{J}_0 - \mathcal{C}_0$, and $u_{0(1)}$ is the first MBA correction to $u_{0(0)}$, calculated for $m^*=0.88$ and the MS potential, whose shape is given by the exponential. θ_0 is the difference between the complete wave function u_0 and the core wave function, $u_{0(0)}$, i.e., the change in the wave function caused by the outer potential.

is given by

$$[\text{second MBA energy}] / [\text{first MBA energy}] = 0.199.$$

This leads to -65.0 MeV for the outer term of each of the S states (1S_0 and 3S_1). This procedure should give a reasonable energy estimate, but a rather poor wave function. The method is easily improved by allowing ϵ to vary with r according to (9.5). The resulting wave function obtained from (9.6) is plotted in Fig. 12, and also the corresponding $\theta_0 = u_0 - u_{0(0)}$. This is the approximate u_0 used in the remainder of this section. Further insight into this wave function is given by Fig. 13 which shows the difference $\chi_0 = \mathcal{J}_0 - u_0$, as well as $\chi_{0(0)} = \mathcal{J}_0 - u_{0(0)}$.

When u_0 is used in the outer integral, we obtain -65.48 MeV for each of the S states. The core term is found to be 35.23 MeV for each S state, so for each state the sum of core and outer contributions to $U(m)$ is estimated as -30.25 MeV. Inclusion of our Pauli and spectral corrections changes this to -29.2 MeV. This may be compared with the Moszkowski-Scott¹⁴ result of -39.5 MeV. The large difference arises from the energy spectra used. Their $U(b)$ is computed "on the energy shell," and is, therefore, continuous with $U(m)$ at k_F . A "best-fit" reference spectrum for their $U(b)$ would have a larger m^* and a smaller Δ than ours, leading to considerably less core repulsion. Even though their spectrum is continuous at k_F , a "best fit" over the range of $k_b = k_F$ to $4k_F$ would lead to a finite Δ and a positive γ^2 . A reasonable "healing distance" is, therefore, assured without explicit use of the exclusion principle, and the remaining Pauli correction should be rather small.

Of course, it is not necessary to use the Moszkowski-Scott potential in the outer integral, once an approximate wave function has been obtained. Numerical integration with the Gammel-Thaler singlet-even potential gives -62.0 MeV for the 1S_0 outer term, and therefore -26.8 MeV for the sum of core and outer terms. To estimate the 3S_1 (deuteron state) term for the Gammel-Thaler potential, we need some approximation for the D wave, $u_{21}^{(0)}$.

A simple general method for the uncoupled states is obtained by subtracting (5.11) from (5.10), and using (9.3).

$$\left[\frac{d^2}{dr^2} - \frac{L(L+1)}{r^2} - \gamma^2 \right] \theta_L = m^* v u_L = m^* v (\theta_L + u_{L(0)}), \quad (9.8)$$

therefore

$$\theta_L = -m^* v u_{L(0)} \left[\frac{L(L+1)}{r^2} + m^* v - \frac{1}{\theta_L} \frac{d^2}{dr^2} \right]^{-1}. \quad (9.9)$$

This is to be solved by iteration, by treating the second derivative term as a perturbation. This method may also be applied to the coupled states, the result for the

deuteron-state D wave being

$$u_{21}^{(0)} = -m^* 2\sqrt{2} {}^3v_T^+ u_{01}^{(0)} / \left[\gamma^2 + \frac{6}{r^2} + m^* ({}^3v_c^+ - 2 {}^3v_T^+ - 3 {}^3v_{L,S}^+) - \frac{1}{u_{21}^{(0)}} \frac{d^2}{dr^2} u_{21}^{(0)} \right] \quad (9.10)$$

Unfortunately this method is not very accurate, since the second derivative term is not a small perturbation—the iterations become unstable at large radii where the potential terms are small. This is why the method was not used for u_0 . On the other hand, its simplicity and ability to handle any form of potential recommend this method for qualitative studies of the higher angular momentum states. The standard solution in terms of the Green's function (5.39) may be used instead of (9.9) to find the wave function at large radii.

Our result for $u_{21}^{(0)}$ is shown in Fig. 13. This wave function gives -70.3 MeV for the 3S_1 outer term. Of this, -29.3 MeV, is due to the tensor force, i.e., the term in (6.14b) involving $u_{21}^{(0)}$. It should be noted that this result is more accurate than a second MBA because the denominator in (9.10) includes the interaction in the D state.

Fourier transforms of the functions χ_0 and $\chi_{21}^{(0)} = -u_{21}^{(0)}$, shown in Fig. 13, are needed in order to calculate the Pauli and spectral corrections. The corresponding transforms $F_0, F_{21}^{(0)}$ [see Eq. (6.35) and (6.36)], are shown in Fig. 14, plotted in units of the core radius squared. Figures 13 and 14 also show $\chi_{0(0)}$ and $F_{0(0)}$ (the results for a pure hard-core interaction) for comparison. The assumed similarity of the S -state wave functions leads to $F_{01}^{(0)} \approx F_0$, therefore (6.37)

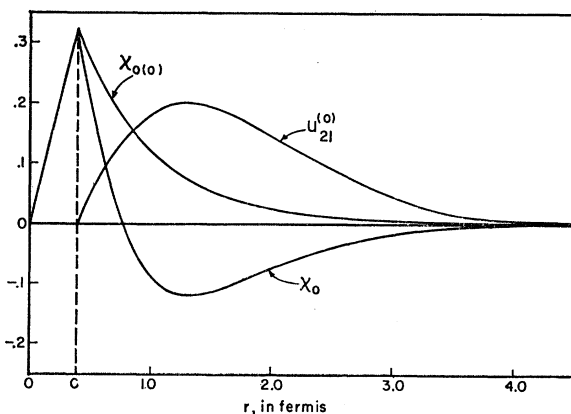


FIG. 13. Difference wave functions for the singlet and triplet S states of an "average pair" in the Fermi sea, showing the distortion, due to the two-nucleon potential, of ψ^R from the form of a plane wave. The D -wave part of the 3S_1 state, $u_{21}^{(0)}$, has no counterpart in the wave function of noninteracting particles; it is a pure "distortion," $u_{21}^{(0)} = -\chi_{21}^{(0)}$. The curve $\chi_{0(0)}$ is the distortion due to a pure hard core; χ_0 is the distortion of the S wave due to the combined attraction and repulsion; it is assumed the same for triplet and singlet states. Note the rapid healing.

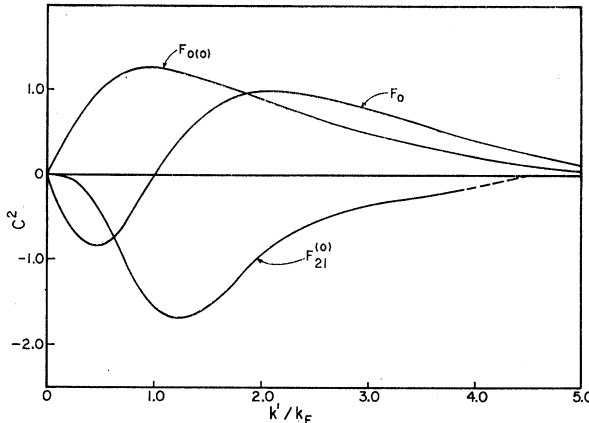


FIG. 14. Fourier transforms of the difference wave functions shown in Fig. 13.

gives $\mathcal{F}_{av} \approx 3(2F_0^2 + F_{21}^{(0)2})$. It is apparent that $u_{21}^{(0)}$ is the major source of both the Pauli and spectral terms, thanks to a rather fortuitous cancellation between the effects on F_0 from the core and the outer potential in the region $k' \approx k_F$. A study of Fig. 13 shows that $\chi_{0(0)}$ is positive definite, and, therefore, $F_{0(0)}$ is also positive definite in the region of interest, $k' \lesssim 4k_F$. On the other hand, the outer potential causes u_0 to "overshoot" \mathcal{J}_0 , leading to a negative dip in χ_0 at large r . For small k' , the Fourier transform weights this negative portion of χ_0 more heavily than the positive peak due to the core. As a result, F_0 is negative for small k' , becoming positive for larger k' . There does not appear to be any fundamental reason why the crossover should occur just at $k' = k_F$.

The total Pauli correction is 5.25 MeV, 2.81 MeV being due to $F_{21}^{(0)}$, and the spectral correction is -1.72 MeV, -1.44 MeV resulting from $F_{21}^{(0)}$. Correction terms from higher angular momenta should be negligible. The effects due to $P \neq 0$ (a) enlarge the region of integration for the Pauli term, and (b) introduce a cross term involving $F_{01}^{(0)}F_{21}^{(0)}$. These corrections may each be of order 1 MeV.

The various terms for each S state (core, outer, Pauli, and spectral) are given in Table III. The Moszkowski-Scott⁴³ results for the Gammel-Thaler potential are also shown for comparison. The MS result for 3S_1 should probably be corrected by minus several MeV for terms of higher than the second order in their expansion method which they did not include.

For 1S_0 the difference between MS and ourselves is again due to the energy spectra used. In their work with the Gammel-Thaler potential, Moszkowski and Scott used the Brueckner-Gammel results for their $U(b)$. Considering the broad range of momenta that occurs in our χ_0 , (see F_0 in Fig. 14), a "best-fit" reference spectrum for their $U(b)$ would have an m^* about the same as ours, but a Δ roughly half of ours. This explains why their 1S_0 state is much more attractive,

viz., because the core repulsion is reduced. The comparison for the tensor force in 3S_1 is at present not understood. Generally Table III should not be considered as a calculation of $U(\bar{m})$ but merely as an illustration of the order of magnitude of the various contributions.

It is gratifying that both the Pauli and the spectral corrections ($G^N - G^R$) are small (5 and 2 MeV, respectively). These numbers should be compared with the total potential energy which we found to be about -87 MeV from Weisskopf's argument (Sec. 8); thus the Pauli correction is about 6%. If the higher corrections to $(G^N - G^R)$ are again around 6% of the first order corrections, their effect would be less than 0.2 MeV for the binding energy. A better estimate, using one of the more recent two-nucleon potentials, is desirable to see whether the error would really be this small.

This small result for $(G^N - G^R)$ has been achieved without an MS separation, and thus illustrates the power of the reference spectrum approximation. (See Sec. 10 for a discussion with MS separation.) Particularly the small contribution of the spectral term is remarkable. It shows that it is not at all necessary to know the particle energies accurately in the range $k_F < k_b < 2k_F$ where they would be difficult to calculate. On the other hand, our results are sensitive to m^* and Δ , hence we must have an over-all knowledge of the particle energies. In this connection we note again that all calculations in this section contain some uncertainty due to our crude treatment of the third-order diagrams shown in Fig. 3. A more careful study is being made.

Formally, of course, it is not necessary to calculate the core and outer terms separately. The total contribution of each partial wave may be found directly in terms of χ by means of (5.2). But this procedure would be less accurate, since the wave functions are never known precisely even if they are obtained from an electronic computer. By comparing (5.1) and (5.2) with and without any outer potential, the form of the outer term in the " χ " method is found to be the left-hand side of the identity

$$(m^*)^{-1}(\gamma^2 + k_0^2) \int_c^\infty \mathcal{J}\theta dr = \int_c^\infty (\mathcal{J} - 3C)vudr. \quad (9.11)$$

This shows that the " χ " method is much less accurate than the "core+outer" method, essentially because

TABLE III. S -state contributions (in MeV) to $U(\bar{m})$, calculated from the Gammel-Thaler potential and the wavefunctions shown in Figs. 12 and 13. The results of Moszkowski and Scott (reference 43), for the same potential, are shown for comparison.

	Outer, central	Outer, tensor	Pauli	Spec-tral	Core	Total	MS total
1S_0	-62.0	...	1.22	-0.14	+35.23	-25.7	-37.2
3S_1	-41.0	-29.3	4.03	-1.58	+35.23	-32.6	-29.4

$u - u_{(0)}$ is much smaller than u . For example, our use of the same u_0 for both S states would lead to the same energies for these states, regardless of the details of v and $u_{21}^{(0)}$, according to the “ χ ” method. In fact, this argument and our expectation that these states would have roughly the same outer energy is the reason we have assumed $u_{01}^{(0)} \approx u_0$. (Note that, because of the core term, the fractional difference between the outer terms is less than this difference for the total of core plus outer.) An extreme example of the difference between the expressions in (9.11) arises when one assumes $u \approx u_{(0)}$. The “ χ ” method gives no outer term at all, but “core+outer” gives the first MBA which accounts for 80% and 45% of the outer terms for 1S_0 and 3S_1 , respectively.

The Fourier transforms in Fig. 14 show that it is important to know $U(b)$ up to, say, $k_b = 3.5k_F$, therefore scattering data have some relevance for nuclear matter at laboratory energies as high as 450 MeV. This is a much higher energy than previously supposed.

10. RELATION BETWEEN NUCLEAR AND REFERENCE MATRIX, MODIFIED MOSZKOWSKI-SCOTT METHOD

In the preceding sections we have calculated the G matrix using the reference spectrum, i.e., G^R . We have also considered the correction, $G^N - G^R$, which must be applied to obtain the actual G matrix in nuclear matter (Sec. 6). In Sec. 9 we gave numerical values for this correction for a special potential. In this section we shall consider the accuracy of the determination of $G^N - G^R$ by an iterative procedure, and we shall find that the method of Secs. 6 and 9 is probably satisfactory. If still higher accuracy is desired the reference spectrum may be combined with the idea of Moszkowski and Scott (MS) of separating the potential into a short- and a long-range part.

The exact relation between G^N and G^R is given by (3.19),

$$G^N = G^R + G^{R\dagger} \left(\frac{1}{e^R} - \frac{Q}{e^N} \right) G^N. \quad (10.1)$$

This is still an integral equation for G^N . Solution by iteration is practical if the first iteration is sufficient, i.e., if G^R can be substituted for G^N in the second term which yields

$$\begin{aligned} \langle \mathbf{k} | G^N | \mathbf{k}_0 \rangle &= \langle \mathbf{k} | G^R | \mathbf{k}_0 \rangle \\ &+ (2\pi)^{-3} \int d^3 k' \langle \mathbf{k} | G^{R\dagger} | \mathbf{k}' \rangle \langle \mathbf{k}' | G^R | \mathbf{k}_0 \rangle \\ &\times \left(\frac{1}{e^R(k')} - \frac{Q(k')}{e^N(k')} \right), \end{aligned} \quad (10.2)$$

or, using (3.18) and (3.9),

$$\begin{aligned} \langle \mathbf{k} | G^N | \mathbf{k}_0 \rangle &= \langle \mathbf{k} | G^R | \mathbf{k}_0 \rangle \\ &+ (2\pi)^{-3} \int d^3 k' \mathcal{E}(k') \langle \phi(k') | \xi(k, \mathbf{P}) \rangle^* \\ &\times \langle \phi(k') | \xi(k_0, \mathbf{P}) \rangle, \end{aligned} \quad (10.3)$$

where $\mathcal{E}(k')$ is given by (6.19),

$$\mathcal{E}(k') = (e_R/e_N)(e^N - Qe^R)|_{k'}. \quad (10.4)$$

Eq. (10.3) is a slight modification of (6.17). Just as there, it is necessary to know the Fourier components of the “wave function distortion” ξ . In Secs. 6 and 9 we have discussed how these Fourier components may be obtained.

Equation (10.4) may be considered as composed of two effects,

$$(1-Q)e_R + (e_R/e_N)(e_N - e_R)Q. \quad (10.5)$$

The first term is the effect of the Pauli principle; contributions come only from occupied states, and depend only on the assumed reference spectrum e_R , not on the actual nuclear spectrum e_N . Indeed, e_N in the states forbidden by the Pauli principle is obviously irrelevant. The second term depends on the difference between the reference and the actual nuclear energy in states outside the Fermi sea, and is minimized by choosing for e_R a good approximation to e_N . However, as shown in Sec. 7, this is only possible over a limited range of k' , and for k' near k_F the difference $e_N - e_R$ tends to be negative, because of the attractive potential. Thus the two terms in (10.5), the Pauli and the spectral term, are of opposite sign and tend to compensate.

It would be possible to choose e_R in such a way that this compensation (in the first order correction term) is exact for the diagonal term $\langle k_0 | G^N | k_0 \rangle$ for some average k_0 , let us say $k_0^2 = 0.3k_F^2$. However, this would still not justify the approximation $G^N \approx G^R$ in the second term of (10.1) which was made in deriving (10.3). For this to be justified, it is necessary that also the important nondiagonal matrix elements satisfy $G^N \approx G^R$. For these elements, the Pauli and spectral term do not, in general, compensate. It is probably necessary, and certainly sufficient for the validity of (10.3) that the Pauli and the spectral term each be small by itself.

We have shown in Sec. 9 that the Pauli correction is about 6% of the total potential energy for the Gammel-Thaler potential. It is reasonable to assume that the higher order corrections, which arise from the fact that the last factor in (10.1) is G^N rather than G^R , are again about 6% of the second-order term (10.2): this would make them about 0.4% of the total potential, giving a contribution of about 0.2 MeV to the binding energy per nucleon. This is a satisfactory accuracy for most purposes; in fact, the fourth and higher order Goldstone diagrams which cannot be calculated very readily, probably give a larger correction. Nevertheless, there

may be cases where the higher order terms in $G^N - G^R$ are larger, especially this might happen if the potential is very large just outside the core, and we, therefore, consider a method which is guaranteed to give $G^N - G^R$ with very great accuracy. For the sake of illustration we only consider central forces beyond the repulsive core. This makes our discussion directly comparable to the work of Moszkowski and Scott.¹⁴ As shown in Sec. 9, the bulk of both the Pauli and the spectral corrections is due to the tensor force, so it is probable that also the separation method does not lead to quite as high a degree of accuracy for tensor forces as we find below for central forces. Special methods have been developed to deal with the tensor force.⁵⁰

Solution for Short-Range Potential

We follow the method of MS and separate the potential into a short- and a long-range part, and we wish to prove that (10.3) is very accurate for the short-range potential alone. For this purpose we go back to (10.1), of which we take the \mathbf{k}, \mathbf{k}_0 matrix element, and then use (3.18), (3.17) to write

$$\langle \mathbf{k} | G_s^R | \mathbf{k}' \rangle = e^R(k) \langle \mathbf{k} | (1 - \Omega_s^R) | \mathbf{k}' \rangle, \quad (10.6)$$

$$\langle \mathbf{k} | (1 - \Omega_s^R) | \mathbf{k}' \rangle = \frac{4\pi}{kk'} \int_0^\infty \mathcal{J}_0(kr) \chi_{0s}(k', r) dr. \quad (10.7)$$

In the last integral, we have replaced ϕ and ξ_s by their $L=0$ components, $j_0 = \mathcal{J}_0/kr$ and $\chi_{0s}/k'r$. This should be justified for the short-range potential if k' is not too large. More generally, sums over L, S, J come in as in Sec. 6. Now χ_{0s} is to be calculated from (5.11) using the short-range potential only,

$$\chi_{0s}'' - \gamma^2 \chi_{0s} = -v_s u_{0s} = -v_s (\mathcal{J}_0 - \chi_{0s}), \quad (10.8)$$

where $v_s = 0$ for $r > d$. The χ_{0s} for all values of k' are to be calculated with the same γ , given by (3.8) in terms of the (fixed) k_0 , because the starting energy must be kept fixed for calculating the entire matrix $\langle \mathbf{k} | G^N | \mathbf{k}' \rangle$, as shown in Appendix A.

Since v_s is restricted to small r , the function χ_{0s}/k' does not depend sensitively on k' as long as k' is moderate. But only for small and moderate k' is the "propagator factor" in (10.1), $(1/e_R - Q/e_N)$, appreciable. Therefore, as long as we consider the short-range potential alone, it is a good approximation to set

$$\langle \mathbf{k} | (1 - \Omega_s^R) | \mathbf{k}' \rangle \approx \langle \mathbf{k} | (1 - \Omega_s^R) | \mathbf{k}_0 \rangle, \quad (10.9)$$

hence also

$$\langle \mathbf{k} | G_s^R | \mathbf{k}' \rangle \approx \langle \mathbf{k} | G_s^R | \mathbf{k}_0 \rangle. \quad (10.10)$$

For this conclusion it is important that $e^R(k)$ rather than $e^R(k')$ occurs in (10.6), i.e., we must make use of

the Hermitean property⁵¹ of G_s^R (Appendix A). We could not easily have deduced (10.10) from the form (3.16) for G_s^R because this involves the derivative x'' which appears to depend on k' , but we have instead used the expressions (3.17), (10.7) for $1 - \Omega$ which involve only the function χ itself.

Inserting (10.10) in (10.1) we obtain

$$\langle \mathbf{k} | G_s^N | \mathbf{k}_0 \rangle = \langle \mathbf{k} | G_s^R | \mathbf{k}_0 \rangle + \left[1 + (2\pi)^{-3} \int d^3 k' \left(\frac{1}{e^R} - \frac{Q}{e^N} \right) \langle \mathbf{k}' | G_s^R | \mathbf{k}_0 \rangle \right]. \quad (10.11)$$

The bracket evidently does not depend on k , hence G_s^N is simply proportional to G_s^R , for all k .⁵² We may then set

$$\langle \mathbf{k} | G_s^N | \mathbf{k}_0 \rangle = (1 - \kappa)^{-1} \langle \mathbf{k} | G_s^R | \mathbf{k}_0 \rangle. \quad (10.12)$$

Inserting into (10.11) yields

$$\kappa = (2\pi)^{-3} \int d^3 k' \left(\frac{1}{e^R} - \frac{Q}{e^N} \right) \langle \mathbf{k}' | G_s^R | \mathbf{k}_0 \rangle \quad (10.13)$$

$$= (2\pi)^{-3} \int d^3 k' [(1 - Q) - Q(e^R - e^N)/e^N] \times \langle \mathbf{k}' | (1 - \Omega_s^R) | \mathbf{k}_0 \rangle, \quad (10.14)$$

where (3.18) has again been used. The bracket in (10.14) has been written so as to separate Pauli and spectral effects, and to put in evidence that the spectral effect is negative.

Equation (10.12) is an "exact" solution of the integral equation (10.11) for G_s^N , provided (10.10) is valid. We can also solve (10.1) "in second approximation," by replacing G_s^N in the last term by G_s^R , as we did in obtaining (10.2). If we then again make the assumption (10.10) we obtain (10.12) with $(1 - \kappa)^{-1}$ replaced by $1 + \kappa$. Thus the relative error in this second approximation is about κ^2 , as might be expected.

To estimate κ we note that the bracket in (10.14) is appreciable only for moderate k' , not for large ones. Therefore the matrix element of $1 - \Omega_s^R$ may be approximated by

$$\langle \mathbf{k}' | (1 - \Omega_s^R) | \mathbf{k}_0 \rangle \approx 4\pi k_0^{-2} \int_0^\infty \mathcal{J}_0(k_0 r) \chi_{0s}(k_0, r) dr \equiv I_R, \quad (10.15)$$

⁵¹ There is, of course, the alternate form of (10.6),

$$\langle \mathbf{k} | G_s^R | \mathbf{k}' \rangle = \langle \mathbf{k}' | G_s^R | \mathbf{k} \rangle^* = e^R(k') \langle \mathbf{k}' | (1 - \Omega_s^R) | \mathbf{k} \rangle^*,$$

$$\langle \mathbf{k}' | (1 - \Omega_s^R) | \mathbf{k} \rangle = 4\pi (kk')^{-1} \int_0^\infty \mathcal{J}_0(k'r) \chi_{0s}^R(k, r) dr,$$

but this is not useful here.

⁵² This simple result breaks down when k becomes so large that the matrix element (10.7) becomes small by the rapid oscillation of $\mathcal{J}_0(kr)$. Then the small difference between $\chi_0(k', r)$ and $\chi_0(k_0, r)$ becomes important, and (10.9) ceases to hold. But then, by the same argument, G^R and G^N are both small.

⁵⁰ E. J. Irwin and M. Razavy (private communication).

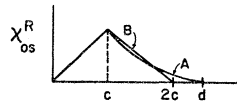


FIG. 15. A = schematic shape of the wave-function distortion due to the short-range potential alone, d = separation distance in modified Moszkowski-Scott method. B = "triangular" approximation to A , used in (10.16).

which is a constant, of the dimension of a volume, characteristic of the deviation of the wave function from a free-particle wave. It is similar to the constants I_P and I_D of MS. For a rough approximation we assume

$$\begin{aligned} \mathcal{J}_0(k_0 r)/k_0 &= r, \\ \chi_{0s}/k_0 &= r, \quad r < c \\ &= 2c - r, \quad c < r < 2c \\ &= 0, \quad r > 2c \end{aligned} \quad (10.16)$$

which gives

$$I_R = 4\pi c^3. \quad (10.17)$$

Actually, the triangular shape for χ_{0s} , (10.16), should be replaced by a more rounded shape, as in Fig. 15, having zero slope at $r=d$ but with $d>2c$; this probably gives about the same result as (10.17). The Pauli effect in (10.14) can now be immediately evaluated and gives, for $P=0$, $k_F=1.5 \text{ F}^{-1}$ and $c=0.4 \text{ F}$:

$$\kappa_P = (2/3\pi)(k_F c)^3 = 0.043 \quad (10.18)$$

The spectral effect requires the knowledge of the spectrum e_N but can then be evaluated by a simple quadrature; we estimate that it is somewhat less than κ_P and of opposite sign. The resulting κ is then less than (10.18) and is further reduced by the fact that, for $k_0>0$, (10.16) is an overestimate. Therefore, we estimate $\kappa \lesssim 0.03$; thus the "second approximation" to G_s^N , (10.2), should have an error of less than 0.1%. This is more than sufficient accuracy for the calculation of G_s^N , especially since this quantity is only about 15% of the total G^N [see below, after Eq. (10.34)]. Thus for the calculation of the diagonal elements of G_s^N , Eq. (10.12) is unnecessary. It is necessary, however, for the accurate calculation of the interference term between short- and long-range forces, the third term in (10.25), as is shown below.

According to (10.12), (10.18), the reaction matrix G_s^N due to short-range forces is very well approximated by the reference matrix G_s^R . The wave-function distortion is of course *not* the same in the nuclear spectrum as in the reference spectrum,

$$1 - \Omega_s^N \neq 1 - \Omega_s^R,$$

especially because of the Pauli principle. Thus G_s is the "simpler" matrix, in marked contrast to the behavior of the matrix elements in a *given* spectrum as a function of the *final state*: The element (10.7) of $1 - \Omega_s^R$

is nearly independent of k , while the element (10.6) of G_s^R is proportional to $e^R(k)$.⁵³

Modified Moszkowski-Scott Method

So far we have not specified the separation distance d of the MS method. We may now choose d so as to justify Eq. (10.15), i.e., the statement that $\langle \mathbf{k}' | (1 - \Omega_s^R) | \mathbf{k}_0 \rangle$ is nearly independent of k' . Clearly this is best fulfilled if $\chi_{0s} \neq 0$ only for small r ; then $\mathcal{J}_0(k'r)/k' \approx \mathcal{J}_0(k_0 r)/k_0$ wherever $\chi_{0s} \neq 0$. The best we can do is to make χ_{0s} vanish entirely beyond d , so we propose to determine d from the condition

$$\chi_{0s}^R(k_0 r) = 0 \quad \text{for } r > d_R. \quad (10.19)$$

This means

$$\mathcal{U}_{0s}^R = \mathcal{J}_0 - \chi_{0s}^R = \mathcal{J}_0 \quad \text{for } r > d_R, \quad (10.20)$$

i.e., the wave function in the *reference* spectrum goes over into the unperturbed wave function beyond the separation distance. This condition replaces that of MS, viz., that the wave function of two *free* nucleons interacting by v_s should go over into the unperturbed wave function,

$$\mathcal{U}_{0s}^F = \mathcal{J}_0 \quad \text{for } r > d_F \text{ (MS).} \quad (10.20a)$$

We prefer our choice (10.19) because the reference G matrix is much closer to the actual G than the free-nucleon G matrix, and it is, therefore, reasonable to make the reference G as good and as simple as possible.

Since χ and χ' are continuous, (10.19) requires that

$$\chi(d - \epsilon) = \chi'(d - \epsilon) = 0. \quad (10.21)$$

It can be shown that the separation distance d exists for any attractive potential at reasonably small k_0 . It is generally larger with our requirement (10.19) than with the MS condition (10.20a). Just like MS, we have the choice of either (a) letting d depend on k_0 , or (b) satisfying (10.18) for some k_0 av and keeping it fixed. In the latter case, χ_0 is small but finite for $r>d$ if $k_0 \neq k_0$ av, and behaves as (3.11). Even with choice (a), however, G_s^R remains Hermitean (Appendix A). We refer to condition (10.19) as the modified Moszkowski-Scott (MMS) method.

We must now obtain the complete reaction matrix G^N from that for the short-range potential G_s^N . According to (A.16) in Appendix A,

$$G = G_s + \Omega_s^\dagger v_l \Omega, \quad (10.22)$$

where the superscript N has been dropped. We rewrite the last term,

$$G = G_s + \left(1 - G_s^\dagger \frac{Q}{e}\right) v_l \left(1 - \frac{Q}{e} G\right), \quad (10.23)$$

and neglect the very small third order term (estimated

⁵³ Also, if we compare the matrix elements for the short-range force in the reference spectrum with those for *free* nucleons, we find that $(1 - \Omega_s)$ is about the same, while G_s is very different. (See Köhler, reference 15.)

about 0.02 MeV below),

$$G_{(3)} = G_s^{\dagger} - \frac{Q}{e} v_l - G_s. \quad (10.24)$$

In the second-order term $v_l(Q/e)G$, we replace G by the first-order approximation $G_s + v_l$ and thus obtain

$$G = G_s + v_l - 2G_s^{\dagger} - \frac{Q}{e} v_l - v_l - v_l. \quad (10.25)$$

The third term is correct in this form only for diagonal matrix elements. Now we use (10.12) and add and subtract a convenient term:

$$\begin{aligned} G^N &= \frac{G_s^R}{1-\kappa} + v_l - \frac{2}{1-\kappa} G_s^{R\dagger} \frac{1}{e^R} v_l \\ &\quad + \frac{2}{1-\kappa} G_s^{R\dagger} \left(\frac{1}{e^R} - \frac{Q}{e^N} \right) v_l - v_l - v_l. \end{aligned} \quad (10.26)$$

The third term here is, apart from the factor $-2/(1-\kappa)$,

$$III \equiv G_s^{R\dagger} v_l = (1 - \Omega_s^R)^{\dagger} v_l, \quad (10.27)$$

whose diagonal element is

$$\begin{aligned} \langle \mathbf{k}_0 | III | \mathbf{k}_0 \rangle \\ = 4\pi k_0^{-2} \int_0^\infty J_0(k_0 r) v_l(r) \chi_{0s}^R(k_0, r) dr = 0. \end{aligned} \quad (10.28)$$

The last equality follows from our definition (10.19) which makes $\chi_{0s}^R = 0$ for $r > d$ while $v_l = 0$ for $r < d$. The vanishing of (10.28) is another great advantage of the MMS method.

The first term in (10.26) is not as accurate as the others. A more accurate result is obtained if (10.12) is not used directly but is inserted into the second term of (10.1), giving for the first term

$$G_s^N = G_s^R + (1-\kappa)^{-1} G_s^{R\dagger} \left(\frac{1}{e^R} - \frac{Q}{e^N} \right) G_s^R. \quad (10.29)$$

This has the further advantage that now the second term of (10.29) can be combined with the fourth term of (10.26) to give the final formula

$$\begin{aligned} G^N &= G_s^R + v_l + (1-\kappa)^{-1} \\ &\quad \times G_s^{R\dagger} \left(\frac{1}{e^R} - \frac{Q}{e^N} \right) (2v_l + G_s^R) - v_l - v_l. \end{aligned} \quad (10.30)$$

Thus the second-order terms [the two last terms of (10.30)] have become very simple. Both of them are small, the last term because Born approximation is good for the long-range potential, the third term because $1/e_R$ is a good approximation to Q/e_N when used in conjunction with G_s^R . If third-order terms are con-

sistently neglected the denominator $1-\kappa$ in the third term should be omitted, but we shall see that it is better retained.

Evaluation of Correction Terms

The most important correction term in (10.30) is the third term which we now rewrite explicitly for the diagonal matrix element, similar to (10.14), (10.15), thus

$$\begin{aligned} G_3^N &= \frac{I_R}{1-\kappa} \int \frac{d^3 \mathbf{k}'}{(2\pi)^3} \left[(1-Q) - Q \frac{e^R - e^N}{e^N} \right]_{k'} \\ &\quad \times \langle \mathbf{k}' | 2v_l + G_s^R | \mathbf{k}_0 \rangle. \end{aligned} \quad (10.31)$$

The bracket has been split into a Pauli term $1-Q$ and a spectral term. For simplicity, the factor $I_R = 1 - \Omega_s^R$ has been assumed to be independent of the intermediate state, \mathbf{k}' . It is evident that there is a double compensation: the attractive potential v_l vs the repulsive G_s^R , and the Pauli effect vs the spectral effect. The attractive potential has mainly low Fourier components, the repulsive short-range potential mainly high ones. We have shown in Sec. 9, especially in Fig. 14, that the Fourier transform of $G^R \approx v_l + G_s^R$ crosses zero near k_F ; that of $2v_l + G_s^R$ is zero at a slightly higher momentum. Thus in the spectral effect the contributions from v_l and G_s^R should compensate very effectively, even more so than in Sec. 9. Therefore, the result for the nuclear binding energy is *very insensitive to the spectrum of particle energies just above the Fermi sea*. This result was already found empirically in the IBM calculations of Brueckner and collaborators, but the above argument clarifies the reason for the lack of sensitivity. Probably the term most sensitive to the particle energies is the second Born term, $v_L(Q/e_N)v_l$, and this is only 0.8 MeV according to MS.

It should not be concluded that the entire particle energy spectrum is unimportant. The behavior of e_N at high k' has a substantial influence on G , as shown in Sec. 7, and contributes significantly to saturation. But this behavior is well approximated by the “effective mass” form for e_R ; thus we have shown that this approximation is very good.

The most important term in (10.31) is the Pauli effect for the long-range potential, i.e., the term $(1-Q)v_l$. Because of its simple structure, the integration over k' can be carried out (for $P=0$ and S states):

$$\begin{aligned} G_{Pl} &= \frac{I_R (2\pi)^{-3}}{1-\kappa} \int_0^\infty 4\pi r^2 dr \int_0^{k_F} 4\pi k'^2 dk' \\ &\quad \times \frac{\sin k'r}{k'r} 2v_l(r) \frac{\sin k_0 r}{k_0 r} \\ &= \frac{4I_R}{\pi(1-\kappa)} \int_d^\infty \frac{dr}{r} (\sin k_F r - k_F r \cos k_F r) \\ &\quad \times v_l(r) \frac{\sin k_0 r}{k_0 r} \end{aligned} \quad (10.32)$$

(notation: P =Pauli, l =long range). Thus, this most important second order term has been reduced to a quadrature involving the long-range potential. Assuming the MS potential (9.4), estimating $d=1.1$ F, inserting (10.17) and (10.18), and setting $k_0=0$ we get

$$G_{Pl} \approx -30 \text{ MeV-F}^3, \quad (10.33)$$

which may be compared with the corresponding ($k_0=0$) matrix element of v_l ,

$$4\pi \int_d^\infty v_l r^2 dr \approx -1000 \text{ MeV-F}^3, \quad (10.34)$$

so that the Pauli correction to v_l , G_{Pl} , is about 3% of v_l . In Sec. 9 without using separation we found a Pauli correction of 6%, but this was largely due to the effect of the tensor force. The point we wish to emphasize, in comparison with Sec. 9, is that here we have also included the main third-order term. Furthermore we can show explicitly that this is small. It is not easy to estimate third-order terms for the method in Sec. 9. The largest third-order term here is represented by the factor $(1-\kappa)^{-1}$. It is, therefore, about 3% of G_P , and the remaining corrections should be even smaller.

Equation (10.32) only gives the contribution of the term with v_l to the Pauli part of (10.31). The contribution of G_s^R to (10.31) is about κG_s^R , as can be seen from the definition (10.14); κG_s^R has a sign opposite to (10.33) and is about 3% of G_s^R , which is by accident the same percentage as (10.33) is of (10.34). Numerically, we estimate from (10.6), (10.15), and (10.17) that for an average value of k_0 in the Fermi sea

$$\langle \mathbf{k}_0 | G_s^R | \mathbf{k}_0 \rangle \approx 140 \text{ MeV-F}^3 \quad (10.35)$$

or about 15% of $\langle \mathbf{k}_0 | G^N | \mathbf{k}_0 \rangle$. Thus the G_s^R part of the correction (10.31) is about 0.2 MeV per particle.

It is interesting that the long-range Pauli term, $I_R(1-Q)v_l$, increases the effect of the potential v_l . This is because it originates from a correction to the short-range wave function, i.e., replacing Ω_s^R by Ω_s^N ; the Pauli effect removes the low-frequency components from that wave function and hence reduces its "repulsive" character. In the (attractive) second-order Born term $v_l(Q/e)v_l$ the Pauli principle reduces the attraction as expected.

The third-order terms are very small. The neglected term (10.24) can be transformed similarly to (10.26)–(10.28), and the result is then related to the fourth term of (10.26) in much the same way as that term is to v_l , except that it does not contain the factor 2 present in (10.26). We therefore estimate (10.24) to be about 3% of (10.31), and thus to contribute about 0.02 MeV (attractive) to the binding energy per particle. The third-order Born term, $v_l(Q/e)v_l(Q/e)v_l$, is probably about 1½% of the second order term, $v_l(Q/e)v_l$, because MS have shown that this second-order term is about 1½% of the first-order term v_l ; this makes the third-

order term about 0.01 MeV in B.E./A. One third-order term has been retained, viz., the denominator $1-\kappa$ in (10.31). If the total (10.31) is about 1.3 MeV (attractive), and $\kappa=0.03$, then this denominator contributes 0.04 MeV to B.E./A (attractive). It is, therefore, the largest of the third-order terms so that its retention seems justified.

Thus, we have proved that our method, using the reference spectrum and MMS separation, gives a highly accurate result in second order. It remains to discuss the relation to the theory without MS separation. In this theory the reference G matrix is, using again (A16),

$$\begin{aligned} G^R &= G_s^R + \Omega_s^{R\dagger} v_l \Omega^R \\ &= G_s^R + \left(1 - G_s^{R\dagger} \frac{1}{e^R} \right) v_l \left(1 - \frac{1}{e^R} G^R \right). \end{aligned} \quad (10.36)$$

Using the first approximation $G^R \approx G_s^R + v_l$ in the last term, and neglecting the third-order term gives

$$G^R \approx G_s^R + v_l - 2v_l \frac{1}{e^R} G_s^R - v_l \frac{1}{e^R} v_l. \quad (10.37)$$

The third term is again zero, by (10.27) and (10.28). The last term may be compared with the last term in (10.25), i.e., with the usual second Born term. The difference between the two,

$$G_t^N - G_t^R \equiv \Delta G_t = v_l \left(\frac{1}{e^R} - \frac{Q}{e^N} \right) v_l \quad (10.38)$$

is just the contribution of the long-range potential to the second-order term in (10.1). Now the important point is that the last term in (10.37) is apt to be appreciably larger than the last term in (10.25) because the long-range potential v_l has mostly matrix elements for small momentum change, thus the Pauli operator Q is very effective in making $v_l(Q/e_N)v_l$ small. Therefore, the last term in (10.37) corrects v_l by an unnecessarily large amount; this correction must then be removed by the further correction $G^N - G^R$. In other words, $G_s^R + v_l$ is a better approximation to the correct reaction matrix G^N than is G^R . This is the main reason why the MMS separation method is more accurate than the direct use of G^R as a first approximation. Moreover, the last term of (10.37) contains strong low-momentum components which have a complicated dependence on k . Therefore, it is difficult to calculate the third-order terms, or even to estimate their magnitude reliably, in contrast to the MMS method. On the other hand, if our estimate in Sec. 9 is correct, the third-order terms in the straightforward G^R method without MS separation are only of order 0.2 MeV per particle, and this is accurate enough for most purposes. Moreover, in Sec. 9 tensor forces gave the main contribution to the second order while in Sec. 10 these forces were omitted. It is, therefore, not clear whether

the MMS method with tensor forces included is really more accurate than the straightforward calculation of Sec. 9, but we believe that its error can be more reliably estimated.

Highly Excited States

All the foregoing discussion in this section applies to the calculation of the nuclear binding energy, or of the particle potential $U(m)$ for states inside the Fermi sea. For states of high k much less care is necessary. First of all, their energy enters the nuclear binding energy only through (10.3), or more specifically, the second term in (10.5). We estimate that an error in $U(b)$ of 1 MeV (on the average over k_b) causes at most 0.1 MeV error in the nuclear binding energy. Hence much less accuracy is required in calculating $U(b)$. Second, the function $\psi(k_0, r)$ for large k_b is almost entirely given by the pure-core function $\mathcal{J}-\mathcal{J}C$ and the correction due to the attractive potential is small, approximately as $(\gamma+\mu)^{-2}$, see end of Sec. 5 and (8.21). Hence the Fourier components of ξ , $\langle \mathbf{k}' | (1-\Omega) | \mathbf{k}_0 \rangle$, are dominated by the behavior of ξ for small r , even if k' is small. The arguments in (10.6) to (10.14) which were made for the short-range potential only, now apply to the complete potential and wave function ξ . Therefore the MS separation is not needed in this case.

The wave function can be obtained directly from (3.10), as is done in Secs. 7 to 9. In most cases the second MBA for the energy gives sufficient accuracy. An exception may be the spin-orbit interaction because this interaction is very large (> 1 BeV) outside the repulsive core, but integration of (3.10) without MS separation is still all right. Incidentally, the correction κ in (10.14) is smaller for large k_0 because the wave function ξ falls more rapidly outside the repulsive core.

For states in the Fermi sea and $L \neq 0$, MS separation is also superfluous: For $L=1$ the most important interaction (spin-orbit) is of very short range, therefore the Pauli correction is small. It can be calculated for the entire $L=1$ interaction in the same simple way as it is calculated for the short-range interaction in (10.14). For $L \geq 2$ the repulsive core and short-range interaction generally are unimportant because $\mathcal{J}_L(k_0 c)$ is very small, and it is, therefore, not worth while to separate them out. In fact, for states with $L \geq 3$ it may be sufficient to neglect the core altogether and use *ordinary* first Born approximation.

11. DISCUSSION

We have shown that the calculation of the Brueckner-Goldstone reaction matrix G is greatly simplified by first calculating a reference matrix. For this purpose, the actual energies of nucleons in all *intermediate* states of the nucleons are arbitrarily replaced by a "reference spectrum"

$$E_R(k) = A + k^2/2m^*, \quad (11.1)$$

i.e., by an effective mass formula. The constants A and m^* can be chosen to fit the actual particle energy spectrum closely over the important range of momenta, especially from $k=2k_F$ to $4k_F$ (Fig. 11). The energy of the *initial* state, occurring in an element of the reaction matrix G , may be deduced from the actual particle energies in nuclear matter.

The particle energies are defined more carefully than in previous work, especially for states above the Fermi sea. In accord with previous calculations,⁴ the G matrix for these states must be calculated off the energy shell, the more so the higher k . This fact, together with the repulsive core, makes the potential energy positive, large, and proportional to k^2 at high k , so that in this limit the *actual* energy is given by a formula of type (11.1) with $m^* < 1$. Approximately, in the limit of large k ,

$$m^* = 1 - (4\pi/3)c^3\rho, \quad (11.2)$$

if we take into account Rajaraman's factor²⁶ of $\frac{1}{2}$ (see beginning of Sec. 4 and end of Sec. 8). In (11.2) ρ is the density and c the radius of the repulsive core. This is about $m^* = 0.94$ for the observed nuclear density ($k_F = 1.5 \text{ F}^{-1}$) whereas the value to be used in the reference spectrum (11.1) (for the important region of k) is about $m^* = 0.88$ or somewhat less (Sec. 8).

When the reference spectrum (11.1) is used it is possible to obtain a simple differential equation in space for the wave function ψ^R which is defined as the Fourier transform of the reference reaction matrix, G^R . This greatly simplifies the treatment of the repulsive core. The differential equation differs from the Bethe-Goldstone²⁰ differential equation by the absence of the integral term which in that theory represents the effect of the Pauli principle: The use of the reference spectrum makes it unnecessary to take the Pauli principle in intermediate states into account when calculating G^R . The resulting simplification makes it possible to give an explicit and simple solution for the reference wave function for a pure repulsive core, and the case of core plus attractive potential can then be treated by a simple perturbation method (Sec. 5). The reference reaction matrix G^R is immediately obtained from the wave function ψ^R by Fourier transformation.

The actual reaction matrix, G^N can be obtained from the reference matrix by solving the integral equation

$$G^N = G^R + G^{R\dagger} \left(\frac{1}{e_R} - \frac{Q}{e_N} \right) G^N, \quad (11.3)$$

in which we take into account (a) the deviation of the actual particle spectrum e_N from the reference spectrum e_R , and (b) the Pauli principle, i.e., the operator Q . It is shown (Sec. 9) that it is usually sufficient to solve (11.3) by one iteration, i.e., by replacing G^N in the last term by G^R . This reduces the calculation of the difference, $G^N - G^R$, to a quadrature. The two corrections, for Pauli principle and for the spectrum difference,

$e_R - e_N$, tend to compensate. This method is amply accurate for the calculation of the energies E_N of states above the Fermi sea and for the $L \neq 0$ interactions in the Fermi sea. For the S states in the sea it is moderately accurate.

Even higher accuracy is obtained if the method of the reference spectrum is combined with the Moszkowski-Scott separation method. It is possible and convenient to define a separation distance d_R , somewhat larger than that of MS, such that the reference wave function for $r > d_R$ goes over exactly into the free particle function, whereas MS put this requirement on the wave function of two interacting nucleons outside of nuclear matter. With this separation method, the reaction matrix in nuclear matter, G^N , can be calculated to an accuracy of better than 0.1 MeV per nucleon, using only quadratures after the solution of the first, simple differential equation for the reference wave function in the short-range potential. We note however that this separation method may perhaps not be capable of quite such high accuracy when tensor forces are considered.

Whether MS separation is used or not, the nuclear binding energy is insensitive to the particle energy spectrum $E(k)$, between k_F and $2k_F$. There is some sensitivity to $E(k)$ between $2k_F$ and $4k_F$ but in this region $E(k)$ is rather easy to calculate. The insensitivity to $E(k)$ directly above the Fermi sea is partly due to a compensation between the attractive long-range and the repulsive short-range interaction.

A great advantage of the MS method and of our modification is that it should permit easy extension of the theory to finite nuclei. The contribution of the short-range forces depends essentially only on the density of nuclear matter, and it should be permissible to use the local density in finite nuclei, at least for approximate calculations. The contribution of the long-range forces can be calculated by Born approximation, and this can be done just as readily for shell model wave functions in a finite nucleus as for plane waves in nuclear matter. Thus the potential to be used in approximate shell model calculations is the long-range part of the nucleon-nucleon interaction, i.e., just the part which is best known from meson theory.

The MS separation is also useful to assess the sensitivity of the nuclear binding energy to the (largely unknown) behavior of the nucleon interaction at short distances. In the MS method, the short-range forces are mainly important for the determination of the separation distance d . But we can determine d , for a given relative momentum k_0 , also from the observed phase shift of nucleon-nucleon scattering for momentum k_0 , together with the well-known nuclear forces at large distance which are given by one- and two-pion exchange. We simply integrate the Schrödinger equation inwards from large r until we reach the point at which the logarithmic derivative of the wave function is equal to that for free, noninteracting nucleons; this

is then the MS separation distance for free nucleons, d_F . The correction from MS separation to our modified separation distance d_R can then be made by perturbation theory, requiring only a rough knowledge of the wave function u between the core radius c and d : but this knowledge is provided, with nearly adequate accuracy, by noting that $u^F = u^R = 0$ at $r = c$ and that the logarithmic slopes of u^F and u^R are the same as for the no-interaction wave function ϕ at d_F and d_R , respectively. The result should be almost independent of the details of the interaction between c and d . The short-range reaction matrix, G_s , also requires mainly a knowledge of the core radius c and the separation distance d .

An accurate method for calculating G is of course not enough to determine the nuclear binding energy; there are two other requirements. One is a quantitative treatment of the higher (\geq fourth) order Goldstone diagrams which may together contribute of the order of 1 MeV per particle. The other is a detailed knowledge of the nuclear force as discussed at the end of Sec. 1. In particular, the exact radius of the repulsive core seems very important for nuclear matter. We have assumed for simplicity that c is the same in all (spin, isospin) states, but the evidence for this is rather poor. We also expect the results to be rather sensitive to the relative amounts of central and tensor force in triplet-even states.

ACKNOWLEDGMENTS

The authors would like to thank Dr. K. A. Brueckner for drawing their attention to the Brueckner-Goldman theory of particle energies in nuclear matter. We are greatly indebted to Professor G. Breit and Dr. Hamada for sending us repeatedly their most recent results on the potential between two nucleons, and on nucleon phase shifts. To Dr. Köhler, Dr. Levinger, Dr. Lomon, Dr. A. M. Green, and Dr. Moszkowski we are grateful for interesting discussions and for keeping us informed on their own methods for nuclear matter calculations, and to Dr. Lomon also for sending us the parameters of his boundary-condition model. Dr. Razavy, E. J. Irwin, and R. Rajaraman who are working at Cornell on related problems, have greatly contributed to this paper by giving us their results before publication.

APPENDIX A. REACTION MATRIX IDENTITIES

Consider two problems A and B , with different potentials v_A and v_B and different propagators

$$P_A = Q_A/e_A \quad (A1)$$

and P_B . We wish to obtain relations between the corresponding reaction matrices G_A and G_B . The Schrödinger equation and the definition of G become

$$\Omega_A = 1 - P_A G_A, \quad (A2)$$

$$G_A = v_A \Omega_A, \quad (A3)$$

and two similar equations with the subscript B . Because of (A2) and its Hermitian conjugate with subscript B , the brackets in the following expression are zero, and it is an identity:

$$G_A = G_A - G_B^\dagger [\Omega_A + P_A G_A - 1] + [\Omega_B^\dagger + G_B^\dagger P_B^\dagger - 1] G_A, \quad (\text{A4})$$

which simplifies to

$$G_A = G_B^\dagger - G_B^\dagger \Omega_A + \Omega_B^\dagger G_A + G_B^\dagger (P_B^\dagger - P_A) G_A. \quad (\text{A5})$$

Using (A3) and its Hermitian conjugate we obtain

$$G_A = G_B^\dagger + \Omega_B^\dagger (v_A - v_B^\dagger) \Omega_A + G_B^\dagger (P_B^\dagger - P_A) G_A. \quad (\text{A6})$$

We first consider (A6) for the case when problems A and B are identical, i.e., when

$$v_A = v_B, \quad P_A = P_B, \quad (\text{A7})$$

in which case we may drop the subscripts. Then we find

$$G = G^\dagger, \quad (\text{A8})$$

if

$$v = v^\dagger, \quad (\text{A8a})$$

and

$$P = P^\dagger. \quad (\text{A8b})$$

The potential is Hermitian, $v = v^\dagger$ for nearly all practical cases.⁵⁴ The second condition $P = P^\dagger$ is more intricate. Using (A1) we see that $P = P^\dagger$ is ensured if

$$Q = Q^\dagger, \quad e = e^\dagger. \quad (\text{A9})$$

The first of these is clearly satisfied: The Pauli operator Q is real and depends only on the "present" state of the two nucleons, hence it is Hermitian. The energy denominator e , however, is the "present" nucleon energy minus the "starting energy" H , as discussed in Sec. 3. If we consider a nondiagonal element of Eq. (A6), going from state \mathbf{k}_0 to \mathbf{k} , we might be tempted to set

$$\begin{aligned} H_A &= E(\mathbf{P} + \mathbf{k}_0) + E(\mathbf{P} - \mathbf{k}_0), \\ H_B^\dagger &= E(\mathbf{P} + \mathbf{k}) + E(\mathbf{P} - \mathbf{k}), \end{aligned} \quad (\text{A10})$$

i.e., to put the starting energy equal to the actual energy of the nucleons in the respective initial state. In this case, $H_B^\dagger \neq H_A$, and therefore $P^\dagger \neq P$ so that G is not Hermitian. To ensure Hermiticity, it is necessary and sufficient that the starting energy be chosen as a constant H , independent of the actual initial state.⁵⁵ Thus the reaction matrix G is a function of the two independent parameters \mathbf{P} and H ; there is a complete matrix $\langle \mathbf{k} | G | \mathbf{k}_0 \rangle$ for each pair of parameters \mathbf{P}, H . We can then, if we wish, choose the matrix corresponding to $H = H_A$ in (A10); the elements $\langle \mathbf{k} | G | \mathbf{k}_0 \rangle$ of the resulting G matrix will then be "on the energy shell" with respect to k_0 .

⁵⁴ See below for the Moszkowski-Scott potential.

⁵⁵ This was recognized by Thouless (reference 31) and by Brueckner and Gammel (reference 4) but, to our knowledge, it has never been stated explicitly that $H = \text{const}$ is required to make G Hermitian.

In the special case of the Moszkowski-Scott potential, a separation distance d is chosen which is a function of k_0 . If we wish to obtain the diagonal element $\langle \mathbf{k}_0 | G_s | \mathbf{k}_0 \rangle$ for the short-range potential, we only need to calculate the complete matrix $\langle \mathbf{k}' | G_s | \mathbf{k} \rangle$ for $d = d(k_0)$ and $H = H_A$ of (A10). This matrix is Hermitian⁵⁶ [the elements of the v matrix $\langle \mathbf{k}' | v | \mathbf{k} \rangle$ all being calculated with $d = d(k_0)$, regardless of k and k'] and the single element $\langle \mathbf{k}_0 | G_s | \mathbf{k}_0 \rangle$ of this matrix is the required answer.

We have thus shown that it is easy to assure that G be Hermitian; hence in (A6) we may replace G_B^\dagger by G_B . However, the wave operator Ω is not Hermitian; in fact, an element of the Hermitian conjugate of (A2) is (dropping the subscript A)

$$\begin{aligned} \langle \mathbf{k}' | \Omega^\dagger | \mathbf{k} \rangle &= 1 - \langle \mathbf{k}' | G^\dagger | \mathbf{k} \rangle P^\dagger(\mathbf{k}), \\ &= 1 - \langle \mathbf{k}' | G | \mathbf{k} \rangle P(\mathbf{k}), \end{aligned} \quad (\text{A11})$$

since P is a diagonal matrix, while

$$\langle \mathbf{k}' | \Omega | \mathbf{k} \rangle = 1 - P(\mathbf{k}') \langle \mathbf{k}' | G | \mathbf{k} \rangle \neq \langle \mathbf{k}' | \Omega^\dagger | \mathbf{k} \rangle. \quad (\text{A12})$$

We now use $G_B^\dagger = G_B$ and assume

$$v_A = v_B, \quad P_A \neq P_B. \quad (\text{A13})$$

Then (A6) becomes

$$\begin{aligned} G_A &= G_B + G_B (P_B - P_A) G_A \\ &= G_B + G_B \left(\frac{Q_B - Q_A}{e_B - e_A} \right) G_A, \end{aligned} \quad (\text{A14})$$

a relation we have used repeatedly in Secs. 3, 6, 9, and 10.

Next we assume

$$P_A = P_B, \quad v_A = v_B + v_C \neq v_B. \quad (\text{A15})$$

For example, v_B may be the short-range potential of Moszkowski and Scott, and v_C the long-range potential. Then (A6) becomes

$$G_A = G_B + \Omega_B^\dagger v_C \Omega_A. \quad (\text{A16})$$

This relation has been derived by Köhler¹⁵ and has been used in our Secs. 2, 5, and 10. It has a very plausible form; apart from the "short-range" reaction matrix G_B we have the second term whose matrix element is

$$\langle \mathbf{k}' | \Omega_B^\dagger v_C \Omega_A | \mathbf{k} \rangle = \int \psi_B^*(\mathbf{k}', \mathbf{r}) v_C(\mathbf{r}) \psi_A(\mathbf{k}, \mathbf{r}) d\tau. \quad (\text{A17})$$

That is, the matrix element of the long-range potential is taken between the wave function in the "short-range" potential B and that in the full potential A , quite analogous to an exact formula in Schrödinger theory comparing two potentials.

It should be noted that (A16) involves Ω_B^\dagger which is not identical with Ω_B . Thus the matrix element between states \mathbf{k} and \mathbf{k}' involves the (complex conjugate

⁵⁶ As pointed out by Köhler, reference 15.

of the) wave function of the final state in potential v_B , viz., $\psi_B^*(\mathbf{k}', \mathbf{r})$ as indicated in (A17). In momentum representation,

$$\begin{aligned} \langle \mathbf{k}' | G_A | \mathbf{k} \rangle &= \langle \mathbf{k}' | G_B | \mathbf{k} \rangle \\ &+ (2\pi)^{-6} \int \int d^3 \mathbf{k}'' d^3 \mathbf{k}''' \langle \mathbf{k}''' | \Omega_B | \mathbf{k}' \rangle^* \\ &\times \langle \mathbf{k}''' | v_C | \mathbf{k}'' \rangle \langle \mathbf{k}'' | \Omega_A | \mathbf{k} \rangle. \quad (\text{A18}) \end{aligned}$$

APPENDIX B. ENERGIES OF HOLE STATES

This Appendix presents the argument, referred to in Sec. 4, for considering the hole-bubble of Fig. 2(b) to be “on the energy shell.” If this diagram is evaluated according to the usual Goldstone rules, the hole-bubble interaction of Fig. 2(b) is even further off the energy shell than the particle-bubble interaction of Fig. 2(a), as shown in (4.11). However, as pointed out in Sec. 4, an argument by Brueckner and Goldman suggests that the hole-bubble interaction should be taken *on* the energy shell.

Brueckner and Goldman use perturbation theory, i.e., v -diagrams, and show that in this case two diagrams, Figs. 6(a) and 6(b), combine to make the interaction effectively on the energy shell [see Eq. (4.12)]. This proof is not directly useful to us since we must deal with G matrices. In this Appendix we shall generalize the Brueckner-Goldman proof⁵⁶ to all orders of perturbation theory so that in fact their result is also valid for the complete hole-bubble interaction. We believe that this was first pointed out by Thouless,⁵⁷ who arrived at this result while studying the single-particle Green's functions of the Goldstone theory. The most direct proof uses time-dependent perturbation theory, and is similar to the original Goldstone demonstration that unlinked diagrams may be factored. We recall that there one sums over all relative time orders for the v interactions, subject only to the restriction that each linked part of a diagram has a unique time order among its own interactions.

A typical v diagram contained in Fig. 2(b) is shown in Fig. 16. (We assume of course that the core is not infinitely hard, and only pass to this limit at the conclusion.) Evaluating this diagram in the conventional manner, we obtain a product of v -matrix elements times

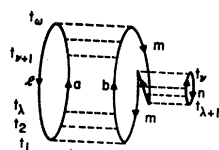


FIG. 16. A typical v -interaction diagram contained in Fig. 2(b). The interactions are shown here in their order of occurrence within the usual Goldstone expansion, Eq. (B2).

⁵⁶ D. J. Thouless, thesis, Cornell University (1958) (unpublished).

an energy factor given by

$$\lim_{\alpha \rightarrow 0} \left(\frac{1}{i\hbar} \right)^{\omega-1} \int_{-\infty}^0 dt_{\omega-1} \int_{-\infty}^{t_{\omega-1}} dt_{\omega-2} \cdots \int_{-\infty}^{t_2} dt_1 \\ \times \prod_{j=1}^{\omega-1} e^{it_j(\delta E_j - i\alpha)/\hbar} = \prod_{j=1}^{\omega-1} \left(-\sum_{k=1}^j \delta E_k \right)^{-1}, \quad (\text{B1})$$

where δE_j is the *change* in the intermediate state energy caused by the j th interaction. In Goldstone's formalism, the δE 's originate from the time factors associated with the matrix elements of the perturbing Hamiltonian in the interaction representation. This gives the ordinary Goldstone result, Eq. (4.11), that the hole bubble is off the energy shell by the amount $\sum_{k=1}^{\lambda} \delta E_k$.

A large number of closely related diagrams may be generated by relaxing Goldstone's time order restriction, which is

$$t_1 < t_2 < \cdots < t_n < t_{n+1} < \cdots < t_\omega = 0. \quad (\text{B2})$$

We now choose to keep the interactions in each of the three uninterrupted ladders in the same relative order as before, but to restrict the interactions in different ladders only by

$$t_\lambda < t_\nu < t_{\nu+1}. \quad (\text{B3})$$

This means that any of the times $t_{\lambda+1}$ to $t_{\nu-1}$ may fall anywhere between t_1 and t_λ , or even below t_1 . The possibility that *all* of these times may fall below t_1 is also included. An example is shown in Fig. 17. Figure 17 can be described in words as follows: There are two ladders in the left half of the diagram, the lower ladder from t_1 to t_λ and the upper ladder from $t_{\nu+1}$ to t_ω , and one ladder in the right half, from $t_{\lambda+1}$ to t_ν . The last interaction on the right t_ν provides an indicator which determines whether a given interaction of the left-hand side of Fig. 17 should be considered part of the upper or the lower G of Fig. 2(b). A heavy line has been placed at the level of t_ν in Fig. 17 to emphasize the special role of this interaction.

The energy factor is then

$$\begin{aligned} \lim_{\alpha \rightarrow 0} \left(\frac{1}{i\hbar} \right)^{\omega-1} &\left[\int_{-\infty}^0 dt_{\omega-1} \cdots \int_{-\infty}^{t_{\nu+2}} dt_{\nu+1} \right] \\ &\times \int_{-\infty}^{t_{\nu+1}} dt_\nu \left[\int_{-\infty}^{t_\nu} dt_{\nu-1} \cdots \int_{-\infty}^{t_{\lambda+2}} dt_{\lambda+1} \right] \\ &\times \int_{-\infty}^{t_\nu} dt_\lambda \left[\int_{-\infty}^{t_\lambda} dt_{\lambda-1} \cdots \int_{-\infty}^{t_2} dt_1 \right] \prod_{j=1}^{\omega-1} e^{it_j(\delta E_j - i\alpha)/\hbar} \\ &= \left[\prod_{j=\nu+1}^{\omega-1} \left(-\sum_{k=1}^j \delta E_k \right)^{-1} \right] \left(-\sum_{k=1}^\lambda \delta E_k \right)^{-1} \\ &\times \left[\prod_{j=\lambda+1}^{\nu-1} \left(-\sum_{k=\lambda+1}^j \delta E_k \right)^{-1} \right] \left(-\sum_{k=1}^\lambda \delta E_k \right)^{-1} \\ &\times \left[\prod_{j=1}^{\lambda-1} \left(-\sum_{k=1}^j \delta E_k \right)^{-1} \right]. \quad (\text{B4}) \end{aligned}$$

Square brackets have been used to distinguish the integrations and energy factors which belong to each of the G 's in Fig. 2(b), while the remaining integrations and the factors in ordinary parentheses refer to the energy denominators between the G 's. The main difference from (B1) is that now the hole-bubble ladder is on the energy shell. This is because $t_{\lambda+1}$ is not restricted from below by t_λ so that the integrand over $t_{\lambda+1}$ does not receive any factor from integrations over preceding t_i 's; the integrand is simply $\exp(i\delta E_{\lambda+1}t/h)$ and the lower limit is $-\infty$. This explains the second square bracket in (B4). The two energy denominators between the three ladders are the same as before, and are equal to each other because

$$\sum_{k=\lambda+1}^{\nu} \delta E_k = 0. \quad (\text{B5})$$

For the same reason, in the first bracket in (B4) the sum over k from $\lambda+1$ to ν may be omitted.

When we now sum Fig. 17 over all intermediate states that can occur in each ladder, and then sum over diagrams having all possible numbers of v 's in each

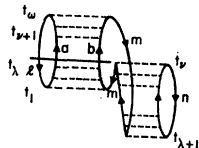


FIG. 17. A time ordering of Fig. 16 permitted by the less restrictive condition, Eq. (B3). The heavy line at t_v separates the interactions which belong to the top and bottom G matrices of Fig. 2(b). Time t_v forms the upper limit for both t_λ and t_{v-1} .

ladder, we obtain the single G diagram of Fig. 2(b), with the hole-bubble interaction taken on the energy shell.

There is a further reason for the choice of time ordering given by (B.3), beyond the fact that it leads to this useful result. It turns out that (B3) generates all possible diagrams which may be considered as insertions in a hole line, such that the insertion part of the diagram is of first order in the density. This is because there is one hole state to be summed over in each of these insertions, viz., the hole n , in Figs. 16 and 17, and the number of possible holes is proportional to $k_F^3 \sim \rho$. Hugenholtz³ has emphasized that the density is an appropriate expansion parameter, supplementing the expansion in powers of G .

Suppose now that the condition $t_v < t_{v+1}$ were relaxed to $t_v < t_\omega$. Then it would be impossible to tell how many of the $\omega + \lambda - \nu$ interactions of the left-hand side of Fig. 17 contributed to the upper G of Fig. 2(b), and how many to the lower. To form the G 's we must sum over all possible combinations of values of λ , $\nu - \lambda$, and $\omega - \nu$, but we must consider each possibility only once. Relaxing $t_v < t_{v+1}$ to $t_v < t_\omega$ would lead to a double summation over the number of interactions in the upper

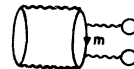


FIG. 18. An iteration of the hole-bubble insertion of Fig. 2(b). The $U(m)$ defined by a single hole bubble also identically cancels this diagram, provided that all hole bubbles are evaluated on the energy shell.

left-hand ladder. Relaxing $t_\lambda < t_\nu$ would lead to the same difficulty. If $t_\nu > t_\omega$ were permitted, the problem of overcounting would occur in a different form. It would become impossible to tell which side of the diagram represented an insertion into the other side. Upon summing over all time orders, all intermediate states, and all numbers of interactions in each of the original ladders, each diagram of the form shown in Fig. 17 would be counted twice. (Momentum conservation requires that $t_\nu > t_1$, or the diagram would vanish.)

It is clear from the derivation that the result (B4) is quite general. Any hole-bubble interaction can be put on the energy shell no matter how complicated the rest of the diagram in which it occurs. The arguments of the last paragraph may be generalized to show that a restriction similar to (B3) is quite reasonable for many higher order diagrams. Overcounting would not necessarily result from v diagrams which violated this restriction, since in a more complicated diagram other features might remain which would distinguish "insertion" from "reduced" parts, but these extra diagrams should be considered as parts of still higher order G diagrams, in order to retain this simplicity for the hole energies. As an illustration, we mention how iterated hole bubbles, such as Fig. 18, may be treated. Figure 19 shows a typical v diagram contained in Fig. 18. If we take as the analog of (B3) the restriction

$$t_\lambda < t_\mu < t_\nu < t_{\nu+1}, \quad (\text{B6})$$

it is easily seen that the hole interactions are both on the energy shell and the energy denominators between the G 's are the same as before. It is interesting to note that time orders with $t_{\mu+1} < t_\mu$ are permitted, in which case *three* holes are simultaneously present in state m .

It is clear that the result (B4) is also valid in time-independent perturbation theory, since the time integration is merely a convenient way of combining the contributions from graphs with different orderings. We have derived (B4) purely algebraically, using a proof by induction, but this does not appear to be instructive.

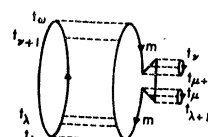


FIG. 19. A v -interaction diagram contained in Fig. 18. The interactions are shown in the standard Goldstone order. Generalizing the time ordering according to Eq. (B.7) leads to an on-energy-shell evaluation of the hole bubbles.

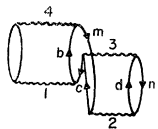


FIG. 20. Lowest order ordinary Goldstone diagram [excluding Fig. 2(b)] contained in an on-energy-shell evaluation of Fig. 2(b).

One thing that this shows, however, is that (B3) could be replaced by

$$t_\lambda < t_{\lambda+1} < t_{\nu+1}, \quad (B7)$$

which is not immediately obvious from the time integration method. This statement corresponds to interchanging top and bottom in diagrams like Fig. 17.

We have discussed in Sec. 4 which types of conventional Goldstone diagrams are taken into account when we calculate Fig. 2(b) on the energy shell. A fairly general example is shown in Fig. 7. The lowest order conventional diagram [apart from Fig. 2(b)] is shown in Fig. 20. Now there is a rather similar diagram, Fig. 21, which is apparently related to the particle bubble of Fig. 2(a) in the same way as Fig. 20 is to the hole bubble. The question therefore arises as to whether a

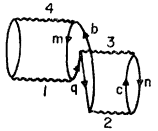


FIG. 21. Another fourth-order Goldstone diagram. In contrast to Fig. 20, this contains different v -matrix elements and an additional independent hole line g . It cannot be generated from Fig. 2(a) by altering the time order.

particle-bubble interaction can also be put on the energy shell. To answer this question, we must examine the v -interaction ladder diagrams which are contained in the G -matrix diagrams. Figures 2(b) and 20 contain the same v -matrix elements; they differ only in the time orders of the v 's. On the other hand, it is easily seen that Figs. 2(a) and 21 involve *different* v -matrix elements. [Fig. 2(a) contains no matrix elements leading to state q .] There are no other Goldstone diagrams which contain the same v -matrix elements as Fig. 2(a) (or Fig. 4) but which have different energy denominators. Therefore, Fig. 2(a) must be taken at its face value and be evaluated off the energy shell. Figure 21 is a

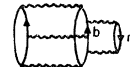


FIG. 22. Simplest generalization of Fig. 2(a) which contains the same number of independent hole lines.

different type of diagram, and is proportional to a higher power of the density since it contains an additional hole line, q . The only generalizations of Fig. 2(a) that are of the same order in the density are of the form shown in Fig. 22. This is a "true" higher order (in G) diagram, but the possibility remains of considering this approximately equivalent to an insertion, following Rajaraman's argument. The crucial point of this discussion is that the hole insertions, such as Figs. 2(b), 16, 18, and 19, naturally contain "kinks" in the Fermion line, m , so that the time order may be altered without changing the v -matrix elements. There are no analogous "kinks" in Figs. 2(a) or 4.